GEMS & GEMOLOGY

VOLUME XXXIII SPRING 1997

THE QUARTERLY JOURNAL OF THE GEMOLOGICAL INSTITUTE OF AMERICA

GEMS & GEMOLGY
SPRING 1997 VOLUME 33 NO. 1

TABLE OF CONTENTS

pg. 5

pg. 33

pg. 43

pg. 64

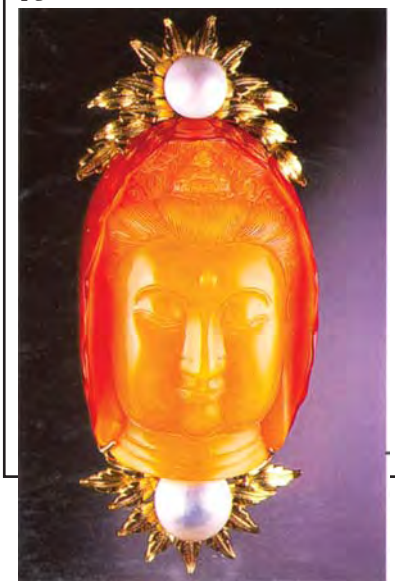

ABOUT THE COVER: Geophysics has the potential to play an increasingly important role in gemstone exploration. Advances in geophysical technology and computer imaging now permit mapping of geologic features at various depths beneath the Earth's surface. Seismic-reflection profiling and georadar are particularly promising for high-resolution mapping of near-surface pegmatites, similar to the one in the Mesa Grande district of San Diego County—the Queen mine—that yielded these beautiful tourmaline crystals. Extremely rare, these "blue tops" measure about 12.5 cm (5 inches) across; the tallest crystal is about 17.5 cm (7 inches) high. Courtesy of Pala International, Fallbrook, California.

Photo © Harold & Erica Van Pelt—Photographers, Los Angeles, CA.

Color separations for Gems & Gemology *are by Effective Graphics, Compton, CA. Printing is by Cadmus Journal Services, Baltimore, MD.*
 ISSN 0016-626X

THE DR. EDWARD J. GÜBELIN MOST VALUABLE ARTICLE AWARD

ALICE S. KELLER, EDITOR

It is with great pleasure that we announce that Dr. Edward J. Gübelin has agreed to have his name associated with *Gems & Gemology*'s most valuable article competition. One of the industry's most respected scientists, Dr. Gübelin's name has been synonymous with gemology for over 60 years. He has written numerous books and articles (including the paper on Nepal rubies in the present issue), published a comprehensive map on world gem localities, and even produced films on the historic Burmese ruby and jadeite deposits. *Photoatlas of Inclusions in Gemstones,* co-authored with John I. Koivula, is perhaps his best-known contribution; the more than 1,400 photomicrographs are unparalleled in both their quality and the information they convey. In Dr. Gübelin's honor, the award has been renamed the Dr. Edward J. Gubelin Most Valuable Article Award.

Beginning this year, as a result of Dr. Gübelin's generosity, the first-place winner of the Dr. Edward J. Gübelin Most Valuable Article Award will receive a plaque, and winners of the second- and third-place awards will be given certificates. Awards of $1,000, $500, and $300, respectively, will also be given to the authors of the three articles that our readers selected as the most valuable papers published in 1996.

Receiving the Gübelin plaque for the 1996 first prize is the article "De Beers Natural versus Synthetic Diamond Verification Instruments," by De Beers researchers Christopher M. Welbourn, Martin Cooper, and Paul M. Spear. This Fall issue article describes the research behind, and the operation of, two ground-breaking new instruments to separate natural from synthetic diamonds. Another article about diamonds, although from a completely different perspective, won second place: A. J. A. "Bram" Janse's "A History of Diamond Sources in Africa: Part II." (Part I of Mr. Janse's article won third place in last year's contest.) John I. Koivula, Robert C. Kammerling, Dino DeGhionno, Ilene Reinitz, Emmanuel Fritsch, and Mary L. Johnson co-authored this year's third-place winner, "Gemological Investigation of a New Type of Russian Hydrothermal Synthetic Emerald." Both the second- and third-place articles appeared in the Spring 1996 issue.

Photographs and brief biographies of the winning authors appear below. Congratulations also to Margaret Alexander of Mimbres, New Mexico, whose ballot was randomly chosen from all submitted to win the five-year subscription to *Gems & Gemology*.

FIRST PLACE

CHRISTOPHER M. WELBOURN ● MARTIN COOPER ● PAUL M. SPEAR

Christopher M. Welbourn

Martin Cooper

Paul M. Spear

Christopher M. Welbourn is principal scientist in the Physics Department at De Beers DTC Research Centre, Maidenhead, United Kingdom. Dr. Welbourn, who joined the De Beers Research Centre in 1978, has a Ph.D. in solid state physics from the University of Reading. He has published several papers on the use of optical spectroscopy and X-ray and cathodoluminescence topography to study diamonds. Research director at De Beers DTC Research Centre, **Martin Cooper** has a B.Sc. in physics from the University of London and a M.Sc. in materials science from Bristol University. **Paul M. Spear** is a research scientist in the Physics Department at De Beers DTC Research Centre. With De Beers since 1986, he has a Ph.D. from King's College, University of London.

SECOND PLACE

A. J. A. "BRAM" JANSE

A. J. A. (Bram) Janse

A. J. A. "Bram" Janse is manager of his own geological consulting company—Archon Exploration Pty Ltd, in Perth, Western Australia—and a director of KWG Resources, Montreal, Canada. During the 38 years he has been involved with diamond exploration, he has worked on projects in Australia, Brazil, Canada, India, and South Africa. He has a B.Sc. in geology and a M.Sc. in petrology and mineralogy from the University of Leiden in the Netherlands, and a Ph.D. in petrology from the University of Leeds in England. He is currently developing an extensive database on diamond and kimberlite occurrences.

From left, John I. Koivula, Dino De Ghionno, and Mary L. Johnson

THIRD PLACE

JOHN I. KOIVULA ● ROBERT C. KAMMERLING DINO DEGHIONNO ● ILENE REINITZ ● EMMANUEL FRITSCH ● MARY L. JOHNSON

Ilene Reinitz

John I. Koivula, chief research gemologist at the GIA Gem Trade Laboratory (GIA GTL), is co-editor of the Gem News section of *Gems & Gemology*. World renowned for his knowledge of inclusions, Mr. Koivula holds bachelor's degrees in chemistry and mineralogy from Eastern Washington State University. The late **Robert C. Kammerling** was vice-president of research and development at GIA GTL, then in Santa Monica, California. A prolific author, he was also an associate editor of *Gems & Gemology* and co-editor of the Gem Trade Lab Notes and Gem News sections. **Dino DeGhionno** is senior staff gemologist at GIA GTL, Carlsbad, California, and a contributing editor to the Gem News section of *Gems & Gemology*. Before he joined GTL, Mr. De Ghionno worked for 14 years as a teacher and later manager of GIA's resident student program in colored stone identification. **Ilene Reinitz** is a research scientist at GIA GTL in New York. A regular contributor to the Gem Trade Lab Notes section and a co-author of several *Gems & Gemology* articles, she has a Ph.D. from Yale University. **Emmanuel Fritsch** is a professor of physics at the Gemology Laboratory, Physics Department, University of Nantes, France. He has a Ph.D. from the Sorbonne in Paris. His research specialties are spectroscopy in gemology, the origin of color in gem materials, and treated and synthetic gems. **Mary L. Johnson,** also a co-editor of *Gems & Gemology*'s Gem News section, is a research scientist at GIA GTL. Dr. Johnson, has co-authored several articles in *Gems & Gemology*, is a Gem Trade Lab Notes contributing editor, and is a frequent contributor to the journal's abstract section. She holds a Ph.D. in mineralogy and crystallography from Harvard University.

Robert C. Kammerling

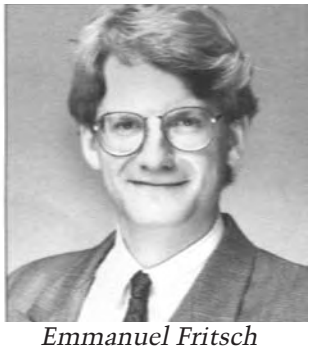

Emmanuel Fritsch

APPLICATIONS OF GEOPHYSICS IN GEMSTONE EXPLORATION

By Frederick A. Cook

Advances in geophysical technology and computer imaging now permit mapping of geologic features at various depths beneath the Earth's surface in more detail than ever before. Geophysical methods, which for some years have been used to explore for diamonds (and many other minerals), also hold promise as important tools in both exploration for new colored stone deposits and assessment of known deposits. Particularly exciting are the use of seismic-reflection and radar-imaging techniques for high-resolution mapping of near-surface pegmatites, veins, metamorphic layering in crystalline rocks, and alluvial deposits in sedimentary rocks. These techniques can produce images of regions only a few centimeters to a few meters in size down to several meters to tens of meters below the surface. Thus, it is now possible to locate directly some buried structures containing gem deposits.

ABOUT THE AUTHOR

Dr. Cook is professor in the Department of Geology and Geophysics, The University of Calgary, Alberta T2N 1N4, Canada.

Acknowledgments: This work was supported by the Natural Sciences and Engineering Research Council of Canada. The author thanks Dr. A. A. Levinson of the University of Calgary for many helpful discussions, constructive criticisms, and editorial suggestions. Dr. A. G. Green of the Swiss Federal Technical Institute in Zurich kindly provided support for recording the georadar data in the Gotthard area of the Swiss Alps. The georadar data used to produce figure 9 were processed at the University of Calgary, and the assistance of A. Van der Velden and Dr. K. Vasudevan in processing those data is greatly appreciated.

Gems & Gemology, *Vol. 33, No. 1, pp. 4–23.*

Much of the exploration for gemstones (even diamonds, in some regions) is conducted with relatively simple, often primitive, techniques. In many areas of known gem occurrences, development and mining involve little more than shovels and screens for alluvial deposits, and explosives plus mechanical tools (such as pneumatic drills) for hard-rock deposits (e.g., pegmatites; figures 1 and 2). In areas where gems are not known to occur, most discoveries are made by chance. This contrasts with the exploration procedures routinely used for many other Earth resources, such as oil and gas or metallic minerals, in which years of regional geologic and geochemical mapping are usually followed by intensive periods of acquiring and analyzing geophysical data. Once target areas are located, more detailed—and usually more expensive—exploration methods (such as drilling or excavation) can be undertaken. However, geophysical techniques have seldom been used to delineate gemstone, particularly colored stone, deposits.

This article describes the principles behind geophysical exploration, together with some applications in diamond exploration and some potential applications in colored stone exploration. Different contemporary geophysical exploration techniques are highlighted, and suggestions are made with regard to how these techniques could be applied to certain types of gem occurrences. As consumer demand for gems continues to rise, and older deposits are depleted, geophysical prospecting has considerable potential for identifying new resources or new areas of gem mineralization at existing occurrences.

GEOPHYSICS AND GEMOLOGY

Geophysics is the application of physical principles (e.g., using magnetism, gravity, or electrical properties) to study the internal structure and geologic evolution of the Earth and other planets. In particular, physical principles are used to study the composition and geologic structure of rocks below the surface. Thus, geophysics includes a number of techniques that can help identify promising localities for mineral exploration.

Figure 1. The discovery of pegmatites, and of gem-bearing pockets in a pegmatite dike, is one of the greatest challenges in gem exploration. These bicolored tourmalines from the Himalaya mine, San Diego County, California, represent some of the fine gems waiting to be discovered in pegmatites worldwide. Courtesy of Pala International, Fallbrook, California; photo © Harold & Erica Van Pelt.

Gemology and geophysics are similar in many ways. The nondestructive techniques that a gemologist uses to determine the identity of a gemstone typically include determination of refractive index (speed of light ratios), specific gravity (density), thermal conductivity, and magnetism (occasionally), as well as describing or mapping internal characteristics (e.g., inclusions, internal growth structure, etc.). A geophysicist also uses generally nondestructive (sometimes called remote sensing) methods. Some of the most common techniques (table 1) include those that measure variations in the speed of vibrational waves (seismic refraction), in rock density (gravity), in the thermal state of the Earth (heat flow), and in rock magnetism (magnetics); as well as those that use imaging to map subsurface structures (seismic-reflection profiling, ground-penetrating radar).

There are essentially two branches of geophysics that apply to studies of rocks: (1) whole-Earth geophysics, and (2) exploration geophysics. In whole-Earth geophysics, geophysical methods are used to map deep and large-scale variations in the Earth's properties, such as the depth and configuration of the Earth's core, the internal characteristics of the Earth's deep *mantle* (the region of the earth between the crust and the core), the depth and structure of the *lithosphere* (the outer shell of the Earth, approximately 100 km deep on average), and the thickness and properties of the *crust* (the outermost layer of the lithosphere, about 10–40 km thick; see figure 3). The lithosphere is generally rigid and consists of a series of "plates" that shift relative to one another (i.e., plate tectonics), thus producing earthquakes, volcanoes, and uplift of mountains. The lithosphere usually reaches its greatest thickness (as much as 300–400 km) beneath ancient continents.

In exploration geophysics, on the other hand, geophysical techniques are used to search for hydrocarbon (oil and gas), mineral (gold, silver, lead, zinc,

Figure 2. This pegmatite pocket from California's Himalaya mine yielded thousands of carats of fine tourmaline. Unfortunately, the discovery of such pockets typically requires hundreds of meters of tunneling and a great deal of luck. Rapid improvements in geophysical prospecting techniques offer the hope that this situation will change in the near future. Photo © Harold & Erica Van Pelt.

etc.), and other economically significant deposits. Hydrocarbon and mineral deposits are usually located in geologic structures that are large enough (sometimes several square kilometers) to be easily mapped by geophysical imaging. Although geophysical results rarely can identify whether economically significant hydrocarbons or minerals are present, they often can pinpoint geologic features that may

TABLE 1. Common geophysical exploration methods and potential applications to gemstone exploration[a].

Method	Principle involved	Usual geologic application	Effective depth	Effective resolution
Gravity	Responds to variations in rock density	Mapping subsurface structure based on variations in density	Meters to 100s of km (depends on spacing of measurements)	100 m to 10s of km (depends on spacing of measurements)
Magnetics	Responds to variations in rock magnetism (usually iron content)	Mapping subsurface structure based on variations in magnetic properties	Meters to 50 km (depends on spacing of measurements)	A few m to 10s of km (depends on spacing of measurements)
Electrical	Responds to variations in electrical conductivity (metals or fluids)	Mapping fluids (e.g., ground water) and metal deposits	Meters to 100s of km (depends on measurement time)	10 m to 100s of km (depends on spacing of measurements)
Heat flow	Responds to variations in temperature at depth; thermal conductivity	Mapping variations in the outflow of the Earth's heat	1 km to 100s of km (depends on knowledge of properties at depth)	A few m to 10s of km (depends on knowledge of properties at depth)
Radioactivity	Responds to variations in radioactivity of rocks	Mapping concentrations of radioactive minerals	A few cm	A few cm to 100s of m (depends on spacing of measurements)
Earthquake seismology	Responds to variations in seismic-wave velocity (varies with rock density)	Mapping large-scale (lithosphere) and deep-Earth structure	To center of earth	10s of km (depends on frequency of signal and wave velocity)
Seismic refraction	Responds to variations in acoustic impedance (density × velocity)	Mapping crustal thickness and regional structure; depth to basement	10 m to 100s of km (depends on length of profiles; energy source)	10 m to 100s of m (depends on length of profiles; energy source)
Seismic-reflection profiling	Responds to variations in acoustic impedance (density × velocity)	Mapping detailed geologic structure and stratigraphy	100 m to 100s of km (depends on length of profiles, energy source)	A few m to 100s of m (depends on frequency of signal and wave velocity)
Ground-penetrating radar (Georadar)	Responds to contrasts in electrical conductivity	Mapping detailed geologic structure and stratigraphy.	Meters to 100 m	About 10 cm to 1 m (depends on frequency of signal and wave velocity)

[a]Not all of these methods are described in detail in the text as their application to gemstone exploration may be limited (e.g., electrical, heat flow). Nevertheless, they may be useful for reconnaissance work under favorable conditions. For additional information on the applications of these techniques, see Telford et al. (1976).

be promising targets. Unlike mineral and hydrocarbon deposits, however, many primary gem deposits—such as those in veins or pegmatite cavities (figure 2)—are no larger than a few meters in diameter. Because of their small size, these deposits are easily missed with conventional mining methods (e.g., trenching or tunneling), and most geophysical techniques cannot produce the resolution (detail) necessary to detect them.

Today, though, new methods of data acquisition and analysis (including sophisticated computer processing) enable some geophysical techniques to resolve geologic features that are as small as a fraction of a meter to a few meters in longest dimension and very shallow, within a few meters of the surface. In addition, improvements in our knowledge of deep geologic structures (tens to perhaps hundreds of kilometers below the surface) now make it feasible to use large-scale reconnaissance geophysical techniques to identify regions of the Earth within which certain kinds of gem deposits might be found. Thus, the science of geophysics has the potential to play an increasingly important role in the exploration and development of some gemstone deposits. It is even possible that specific exploration strategies could be developed using geophysical techniques to optimize: (1) opportunities of for success in exploring for gems, and (2) knowledge of existing deposits (e.g., their extent and thus, potentially, their value) .

THE "RESOLUTION PROBLEM"

The objective of all geophysical methods is to produce an image of the Earth's interior, usually by making measurements at the surface. The type of

Relative cost	Limitations	Comments	Potential application in gem exploration
Low ($100s per day); cost increases for greater detail	Inherent ambiguity between rock geometry and density limits usefulness in exploration	Used for reconnaissance work and as a measurement for density estimate	Reconnaissance; thickness of crust and lithosphere
Low ($100s per day); cost increases for greater detail	Inherent ambiguity between rock geometry and magnetism limits usefulness in exploration	Used to map kimberlite pipes; may also assist in mapping regional geologic structures in basement	Delineating kimberlites; mapping regional geologic structures
Low ($100s per day); cost increases for greater detail	Inherent ambiguity between rock geometry and conductivity limits usefulness in exploration	Used to explore for metal deposits; may assist mapping lithosphere thickness and basement structures	Reconnaissance; thickness of lithosphere; mapping kimberlites
Low, but usually requires costly drillholes at $1000s per drillhole	Requires drillholes, thus limiting number of measurements; inherent ambiguities in calculation	Used to calculate temperature at depth, geothermal energy	Reconnaissance; thickness of the crust and lithosphere
Low ($100s per day); cost increases for greater detail	Limited penetration; not useful for regional studies	Used to explore for radioactive mineral deposits	Might help to indicate presence of accessory radioactive minerals
Low to moderate; cost increases with number of receiving stations	Low resolution; not useful for detailed structure	Used for mapping variations of seismic velocity in the mantle	Reconnaissance; thickness of the lithosphere in diamond exploration
Moderate ($100s–1000s per day); cost per kilometer increases with number of receiving stations	Low resolution; not useful for detailed structure	Used for mapping variations in depth to mantle and depth to basement	Reconnaissance; thickness of the crust; depth to basement beneath alluvial deposits
High ($1000s per day); cost increases for greater detail	Relatively expensive; not easy to image shallower than 50 m	Most widely used geophysical method in hydrocarbon exploration due to good image quality	Reconnaissance; thickness of the crust; detailed structure; mapping of alluvial deposits
Low ($100s per day)	Signal can only penetrate up to 50 or 100 m; quality may be severely affected by surface material	Used in mapping near-surface features such as archeological sites, pipelines, tunnels, etc.	Alluvial deposits; delineating pegmatite cavities

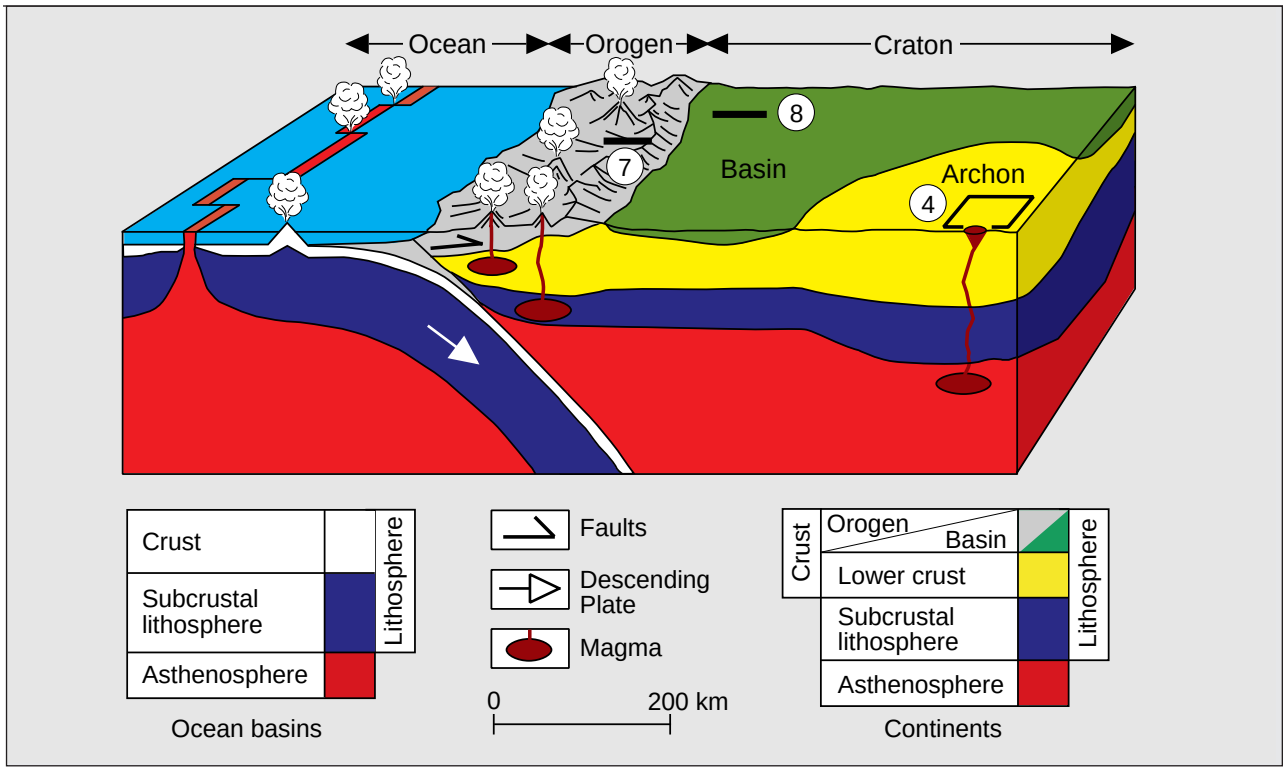

Figure 3. In this schematic diagram, normal lithosphere is segmented into the tectonic plates of the Earth's surface, with unusually thick lithosphere (combined crust and subcrustal) under archons (portions of cratons with an age of formation exceeding 2,500 million years [Janse, 1994]), where diamonds may form. Cratons are areas of the continent that have been stable for long periods of geologic time, and orogens are regions that have been subjected to folding and faulting. Geophysical techniques may be applied in different areas and at different scales to delineate gem deposits. For example, some methods are useful on a reconnaissance scale to delineate thick lithosphere, where most primary diamond deposits are found, as well as to identify regions of thin lithosphere, where economic primary diamond deposits are very unlikely to occur. Other geophysical methods are more useful for intermediate-scale exploration. Magnetic surveys, for example, respond to differences in properties between kimberlites and surrounding rocks and assist in locating specific areas for exploration (figure 4), whereas seismic profiles assist in delineating the deep geometry of mountains (figure 7) and basins (figure 8). Approximate positions of data in figures 4, 7, and 8 are shown as circled numbers.

image depends on what parameter(s) are measured by the particular method being used (again, see table 1). The value of a technique depends on its *resolution*, that is, its ability to distinguish responses from different types and sizes of geologic features.

In all cases, the measured response includes the combined effects of rocks between the target zone (area of interest) and the surface; in some cases, it also includes features below the zone of interest. Consider the following analogy. In measuring the density (specific gravity) of a gem, a gemologist weighs a sample first in air and then in water, and calculates the specific gravity according to how much water is displaced. In fact, however, the specific gravity of the sample is affected by the specific gravity of the gem material plus the specific gravities of any inclusions, some of which may be lighter (e.g., air or water) or heavier (e.g., heavy minerals) than the host gem. For example, an emerald that has many pyrite (S.G. ~ 5.00) inclusions will have a specific gravity that is greater than for beryl alone (2.70). The inclusions thus add *noise* (i.e., an unwanted signal) to the result, which causes the measured specific gravity to deviate from the theoretical value of the pure gem material or even from the value typical for relatively inclusion-free material.

The geophysical method analogous to specific gravity is the measurement and analysis of the Earth's gravity field (Box A; table 1). After accounting for large-scale variations caused by the Earth as a whole (such as its shape and size), the remaining signal (e.g., the pull of gravity) is a function of variations in the densities of rocks at depth. When a geophysicist measures the Earth's gravity field at a location on the surface, the reading includes the

BOX A: GRAVITY AND MAGNETIC METHODS

Subtle variations in the Earth's gravitational pull are brought about by differences in the density of large masses of rock. These variations can be identified by the gravity method, which is analogous to measuring specific gravity. In it, a gravity meter, or gravimeter—a sensitive mass-spring system that weighs about 5–7 kg (10–15 pounds)—is carried (usually on the ground, although sometimes in an airplane) from location to location, measuring the pull of the earth's gravity field (figure A-1). When a gravity measurement is taken over an object with a high density, the object pulls on the mass and is recorded as an increase in gravity (figure A-1); decreases in gravity occur over low-density objects.

Once appropriate corrections for elevation and latitude are made to the recorded gravity data, the resulting values (anomalies) represent variations in mass (density) at depth. A problem inherent in interpreting these kinds of data is that the actual measured value is the sum of responses of all mass variations at depth (e.g., A and B in figure A-1). This makes it difficult to determine the subsurface structure with much precision from this method alone, so gravimeter data are usually used in conjunction with magnetic and other data.

The magnetic field at any location is a combination of the field produced by the Earth's core plus effects from nearby magnetic objects, such as iron-bearing rocks. Magnetic data are acquired in much the same way as gravity data, except that a magnetometer is used to measure the magnetic field on or above the surface. Once the Earth's field is removed from the measured signal, the resulting anomalies can be interpreted in terms of geologic features. Normally, rocks that contain large amounts of iron (e.g., kimberlites) produce large magnetic anomalies (see text figure 4). One advantage that the magnetic method has over most other methods is that a magnetometer can be carried behind an airplane, thus allowing the acquisition of large amounts of data in a short time. Interpretation of magnetic anomalies is similar to interpretation of gravity anomalies. Aeromagnetic surveys have been broadly used in the exploration for diamond deposits in Australia, Africa, and, most recently, Canada.

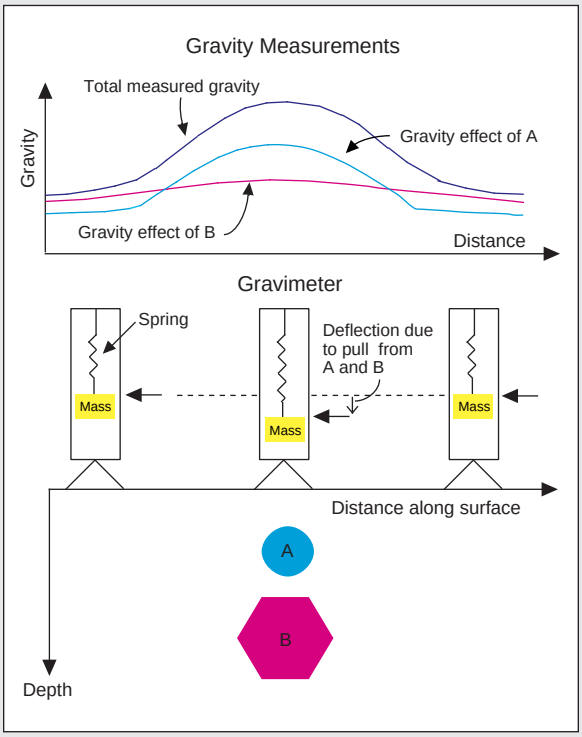

Figure A-1. In this schematic illustration of the gravity method, a gravity meter (gravimeter), which is essentially a mass-spring system, is placed at a series of locations along the surface. The displacement of the mass is a function of the strength of the gravity at each location. Following corrections for elevation and latitude, the remaining signal consists of a series of anomalies that represent the combined gravitational attraction of local geologic features (A and B in this figure).

combined effects of all rocks below the area being measured, from great depths to the surface. The analysis must account for as many effects as possible, so that resultant *anomalies* (in this context, deviations from uniformity or normal values in an exploration survey) can be interpreted. However, it is often difficult to separate the effects of different masses of rock, because their shapes and densities are not usually known. Because such detailed knowledge of subsurface rock types and geometries is not yet available, geophysicists cannot resolve variations in rock density to a few meters in size, as would be necessary for many gem exploration applications. Similar difficulties exist in measuring the Earth's magnetic field (table 1), although high-precision instruments and detailed measurements now permit greater resolution than ever before.

In fact, interpretations of virtually all geophysical measurements require careful understanding of the possible causes of the background noise that affects resolution. Usually more than one method of exploration must be applied before an economic

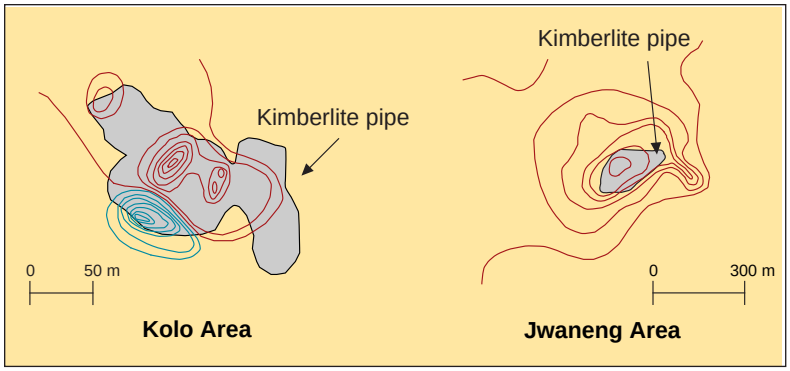

Figure 4. Magnetic anomalies from kimberlites tend to be roughly circular in map view (modified from Atkinson, 1989). On these maps of two kimberlites in Africa, Kolo and Jwaneng, the red lines represent magnetic highs (regions of high iron concentrations), the blue contours represent magnetic lows, and the gray stippled areas are outlines of the kimberlite pipes. Map information taken from Burley and Greenwood (1972, for the Kolo area) and Lock (1985, for Jwaneng).

deposit can be clearly identified. The problem of background noise is even greater for conditions of analysis that might provide the detailed resolution necessary to delineate most types of gem deposits.

Nevertheless, when much larger-scale variations are considered (such as changes in the lithosphere or locating some large features that may contain gems), geophysics can and does play an important role. Such is the case in diamond exploration.

CURRENT USE OF GEOPHYSICS IN DIAMOND EXPLORATION

Primary Deposits. Geophysical techniques are commonly used to locate promising regions for primary diamond deposits (Atkinson, 1989; Smith et al., 1996), which are found in two types of rare igneous rocks, kimberlites and lamproites. The magmas from which these igneous rocks crystallized originated in the Earth's mantle at depths of more than 150–200 km. As they ascended to the surface, these magmas traveled through the lower part of the continental lithosphere, where the diamonds probably formed (again, see figure 3). Sometimes, these magmas carried some of the diamonds along with them. We know, then, that primary diamond deposits form in regions where the continental lithosphere is thick (150–200 km or more); to be economic, the kimberlites or lamproites must be present at or near the surface (Levinson et al., 1992).

The presence of kimberlites or lamproites can be detected by geophysical methods, particularly by magnetic and electrical techniques. Kimberlites and lamproites typically have high iron concentrations, so they often are more magnetic and more electrically conductive than the rocks they have intruded (Atkinson, 1989; Hoover and Campbell, 1994; Smith et al., 1996). Furthermore, they usually form circular or irregularly shaped structures (in map view), so that they can be pinpointed by magnetic (figure 4) and electrical measurements (Smith et al., 1996), even if they are covered by a thin blanket of sedimentary rocks.

However, only a small fraction of kimberlites contain diamonds in economic amounts, and these tend to be in areas with thick lithosphere. Thick lithosphere is more likely to have economic kimberlite or lamproite deposits because diamonds form from carbon (or carbon-containing compounds such as methane and carbon dioxide) at pressures corresponding to 150–200 km depth. The lithosphere is usually about 100 km thick, so a 150–200 km thick lithosphere is uncommon and would appear as a "keel" or "root," much like the lower part of an iceberg. Thick lithosphere tends to occur beneath old continental *cratons* (those parts of the earth's crust that have attained stability, and have been little deformed for prolonged periods), because that is where there has been the greatest amount of time for the lithosphere to cool and thicken (billions of years, as compared to a few hundred million years for oceanic regions). Thus, methods that measure the thickness of the lithosphere can be valuable in assessing whether a region might contain diamondiferous kimberlites. Figure 5, for example, illustrates the various thicknesses of the lithosphere under North America, with specific reference to the recently discovered diamond deposits in Canada. Lithospheric roots are higher in density than the surrounding mantle material, so geophysical techniques that respond to density are useful (e.g., gravity and earthquake seismology; again, see table 1).

Measurements of seismic-wave velocity provide some estimation of variations in rock density as well as of the rigidity (strength) of the rocks. Because rocks in the mantle part of the lithosphere usually are denser and more rigid, they have higher seismic-wave velocities than adjacent rocks of the partly

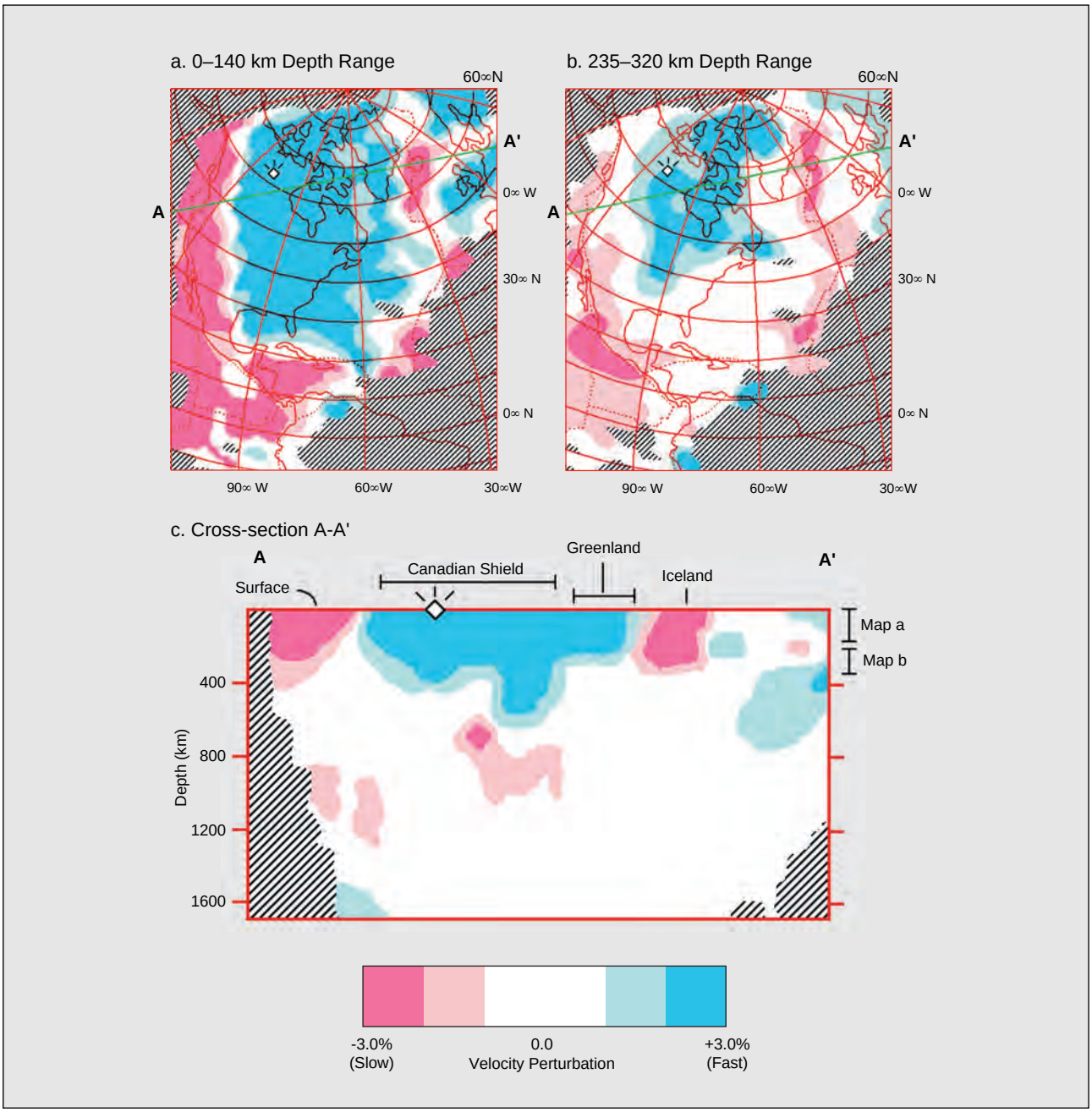

Figure 5. The thickness of the lithosphere beneath continents may be estimated by measuring the velocities of seismic waves. Two maps of North America (a and b) show estimates of seismic-wave velocity for different depth ranges. Areas of increasingly high velocity (and probably increasingly rigid material) are represented by light to dark blue, whereas areas of lower velocities (and probably less rigid, partly molten material) appear pink to red. (a) For depths from the surface down to 140 km, this map shows high velocities under the center of the continent, where the lithosphere is thick. The velocities tend to decrease slightly near the edges of the continent, where some partly melted rock is closer to the surface. (b) For the depth range 235–320 km, only the central part of the continent (Canadian Shield) has high velocities and, thus, more rigid rock; this is the area where major primary diamond deposits have recently been found (diamond symbol). In both maps, dotted lines represent the boundaries between tectonic plates, and the scale at the bottom indicates perturbation of seismic-wave velocity from expected values. A-A' is the location of the cross-section of (c). Diagonal-lined areas have no data. (c) Cross-section A-A' through the North American continent illustrates seismic-wave velocity as a function of depth. Again, the dark blue (high velocity) region extends to 300–600 km depth beneath the central part of the continent (Canadian Shield). The depth ranges of maps a and b are shown on the right of the diagram. Figures are modified from Grand (1987).

molten *asthenosphere* (the part of the Earth's mantle that is located below the lithosphere and that acts somewhat like a fluid; figure 3). The top of the asthenosphere is found typically between about 100 and 200 km, but it is sometimes much deeper beneath ancient cratons (again, see figure 3). Thus, maps of wave velocities (measured from earthquake waves) at different depths have anomalously high values (hence, high densities and greater strength) deep below the thick cratons (Grand, 1987). The dark blue areas of figure 5 represent regions with high density and are interpreted as the lithospheric roots. Once the lithospheric roots have been located, higher-resolution magnetic and electrical data may allow identification of anomalies associated with individual kimberlite or lamproite structures. These are the kimberlite structures that should receive the most intensive study (Atkinson, 1989; Smith et al., 1996). Of course, identification of kimberlite fields in areas of thick lithosphere does not guarantee that economic diamond deposits will be found. Without these conditions (kimberlites/lamproites *and* thick lithosphere), though, the possibility of economic primary deposits is severely diminished.

Atkinson (1989) states that geophysical techniques, specifically magnetics, were used as early as 1932 to locate the boundaries of kimberlite pipes. Gravimetric and resistivity surveys were also used for similar purposes. All these early attempts were conducted on the ground. Following World War II, however, aeromagnetic surveys were flown as part of exploration for kimberlite, with the Russians being the first to use this method extensively in Yakutia. Since the early 1970s, aeromagnetics have been used in many places, such as Australia and Botswana, resulting in the discovery in the late 1970s of the Ellendale lamproites in Western Australia. Today, geophysical techniques, particularly aeromagnetics, are used throughout the world in exploration for kimberlites, such as in the Northwest Territories, Canada (Smith et al., 1996).

Secondary (Including Alluvial) Deposits. Exploration for secondary diamond deposits (alluvial, beach, marine deposits etc.) involves identification of the sedimentary layers within which diamonds occur. Diamonds may be transported long distances (hundreds of kilometers) from their primary source locations, collecting in deposits that are no longer situated on thick lithosphere. Consequently, geophysical exploration for secondary diamond deposits requires techniques that allow mapping of detailed features at shallow depths. For example, in South Africa and Namibia, diamond deposits in river gravels are found at the edge of, or even offshore from, the African continental craton (Gurney et al., 1991), where the lithosphere is probably thin. In such cases, it is necessary to explore with methods that allow mapping of the shallow subsurface geometry of the diamondiferous sediment layers. Because this approach is essentially the same for all alluvial gems, colored stones as well as diamonds, it is discussed in greater detail below.

USES OF GEOPHYSICS IN COLORED STONE EXPLORATION

Colored stones are found in a much greater variety of geologic environments than are diamonds, and many of the most valuable gem deposits occur where the stones are concentrated into secondary (alluvial) environments after redistribution from their primary source locations. Also unlike diamond deposits, primary colored stone deposits—such as those found in pegmatites, in igneous intrusions in metamorphic or sedimentary rocks, in vugs in volcanic rocks, and the like—tend to be associated with geologic features on the order of a few meters or less. As is the case with diamonds, however, for a colored stone deposit to be economic it must be located within a few meters or tens of meters from the surface. Hence, whether the colored stone deposits being investigated are primary or secondary, the methods chosen must be able to delineate the near-surface geology in some detail.

In the past, geophysical techniques generally have not been as useful for mapping the extremely shallow part of the Earth (upper few meters to tens of meters) as they have been for greater depths; the more established techniques—such as gravity and magnetic measurements or electrical and seismic methods—simply have not had the resolution necessary to map the near-surface in detail. This is why we rarely hear of geophysics being used in colored stone exploration. However, this situation has changed in the past five to 10 years.

Some geophysical techniques are now being adapted for application to near-surface geologic interpretation, primarily to address geologic factors in environmental problems such as waste disposal (Beres et al., 1995; Lanz et al., 1994). Some of these methods are also being used in a limited way to explore for gemstones (e.g., Patterson, 1996; William Rohtert, Kennecott, pers. comm., 1997). Because most geophysical exploration techniques (such as

gravity and magnetics; see Box A) can be acquired and processed with high resolution, they are appropriate for certain specific, near-surface, exploration targets. For example, magnetics may be useful in mapping locations of some gem-bearing igneous dikes that have intruded into sedimentary strata (because igneous rocks usually contain large amounts of iron compared to most sedimentary rocks), or in mapping iron-rich sedimentary rocks. In fact, magnetics have been used to map concentrations of ironstone deposits that contain precious opal in Queensland, Australia (Senior et al., 1977). Magnetic anomalies coupled with anomalies in radioactivity have also been helpful in outlining possible areas for exploration of red beryl in Utah (William Rohtert, pers. comm., 1997; figure 6).

Nevertheless, it is rare for these (gravity, magnetics) and most other geophysical methods to be used for mapping alluvial deposits or other geologic features (e.g., veins, cavities, pegmatites, metamorphic layering) that contain gemstones. The reason for this is exactly the same as that for the difficulties that arise in interpreting specific gravity readings: The ambiguities inherent in the analyses preclude obtaining the necessary subsurface geometry and resolution. Because these methods have somewhat limited use in colored stone exploration, they will not be discussed further.

There are, however, two methods that have proved valuable for mapping subsurface geology—seismic-reflection profiling (Box B) and ground-penetrating radar (georadar; Box C)—that may also have broad applicability to gemstone exploration. Although these respond to different physical properties, the images of subsurface geometry produced by both of these geophysical exploration techniques are consistently superior to those of the other methods for mapping geologic layering. Illustrations of these methods clarify their potential value.

Seismic-Reflection Profiling. *The Method.* Seismic-reflection profiling was first used in the 1920s to map subsurface geologic structures in the search for oil and gas. Since then, it has become the most important tool in exploration geophysics; more than 90% of geophysical exploration for hydrocarbons is accomplished with seismic profiling. This is because the technique produces results that are similar to geologic cross-sections (figure 7). Although interpreting these data often requires specific skills, particularly knowledge of how seismic waves propagate through rocks, with these skills the geometry of the rock layers beneath the surface can often be determined with precision (again, see Box B).

Figure 6. Kennecott geologists used a combination of magnetic anomalies and radioactivity anomalies to outline potential deposits of red beryl in Utah's Wah Wah Mountains. The 10 × 9 × 8 mm crystal and 0.76 ct cut stone shown here represent some of the fine red beryls found at this locality. Courtesy of Michael M. Scott; photo © Harold & Erica Van Pelt.

The layers on the image in figure 7 represent reflections from boundaries between different rocks or, more specifically, between rocks with different properties (seismic velocity and density). By determining how fast the waves travel in the rock layers below the surface, we can convert the travel times to the reflecting surfaces to the depths of those surfaces (figure 7b). Thus, if a wave travels at about 5 km (3 miles) per second, a two-way (round-trip) time of 5 seconds represents 12.5 km depth (5 km/second × 5 seconds ÷ 2). With the data displayed this way, we are essentially looking at a cross-section of this portion of the Earth (about 50 km long × 20 km deep in the example in figure 7), in a manner similar to a CAT scan or an X-ray image of a portion of the body.

The profile in figure 7, which was taken in the Rocky Mountains of southwestern Canada, reveals a cross-section of some deformed (faulted and folded)

BOX B: SEISMIC-REFLECTION PROFILING

In seismic-reflection profiling, vibrational waves are generated on the Earth's surface and travel into the subsurface; there, they reflect off rock layers and return to the surface, where they are received by a row of sensors. It is the most common geophysical technique in hydrocarbon exploration and has been developed to a very sophisticated level. As for all of these techniques, the basic components for seismic-reflection profiling are field acquisition, data processing, and interpretation (figure B-1). In data acquisition, a source of elastic (vibrational) energy such as a small explosion or a large vibrator truck (figure B-2) produces the signals that penetrate into the Earth and are reflected back. A series of sensors (geophones; figure B-3) are positioned along the surface and are connected to a recording truck by cable or radio communication. These sensors measure variations in arrival times and amplitudes of waves, which relates to the densities and velocities of the different rock types. At the recording truck, the received signals are recorded through a computer onto magnetic tape.

The geometry of the field recording allows signals from a single point on a boundary (P in figure B-1) to be recorded at different geophone positions as the process is repeated at subsequent locations. This means that the separate reflections from P can be added together in data processing to enhance the signal from the layer boundary and thus identify the rock formation (or type of formation) that boundary represents.

Data processing is usually time consuming, and requires that a highly trained individual make judgments about parameters as different computer programs are applied (figure B-1). The basic sequence requires inputting the data from a field tape to the computer facility, displaying the field data (step 1 in figure B-1); editing bad traces (step 2; a trace is the series of signals recorded at a specific geophone for a single source vibration); collecting the signals of vibrations that were reflected from a single point from different geophone locations (step 3); removing noise from the waves that travel along the ground surface, rather than from those that reflected from depth (step 4); lining up these signals (step 5) and summing them into a single composite trace (step 6); applying different filters to enhance the pulse (step 7); and displaying the final section for each reflection point (step 8). Data presented in this article were processed through these steps. The final procedure is to interpret the data (step 9 in figure B-1), which requires that the analysts use as much geologic information as possible, as well as any other relevant geophysical information, to optimize the result. Because seismic-reflection profiling has potential for identifying relatively small geologic features (see discussion in the text), it has promise for gem exploration.

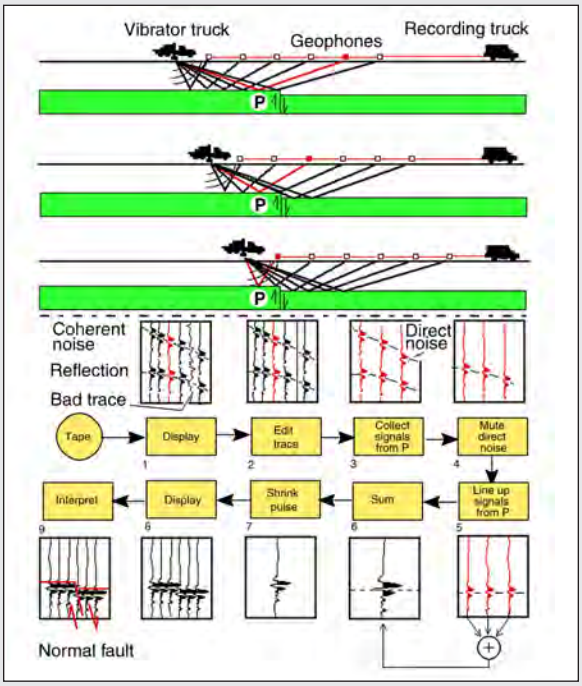

Figure B-1. This schematic drawing shows the many steps (described in the box) that are required to collect and analyze data in the seismic-reflection profiling technique (modified from Cook et al., 1980).

Figure B-2. Vibrator trucks—typically three or more in tandem—are commonly used as a source of energy for seismic-reflection work. Each of these trucks vibrates a signal of known frequency and energy for several seconds. These signals travel into the Earth until they are reflected back to the surface by a rock layer. Photo courtesy of K. W. Hall.

Figure B-3. Geophone sensors, each about 4 cm across the top, are placed on the ground surface to record the vibrations returned from beneath the surface. Photo courtesy of K. W. Hall.

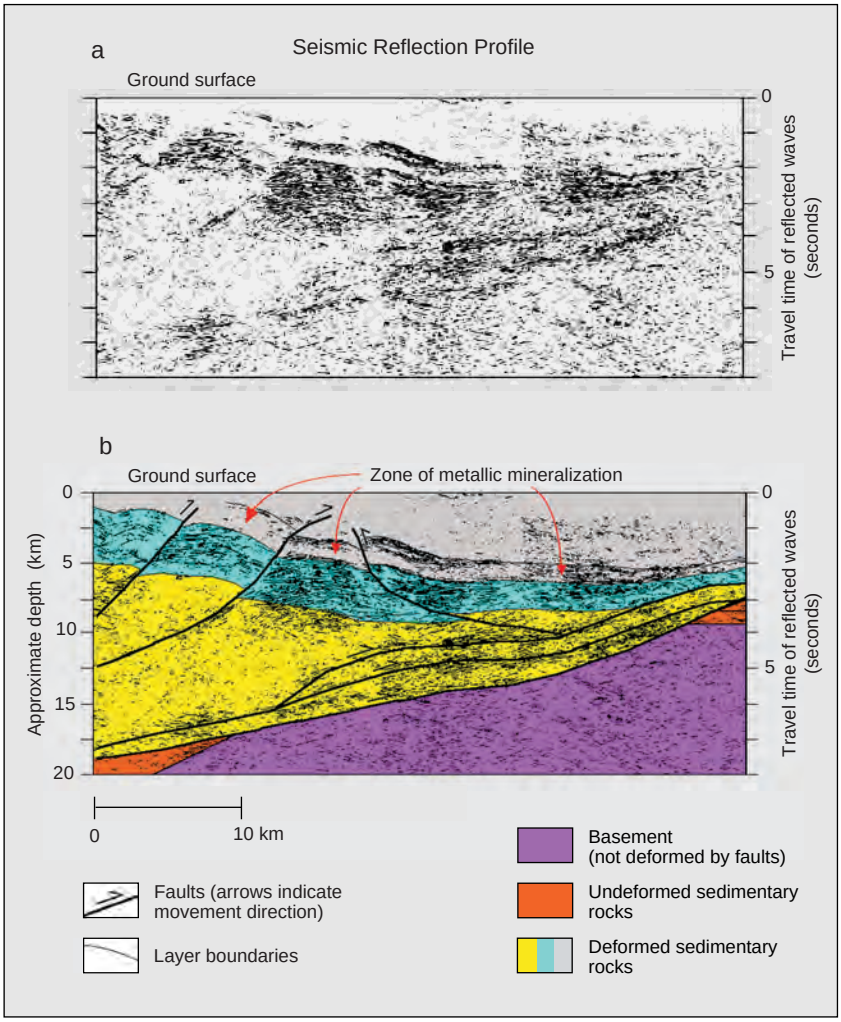

Figure 7. (a) This seismic-reflection profile, taken in the Rocky Mountains of southwestern Canada, is plotted with the horizontal axis as distance along the ground surface and the vertical axis as time (in seconds) for waves to travel from the surface (0) to a reflecting boundary (linear features on the data) and back to the surface. (b) Geologic interpretation of the data in (a) reveals different rock types, as shown by the colored areas, and faults. In this interpretation, sedimentary rocks were deformed by folding and faulting above undeformed basement rocks. A drill hole (not shown) about 10 km to the left of this profile penetrated a zone that was found to have large concentrations of metallic minerals (lead, zinc, silver). See figure 3 for the position of this profile relative to other geologic features. Adapted from Cook (1995).

sedimentary rocks. A drill hole located 10 km to the left of the section intersected the prominent layers observed; thus, these layers could be interpreted with some certainty. Furthermore, the drill hole also intersected a zone of metallic (lead, zinc, silver) mineralization that has not been exploited. This mineralization zone is associated with a stratum that can be followed as a recognizable layer, sometimes even across faults, for tens of kilometers on these and related seismic-reflection data. Thus, while the method does not actually produce images of the lead, zinc, or silver minerals, it does allow us to map the geometry and extent of the layer that may contain the minerals.

The large-scale profile (about 100 km long) in figure 8 illustrates an application of the method in a reconnaissance survey. This seismic-reflection cross-section of an area in western Canada required about two to three weeks of field work and another four to six weeks of computerized data analysis (again, see Box B). Layers are visible from near the surface to the base of the section (about 30–40 km depth). In this instance, the method provided an image of a previously unknown, ancient (Precambrian, or older than 570 million years) basin that lies above westward-thinning crust and below young, flat-lying sedimentary rocks (figure 8b; Cook and Van der Velden, 1993).

While details of the interpretation are not of major importance here, it is easy to see how seismic-reflection profiling can be used to map the deep geologic boundaries, and thus how it could be a valuable reconnaissance tool. But is this technique applicable to the very shallow part of the Earth, where gemstones might be recoverable? To a large extent, the answer to this question depends not only on the depths in question, but also on how small a feature the technique can detect; that is, on the resolution of the signal.

Resolution of the Data. The resolution of seismic-reflection data depends on the wavelength (L) of the

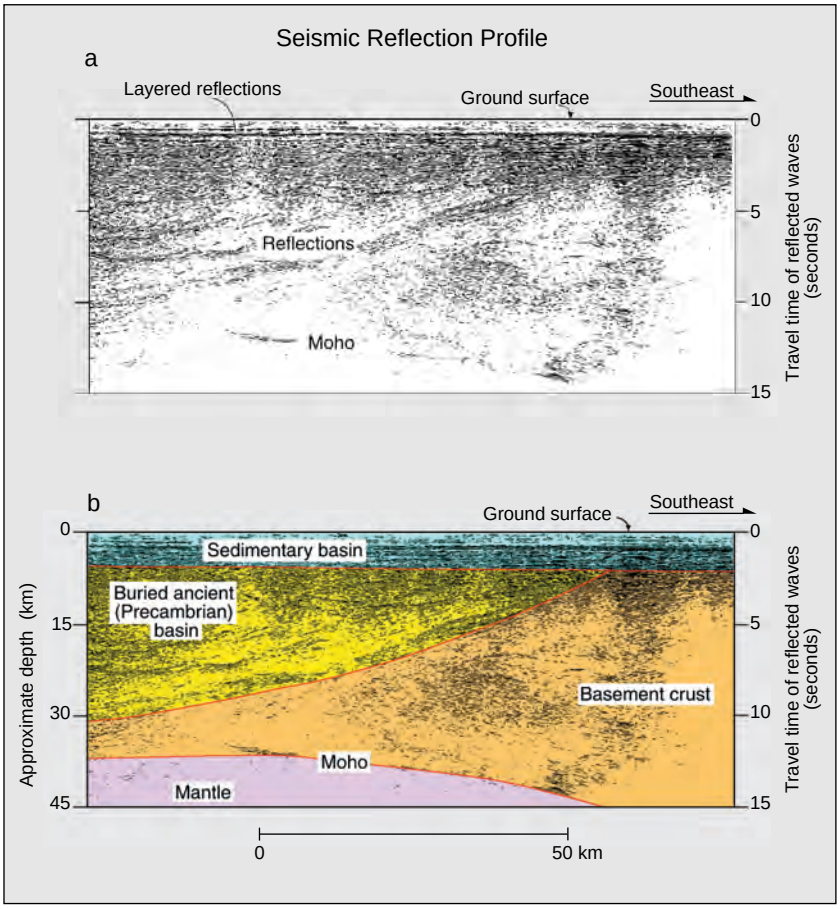

Figure 8. (a) This seismic-reflection profile taken in northeastern British Columbia shows a decrease in thickness of the crust (depth to the top of the mantle, or Moho). (b) Interpretation of the data reveals that the flat layers between 0 and about 2 seconds are relatively young sedimentary rocks, which rest on Precambrian crystalline (granite and metamorphic) rocks (orange—right) and Precambrian sedimentary basin rocks (yellow—left). The Moho (Mohorovicic discontinuity), the transition from the crust to the mantle, lies at about 45 km on the southeast and about 35 km on the northwest. Inasmuch as some gem deposits may depend on variations in crustal thickness (e.g., some gem corundum deposits appear to be located in areas where the crust is 40 or more km thick; Levinson and Cook, 1994), mapping the thickness of the crust could prove valuable for reconnaissance. (For this figure, the approximate depth values have been calculated assuming an average seismic-wave velocity of 6 km/sec, rather than 5 km/sec as in figure 7, because of different characteristics of the rocks.) Figure is modified from Cook and Van der Velden (1993).

signal, which is a function of the frequencies (f) of the waves that are used, as well as on their velocities (V) through the rocks. The following equation summarizes the relationship between these parameters:

$$L = V / f$$

In general, the smaller the wavelength of the signal, the smaller the feature that can be detected and the higher the resolution of the measurement. In practice, it is possible to obtain seismic frequencies up to about 100 cycles per second in the shallow subsurface (first 20–50 m), where the seismic-wave velocity varies from about 6.0 km/sec in many crystalline (e.g., granite) rocks to about 2.0 km/sec in loose sedimentary rocks (e.g., gravels). Using f = 100 in the equation above, we find that L = 60 m (0.06 km) for granites and L = 20 m (0.02 km) for loose sedimentary rocks. The resolution of the method is determined by the lower limit of size of the feature that can be imaged. In seismic profiling, geophysicists have found that this limit is about one-fourth times the wavelength of the signal, or about 15 m for granitic rocks and about 5 m for loose sedimentary rocks. This means that we can, in principal, map features on the order of 5 m thick in some areas (e.g., alluvial deposits), which approaches the resolution necessary for effective gem exploration. For example, it might be possible to map the locations of large dikes (e.g., pegmatites) or the geometry of important geologic layers, such as a gem-bearing gravel. However, it would still be difficult to identify pockets or cavities smaller than 15 m in diameter.

We cannot change the speeds of the seismic waves in the rocks (which largely depend on the kinds of minerals the rocks contain), but we can vary the frequency of the source of seismic waves to improve the resolution. However, the Earth does not always cooperate, because it absorbs high-frequency signals very easily. (This is why the booming low frequencies of a stereo sound system can be heard for a long distance, while the higher- frequency signals are readily absorbed.) Additional technical problems make it difficult to use the seismic-

reflection technique for depths less than about 20 m. Nevertheless, as technical advances improve seismic-reflection profiling for applications to geologic problems in the shallow subsurface, it may become an important tool in gem exploration.

Cost. Another important consideration is that seismic-reflection profiling can be relatively expensive; exact costs depend on the parameters (e.g., the spacing of the receiver points) that are used in the field. Although acquiring high-resolution shallow data is usually less expensive than acquiring deep reflection data (because the area surveyed is smaller), survey costs of several thousand dollars per day are not unusual, and a proper survey usually takes one or more weeks. Thus, even if the technique is refined to the point where meter-scale resolution is possible in the uppermost few meters, the costs may be prohibitive for many gem-exploration applications. Fortunately, there is a less-costly alternative for some situations—georadar.

Georadar. *The Method. A*lso known as ground-penetrating radar, or GPR, georadar is finding a number of geologic applications in the shallow subsurface (Box C). Radar has been used for about 15 years to map thicknesses of ice sheets and glaciers. More recently, it has been applied in mapping underground pipes and building foundations, shallow archeological sites (Imai et al., 1987), the geometry of landfill sites (Lanz et al., 1994), the geometry of sediment deposits (Beres and Haeni, 1991; Smith and Jol, 1992; Beres et al., 1995), and fracture systems in some crystalline (metamorphic and igneous) rocks (Piccolo, 1992; Grasmueck, 1996). Based in part on work by Grasmueck (1995, 1996), and in part on results from the author's own experiments (figure 9), it is proposed here that, if carefully performed, radar may be applicable to gemstone exploration in many instances.

When most of us think of radar, we think of air traffic controllers or military personnel monitoring the positions of airplanes or missiles. However, if a radar (radio wave) signal is directed into the ground, it can penetrate some distance and then reflect off rock layers beneath the surface (again, see Box C). The distance that a radar signal penetrates depends on the absorptive properties of the rocks through which it is traveling. The property that most affects penetration is probably electrical conductivity, a measure of how easily an electrical signal travels through a material. The more electrically conductive a material is, the more it absorbs a radar signal. Metals, as well as clay-rich and saltwater-rich materials, are very electrically conductive; consequently, they prevent radar signals from being transmitted very far because they absorb much of the energy. Like ice, fresh water, and air, granite is largely transparent to radar signals; thus, the signals travel through it readily. This characteristic is key to the success (or failure) of the method. When a radar signal impinges on a boundary between nonconductive and conductive materials, some of the energy reflects back to the surface, where a receiver can measure it. Where there are large contrasts in electrical conductivity, large amounts of signal energy may be reflected.

As with a seismic section, the travel time to and from each reflector is measured and, if the wave velocity is known, the depth can be determined. Reflected signals received by instruments on the surface are recorded in the field and stored for later computer enhancement. Many of the computer-enhancement techniques that have been developed for seismic-reflection images are also applicable to radar images (Fisher et al., 1992; Grasmueck, 1996). The result, when recording a single profile or line, is a cross-section—much like a seismic-reflection section—that has a series of coherent signals, each of which corresponds to a reflection from a rock interface (or an abrupt change in rock properties) at depth.

There are, however, two major differences between seismic-reflection data and georadar data. First, the frequencies and velocities of radar signals are much higher than those of seismic data: Radar signals travel at the speed of light in air (300,000 km per second) and about one-third of that speed in granite (Davis and Annan, 1989). Second, radar signals respond to the electrical properties of the material, whereas seismic signals respond to the *elastic* properties of the material. (Elastic properties are measures of how easily a material deforms, such as when it vibrates.) Both of these characteristics of radar (higher frequencies and electromagnetic waves), prevent radar signals from penetrating very deeply into the rocks; in figure 9, for example, the radar section corresponds to only 60 m of rock, as compared to the 45 km depth for the seismic section of figure 8b. Even more importantly, radar signals in the shallow subsurface often have wavelengths of about one meter or less, providing a resolution to 0.25 m (25 cm), which is potentially useful for gem exploration.

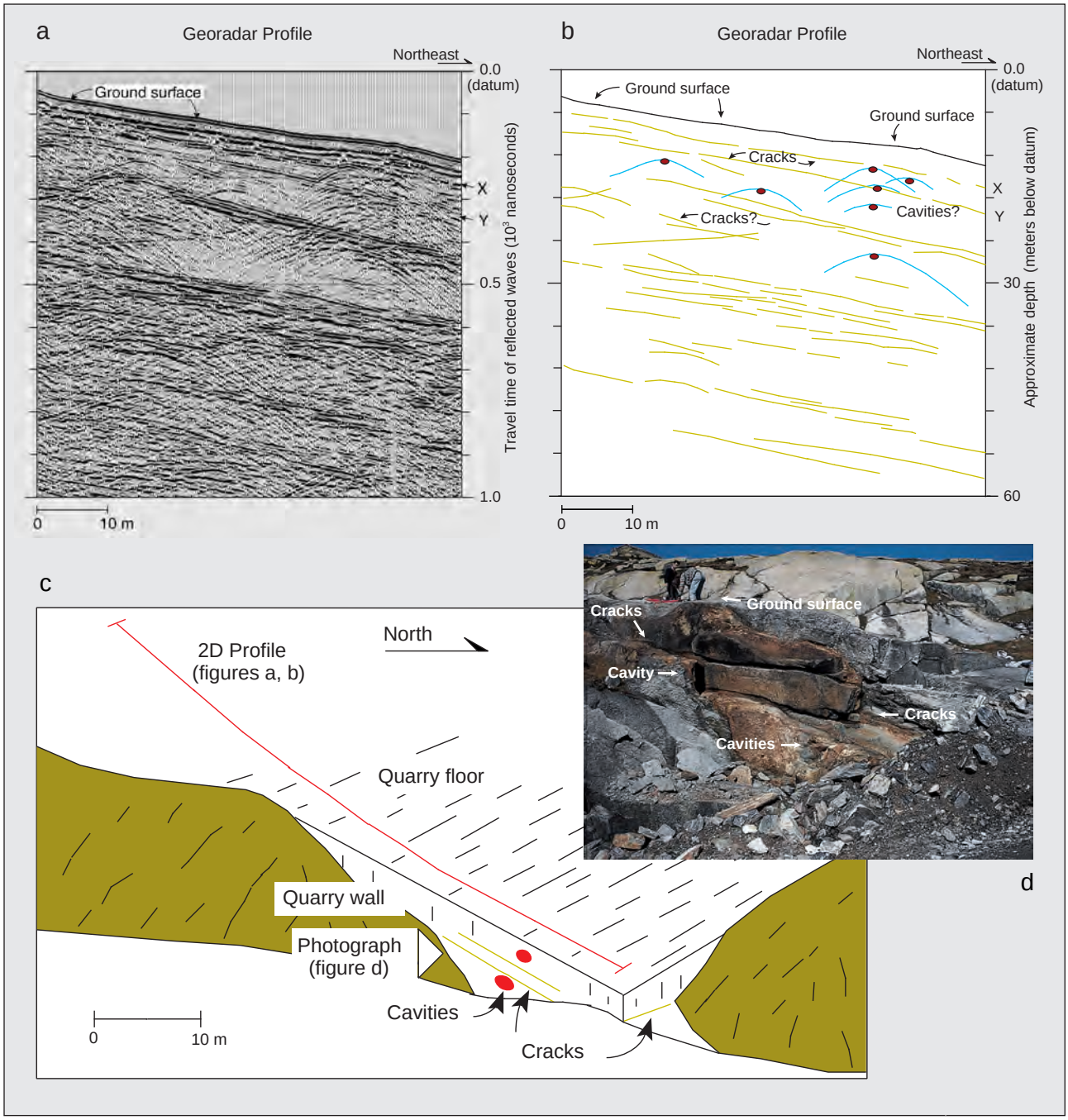

Figure 9. This georadar profile (a) was recorded by the author in a gneiss in southern Switzerland. Here, reflections are caused by differences in electrical properties, and the depth of penetration is about 50–60 m (compare with figures 7 and 8). Thus, the resolution is significantly more detailed than that for seismic profiling. Note that the datum (0.0 time line) is above the northeast-sloping ground surface. Interpretation of the data (b) reveals that prominent reflections at a depth (below the ground surface) of about 3 m (reflection X) and 6 m (reflection Y) on the right side of the section are probably cracks that are only a few centimeters thick (as interpreted on another dataset in the area by Grasmueck, 1995; see also [d] below). Red dots represent discontinuities, such as cavities or small faults, that give rise to the arcuate features (blue lines). The schematic diagram in (c) illustrates the relationship between the location of the georadar profile of (a) and (b) and the photograph of (d), an outcrop where a zone of mineralization (including cavities and small faults) is exposed. The outcrop is in a quarry wall immediately beneath the ground surface on the right side of the profile in (b).

Georadar in Three Dimensions. Most georadar recordings, as with most seismic-reflection recordings, are made along lines that result in a two-dimensional profile (horizontal distance in one direction and vertical depth, or distance through a feature, in the other; see Box C and figure 9). However, pockets or cavities that are small (e.g., one meter or less in diameter), but nevertheless productive, would be easy to miss unless profiles were recorded very close together. In such a situation, it might be desirable to acquire data in three dimensions (two horizontal and one vertical; figure 10), as described, for example, by Beres et al. (1995). Although three-dimensional data require somewhat more effort in both recording and data processing, the resulting information provides images of the internal structure of a volume of rock, rather than a single cross-sectional profile; features such as cavities or mineralized zones may be much more apparent and less likely to be missed. Preliminary results from an experiment conducted by the author and a colleague (J. Patterson) within a pegmatite have shown that it is possible to outline the three-dimensional geometry and size of a pocket.

Georadar is not very expensive relative to seismic profiling. A three-dimensional survey, with accompanying profile lines like the one shown in figure 10, requires about two to four person days of field time and perhaps two to four weeks of computer work. A similar three-dimensional seismic-reflection survey would have required 10 times as much effort.

Possible Uses of Georadar Profiling in Gemstone Exploration. Three characteristics of georadar make it a potentially useful method for gemstone exploration:

1. Radar provides very high resolution (to as small as 25 cm) images of the near-surface environment (in some cases, in the first few meters to tens of meters beneath the surface).
2. Georadar data are comparatively inexpensive to acquire and process.
3. Crystalline (granitic and metamorphic) rocks, in which many gem deposits typically occur, are relatively transparent to radar signals. However, the cavities or pockets that contain the gems (e.g., fluid-filled fractures, hydrothermal veins, clay-filled pockets in pegmatites, etc.) are likely to have electrical properties very different from the surrounding rocks. They could therefore produce very prominent reflected signals (figures 9a and b).

As noted earlier, most economic gemstone deposits presently are found at the surface or within a few meters to tens of meters of the surface. Examples include various alluvial deposits (where diamonds, rubies, sapphires, spinels, and many other gems are found), silica-rich sedimentary or volcanic rocks (such as some opal deposits in Australia and Mexico, respectively), pegmatite dikes (where quartz, beryl [figure 11], tourmaline, and a variety of rare gems are found), and lamprophyre (ultramafic) dikes (such as Yogo Gulch, Montana, where sapphires are found). Each of these deposit types may, if conditions are appropriate, be amenable to exploration using georadar or, in some cases, other geophysical tools.

For example, exploration for gemstones in sedimentary rocks, such as alluvial and some opal deposits, requires mapping of the subsurface geometry of the sedimentary layers. Georadar, and sometimes high-resolution seismic-reflection data, can be very effective tools for constructing such maps. The data illustrated in figure 10 were recorded to map the three-dimensional geometry of sedimentary layers near the surface (Beres et al., 1995). Detail is provided to 15 m depth. If one of the layers in such a survey (e.g. that labeled R2) were known to have high concentrations of gems (diamonds, corundum, spinels, etc.), it would be easy to follow that layer in the subsurface to predict its extent, its continuity, and thus the potential value of the deposit.

Exploration for primary deposits in granitic and metamorphic rocks is equally promising. Radar is already being used to locate high-quality (unfractured) ornamental rocks in quarries (Piccolo, 1992); thus, there may be applications for locating zones of high-quality jade or other massive gem materials. Highly fractured, lower-quality material would have measurably different properties from solid material.

Radar has been tested in some pegmatite deposits in California (Patterson, 1996), and at the Alma, Colorado, rhodochrosite deposits (Brian Lees, pers. comm., 1996) with limited success. In both areas, georadar has been useful for mapping subsurface structures. At the Colorado rhodochrosite deposits, for example, the technique has been successfully used to map faults associated with the deposit. However, it has been less successful in producing images of crystal-bearing pockets, probably because the pockets are very small (commonly less than 25 cm; Brian Lees, pers. comm., 1996).

BOX C: GEORADAR

Radio waves reflecting from contrasts in electrical conductivity can be detected by sensitive antennas. The georadar method is similar to seismic-reflection profiling in that a source of energy (radio waves in this case) is sent through a transmitting antenna (antenna T in figure C-1 and C-2) into the ground, and the returned signal is detected and collected at a receiving antenna (R in figure C-1 and C-2). The received signal is stored on a computer for later display and data processing. The simplicity and portability of georadar systems (figure C-3) allow the instruments to be used horizontally, such as into or through walls (e.g., figure C-2). Anomalous objects such as cavities (e.g., in a pegmatite) would appear as traces with unusual shapes or arrival times (figure C-2).

Figure C-1. This schematic diagram illustrates the georadar method for profiling along the Earth's surface. The transmitting antenna (T) sends a pulse into the ground, where it is reflected back to a receiving antenna (R). The signal is sent through cable to a computer, where it is stored on disk for later display and processing.

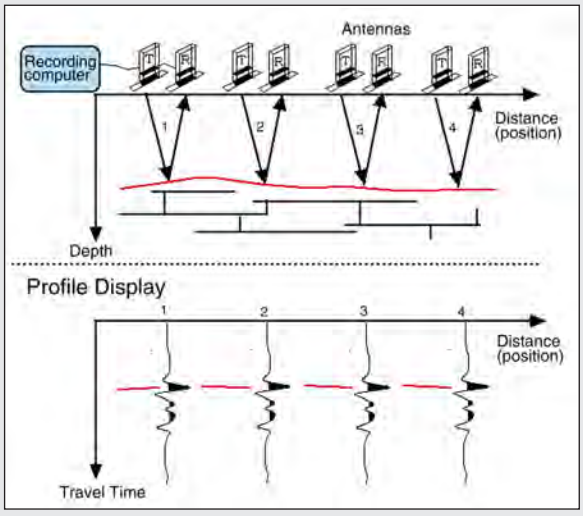

Figure C-2. This schematic diagram illustrates the georadar method for recording waves that are transmitted through an object (a wall) to detect anomalous zones such as cavities. Here the transmitting and receiving antennas are placed on opposite sides of the wall, and the anomalous zone appears in the data as an unusual waveform or arrival time.

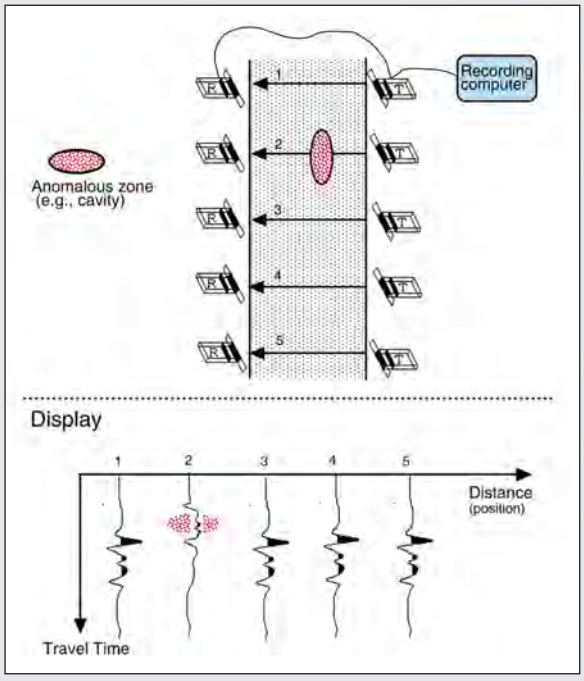

Figure C-3. The equipment required for georadar is very portable, and the procedure is not labor intensive. In this photo of a georadar field crew working in western Canada, the person in the foreground is setting the antennas, one for transmitting the radar pulse and the other for receiving the returned signal. The person in the background is carrying the instruments that control the signals and record them onto magnetic tape or disk. The wire along the ground connects the antennas to the recording instruments. Photo courtesy of D. G. Smith.

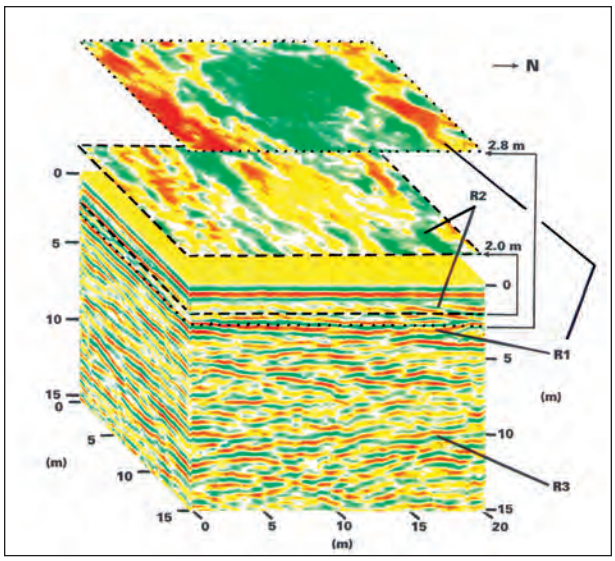

Figure 10. (top) These georadar data were acquired in northern Switzerland to map sedimentary (alluvial) structures in the near-surface (modified from Beres et al., 1995). R1, R2, and R3 are positions of reflected signals. Horizontal "slices" at 2.8 and 2.0 m are shown above the cube to illustrate how reflections R1 and R2 can be followed in three dimensions. If R2 were a gem-bearing gravel, it could be mapped easily over the region to determine both its lateral and vertical extent. R3 is another boundary at about 10 m depth. Knowledge of gem concentrations within this structure could thus be used to predict the total value of the deposit. The colors represent reflected waves from different layer boundaries. (Bottom) A two-person radar team works on sedimentary strata exposed in cross-section. The right-dipping layers are about the same size as layers R2 above, thus illustrating the kind of detail that may be possible with this georadar application. Photo courtesy of D. G. Smith.

Limitations of Georadar in Gem Exploration. Georadar is not a panacea for gemstone exploration at shallow depths. Some gem deposits in sedimentary rocks, such as some alluvials and some opal deposits, may have large quantities of clay near the surface. In such cases, the radar signal might not penetrate more than a few centimeters (Davis and Annan, 1989), and thus georadar would not be appropriate.

Pegmatite deposits in which the granitic rocks have weathered to produce a layer of surface clay are also problematic for radar, again because the clay absorbs much of the signal. This is commonly the case in southern California (Jeffrey Patterson, pers. comm., 1996). However, exposed pegmatites and deposits in relatively dry, sandy regions or in glacially scoured areas could be excellent environments for radar detection of underground cavities and fractures (figure 9). Hence, georadar may be an appropriate tool for the first 20–40 m depth if there is not a layer of clay or saline fluid near the surface. If the desired target is at a greater depth, or if the surface is not conducive to radar-signal penetration, other methods such as reflection seismology or magnetics (see table 1) may be appropriate. Therefore, surface and near-surface conditions must be investigated, usually with field observations or other tests, before deciding which technique(s) to use.

STRATEGIC APPLICATION OF GEOPHYSICS IN GEMSTONE EXPLORATION

Application of geophysical methods to gemstone exploration begins with establishing the nature of the target. In some cases, geophysical programs that address continental-scale measurements may be useful to identify regions appropriate for more intensive exploration. This approach is commonly used in exploring for diamonds, but it may also be applicable in exploring for gem corundum. Some gem corundum is found in alkali basalts that originated as magma below 50 km depth and picked up corundum from the lower crust (30–50 km) beneath continents as the magma traveled to the surface (Levinson and Cook, 1994). Thus, methods that allow the thickness of the crust to be mapped from place to place could be valuable. The seismic section of figure 8 is an example of a change in the thickness of the crust from about 40 km on the east to about 30 km on the west. Alkali basalts found east of this change would be more likely to contain corundum than those found west of it, if the theory

Figure 11. Georadar has great potential in pegmatite exploration, with the potential to locate gem pockets such as the one in which this superb aquamarine crystal (7.5 cm long) was found. Courtesy of Michael M. Scott; photo © Harold & Erica Van Pelt.

proposed by Levinson and Cook (1994) is correct; that is, that alkali basalt–hosted gem corundum originates in thick crust.

For other types of colored stone deposits, geologic mapping and serendipity will necessarily continue to play major roles. However, geophysics may be useful in delineating the extent of a newly discovered deposit, as well as in identifying specific targets (e.g., cavities) to investigate. In these cases, it is likely that high-resolution seismic reflection and, especially, georadar will soon become important exploration tools.

Following is a strategy to evaluate the potential usefulness of geophysical methods in a particular exploration venture:

1. Define the target (potential gem deposit, or regional structure) in terms of its:
   a. Size: If the target is the entire thickness and lateral extent of the lithosphere, and the desire is to establish likely regions for detailed work (e.g., diamond exploration), then only low-resolution techniques may be required.
   b. Depth: The greater the depth of a target is, the lower the resolution that can be provided by geophysical techniques.
   c. Geologic environment: Alluvial deposits may be imaged by techniques that provide stratigraphic information; primary deposits may require more direct images, such as of cavities.
   d. Physical properties: Knowledge of physical properties allows predictive models to be constructed. Such properties include seismic-wave velocity, density, magnetic characteristics, and electrical conductivity.
2. Acquire existing "test" data. "Regional" data sets (e.g., gravity, magnetics, occasionally seismic) often are available from government agencies. Such data can provide a considerable amount of background information, such as the thickness of the crust, the lithosphere, and so on.
3. Evaluate the costs versus the potential return.

Initial field testing is advised, particularly with high-resolution techniques such as radar. For example, it may be worthwhile to record a single radar profile to determine if near-surface clay layers are a problem. Such a test could also indicate whether a larger-scale survey, or even a three-dimensional survey, might be appropriate.

SUMMARY

Today, geophysical methods are sometimes used in diamond exploration, but they are not commonly applied for either exploration or exploitation of colored gemstone deposits. Part of the reason for this is historical: People searching for gems have not previously used these techniques and often are not familiar with them. Much of the reason, however, is technical: Geophysical methods simply have not had the resolution to be effective in either finding or delineating gem deposits, which are typically small. In addition, many geophysical techniques are expensive and require sophisticated equipment and technical expertise.

As technology progresses, however, the resolution of these techniques is being enhanced. Seismic-reflection data, for example, may now resolve features as small as a few meters; 10 years ago, it was difficult to resolve features of even 20 m. Georadar,

too, was in the early stages of development as an application to subsurface studies a decade ago. Since then, the methods for acquiring and processing such data have improved measurably. It is now possible to analyze georadar data in the field with small recording systems and computers; more than five years ago, the equipment was much more cumbersome, if it existed at all.

In the future, as resolution continues to improve, and as data collection and analysis become even easier, it is likely that these and other geophysical techniques will become valuable tools for gemstone exploration. Even today, georadar holds potential for locating gem-bearing structures in pegmatites, alluvial beds, and alkali basalts, among other types of occurrences.

REFERENCES

Atkinson W.J. (1989) Diamond exploration philosophy, practice, and promises: A review. In J. Ross, Ed., *Kimberlite and Related Rocks, Vol. 2, Proceedings of the Fourth International Kimberlite Conference*, Geologic Society of Australia Special Publication 14, Blackwell Scientific Publications, Oxford, England, pp. 1075–1107.

Beres M., Haeni F. (1991) Application of ground-penetrating radar methods in hydrogeologic studies. *Ground Water Research*, Vol. 29, pp. 375–386.

Beres M., Green A., Huggenberger P., Horstmeyer H. (1995) Mapping the architecture of glaciofluvial sediments with three-dimensional georadar. *Geology*, Vol. 23, No. 12, pp. 1087–1090.

Burley A.J., Greenwood P.G. (1972) Geophysical surveys over kimberlite pipes in Lesotho. *Institute of Geologic Sciences of London, Geophysical Division*, Reference 540 1069/72 (cited in Atkinson, 1989).

Cook F.A. (1995) Lithospheric processes and products in the southern Canadian Cordillera: A Lithoprobe perspective. *Canadian Journal of Earth Sciences*, Vol. 32, No. 10, pp. 1803–1824.

Cook F.A., Brown L.D., Oliver J.E. (1980) The southern Appalachians and the growth of continents. *Scientific American*, Vol. 234, No. 4, pp. 126–139.

Cook F.A., Van der Velden A.J. (1993) Proterozoic crustal transition beneath the Western Canada sedimentary basin. *Geology*, Vol. 21, No. 9, pp. 785–788.

Davis J.L., Annan A.P. (1989) Ground-penetrating radar for high-resolution mapping of soil and rock stratigraphy. *Geophysical Prospecting*, Vol. 37, No. 5, pp. 531–551.

Fisher E., McMechan G.A., Annan A.P. (1992) Acquisition and processing of wide-aperture ground-penetrating radar data. *Geophysics*, Vol. 57, No. 3, pp. 495–504.

Grand S.P. (1987) Tomographic inversion for shear velocity beneath the North American plate. *Journal of Geophysical Research*, Vol. 92, No. B13, pp. 14,065–14,090.

Grasmueck M. (1995). Development of a georadar system for three-dimensional imaging of the subsurface and its application to studies of crystalline rock bodies. Ph.D. dissertation, Swiss Federal Institute of Technology, Zurich, 104 pp.

Grasmueck M. (1996). 3D ground-penetrating radar applied to fracture imaging in gneiss. *Geophysics*, Vol. 61, pp. 1050–1064.

Gurney J.J., Levinson A.A., Smith H.S. (1991) Marine mining of diamonds off the west coast of southern Africa. *Gems & Gemology*, Vol. 27, No. 4, pp. 206–219.

Hoover D.B., Campbell D.L. (1994) Geophysical model of diamond pipes. In W. D. Heran, Ed., *Codicil to the Geophysical Expression of Selected Mineral Deposit Models*. United States Geologic Survey Open File Report 94–174, pp. 32–36.

Imai T., Sakayama T., Kanemori T. (1987) Use of ground-probing radar and resistivity surveys for archaeological investigations. *Geophysics*, Vol. 52, No. 1, pp. 137–150.

Janse A.J.A. (1994) Is Clifford's rule still valid? Affirmative examples from around the world. In H. O. A. Meyer and O. H. Leonardos, Eds., *Proceedings of the Fifth International Kimberlite Conference, Vol. 2, Diamonds: Characterization, Genesis and Exploration*, Companhia de Pesquisa de Recursos Minerais (CPRM), Rio de Janeiro, Brazil, pp. 215–235.

Lanz E., Jemmi L., Mueller R., Green A., Pugin A. (1994) Integrated studies of Swiss waste disposal sites from georadar and other geophysical surveys. In J. D. Redman, A. P. Annan, J. P. Greenhouse, T. Klym, and J. R. Rossiter, Eds., *Proceedings of the Fifth International Conference on Ground Penetrating Radar*, Waterloo Center for Groundwater Research, Kichener, Canada, pp. 1135–1150.

Levinson A.A., Gurney J.J., Kirkley M.B. (1992) Diamond sources and production: Past, present, and future. *Gems & Gemology*, Vol. 28, No. 4, pp. 234–254.

Levinson A.A., Cook F.A. (1994) Gem corundum in alkali basalt: Origin and occurrence. *Gems & Gemology*, Vol. 30, No. 4, pp. 253–262.

Lock N.P. (1985) Kimberlite exploration in the Kalahari region of southern Botswana with emphasis on the Jwaneng kimberlite province. In *Prospecting in Areas of Desert Terrain*, Institute of Mining and Metallurgy, London, pp. 183–190 (cited in Atkinson, 1989).

Patterson J.E. (1996) Modeling miarolitic cavities in a pegmatite dike using subsurface interface radar, Little Three mine, Ramona, California. In *The Spirit of Inquiry*, undergraduate research sponsored by the Honors Center, University of Arizona, p. 17.

Piccolo M. (1992) GPR applications for the definition of unconformities in a Carrara marble quarry (Massa Carrara—Italy). In P. Hanninen and S. Autio, Eds., *4th International Conference on Ground Penetrating Radar*, Geologic Survey of Finland, Special Paper 6, pp. 223–228.

Senior B.R., McColl D.H., Long B.E., Whitely R.J. (1977) The geology and magnetic characteristics of precious opal deposits, southwest Queensland. *BMR Journal of Australian Geology and Geophysics*, Vol. 2, pp. 241–251.

Smith D.G., Jol H.M. (1992) Ground-penetrating radar investigation of a Lake Bonneville delta, Provo level, Brigham City, Utah. *Geology*, Vol. 20, No. 12, pp. 1083–1086.

Smith R.S., Annan A.P., Lemieux J., Pederson R.N. (1996) Application of modified GEOTEM system to reconnaissance exploration for kimberlites in the Point Lake area, NWT, Canada. *Geophysics*, Vol. 61, No. 1, pp. 82–92.

Telford W.M., Geldart L.P., Sheriff R.E., Keys D.A. (1976) *Applied Geophysics*. Cambridge University Press, Cambridge, 860 pp.

RUBIES AND FANCY-COLOR SAPPHIRES FROM NEPAL

By Christopher P. Smith, Edward J. Gublein, Allen M. Bassett, and Mache N. Manandhar

Gem-quality rubies and fancy-color sapphires have been recovered from dolomite marble lenses located high in the Himalayan mountains of east-central Nepal (Ganesh Himal). First discovered in the early 1980s, these deposits have had only limited and sporadic production because of their isolated locations, high altitudes, and harsh seasonal weather conditions. The precise locations and geology of the two best-known deposits are described. In addition, 27 polished samples and 19 rough crystals and mineral specimens were thoroughly investigated to document their gemological characteristics and crystal morphology. The most distinctive internal features are their color-zoning characteristics, various cloud-like and other patterns, as well as a wide variety of mineral inclusions, some of which have not been seen in rubies from other sources.

ABOUT THE AUTHOR

Mr. Smith is a research gemologist residing in Lucerne, Switzerland. Dr. Gübelin is a gemologist and co-author of the Photoatlas of Inclusions in Gemstones *and various other books and publications. Dr. Bassett is retired professor of geology, California State University, San Diego, and technical director of Himalayan Gems Nepal; he resides much of the year in Katmandu, Nepal. Mr. Manandhar is general director of Himalayan Gems Nepal, Katmandu, Nepal.*

Gems & Gemology, *Vol. 33, No. 1, pp. 24–41*

Nepal is a small mountainous country situated along the Himalayan mountain chain in southern Asia.Landlocked by Tibet (China) to the north and India to the east, south, and west, Nepal's surface area covers only 140,000 km^2; it has approximately 20 million inhabitants. Southern Nepal is the birthplace, more than 2,500 years ago, of Siddartha Gautama, the founder of Buddhism. For many centuries, Nepal was closed off from the rest of the world. Only since it emerged from a feudal state in 1950, have the minerals and gemstones of Nepal begun to enter the world economy. Although Nepal has a reigning monarch, a multiparty democracy was established in 1990.

Most widely recognized for having the highest elevation of any country in the world, Nepal is the home of Mount Everest (8,848 m/29,028 feet above sea level). In all, seven of the eight highest peaks in the world can be found in this country's rugged terrain.

Although Nepal has limited industrial development and relatively meager mineral wealth, it is blessed with a broad range of gem minerals that includes tourmaline, beryl, garnet, quartz, spinel, danburite, hambergite, kyanite, apatite, sodalite, zircon, sphalerite, epidote, diopside, iolite, feldspar, pyrite, hematite, andalusite, lepidolite, and corundum (Bassett, 1979; 1984; 1985a and b; 1987). Gems have been recovered in Nepal since 1934, when tourmaline and aquamarine were first discovered there (Bassett, 1979). However, not until the early 1980s did rubies and sapphires begin to appear (figure 1).

As the story was told to authors AMB and MNM, goat-herders of the Tamang ethnic group first spotted red crystals in 1981, high in the Ganesh Himal massif of the Dhading District in east-central Nepal. These stones were brought to the capital city (Katmandu) to sell for shop displays, where they were identified as rubies. The first official report of corundum in Nepal was made by Baba (1982), who erroneously described

Figure 1. Since the early 1980s, rubies and fancy-color sapphires have been recovered in the Himalaya Mountains of east-central Nepal. The Nepalese rubies shown here range from 0.50 to 2.50 ct. Jewelry courtesy of the Gold Rush, Northridge, California; photo by Shane F. McClure.

ruby/corundum coming from the Taplejung District, in eastern Nepal. Soon after, however, it was determined that the source was actually in the Ganesh Himal (Dhading District), and many staked claims there, hoping to make their fortunes. For the most part, however, these earlier miners lacked any understanding of gemstone recovery methods or of the geology and challenging topography of the mountainous region, so these early efforts met with limited success. It was not until 1984 that one of the authors (AMB) made the first geologic study of the corundum-producing region at Ganesh Himal (Bassett, 1984). After concluding this investigation, AMB joined with MNM to found Himalayan Gems Nepal, which acquired the leases to the two most commercially viable claims, known as Chumar and Ruyil. Himalayan Gems Nepal began officially recognized mining activities during 1985. They also set up a cutting factory to bring these rubies and fancy-color sapphires to the gem and jewelry markets. Several other parties also mined unofficially in the surrounding region.

None of these mining ventures lasted long, however, because of the isolated locations, harsh weather conditions, and difficulties encountered in efforts to develop larger-scale mining. All of the claims were eventually abandoned by their owners. Today, local Tamang farmers continue rudimentary mining; they bring their production to Katmandu for sale and distribution. As a result, throughout the mid- to late 1980s and early 1990s, the production of gem-quality rubies and fancy-color sapphires was sporadic. Although Himalayan Gems Nepal also ceased active mining after about two years, they continue to buy gems from the local farmers and cut them in their factory.

Since mid-1996, two other deposits—Shelghar and Shongla—have produced corundum that is comparable in quantity and quality to Chumar and Ruyil. During studies in 1985, AMB determined that the geology of these two deposits is identical to that of Chumar. Besides these four producing deposits, two others (Pola and Sublay) are known to have potentially significant amounts of corundum,

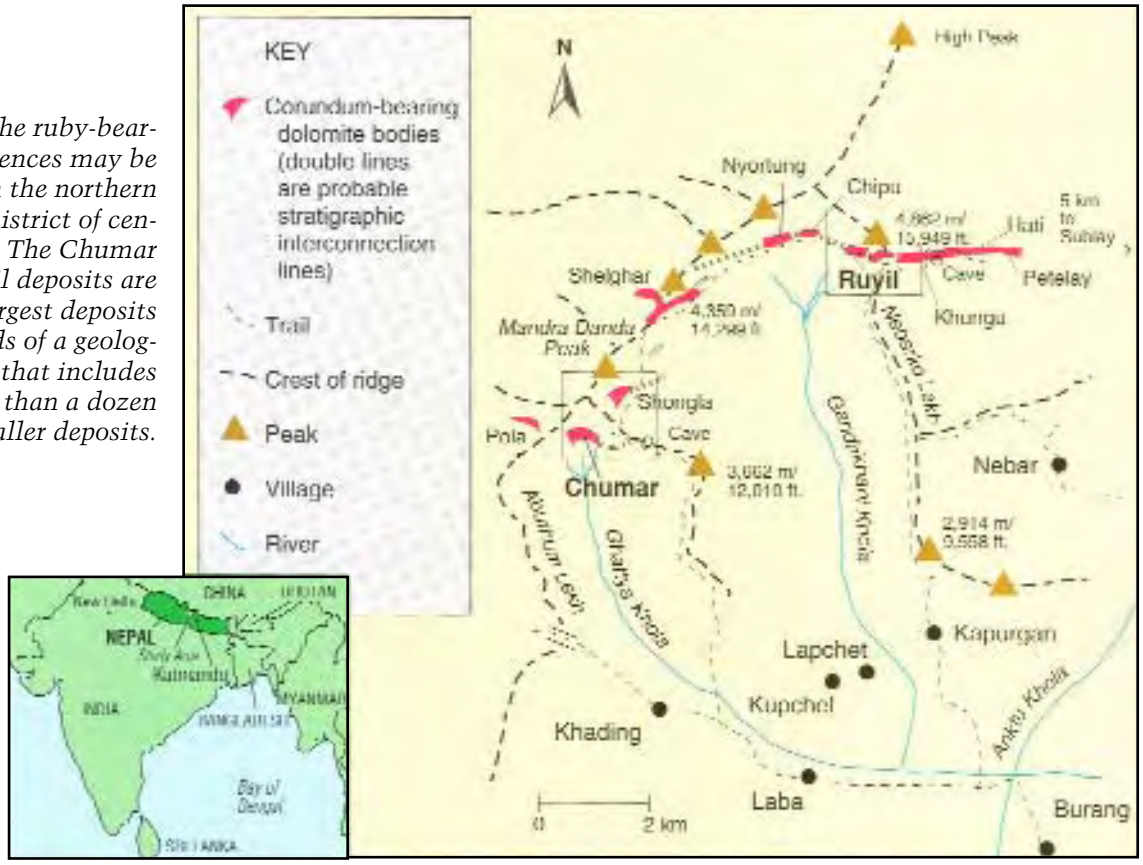

Figure 2. The ruby-bearing occurrences may be found in the northern Dhading District of central Nepal. The Chumar and Ruyil deposits are the two largest deposits and the ends of a geologic chain that includes more than a dozen smaller deposits.

but they have not yet been mined. However, Chumar and Ruyil remain the most recognized deposits of commercial-grade and finer quality rubies and pink sapphires in Nepal.

One of the authors (AMB) was told that blue sapphires are currently being recovered from the Taplejung District of eastern Nepal. The authors have examined a few non-gem-quality specimens, but there is no additional information on the amount or quality of the material being unearthed. The claim holder reports, however, that the sapphire crystals occur in outcrops on the slopes of the mountain known as Sapphire Hill, approximately 1.5 km northwest of the small village called Khupatal, north of the Tamur River in the Taplejung District. Contrary to Baba's 1982 report, our investigations yielded no evidence that rubies have ever been found in this district.

The first in-depth study of ruby from Nepal was provided by Harding and Scarratt (1986). Soon after, researchers in Germany also described fancy-color (pink and violet) sapphires from unspecified deposits in Nepal (Kiefert and Schmetzer, 1986, 1987). A detailed investigation of one very fine gem-quality ruby from Nepal was reported in 1988 (Bank et al., 1988). Robinson et al. (1992) were the first to mention a specific deposit, named Chumar, for the corundum occurrences. Overviews on gems from Nepal also described corundum deposits (e.g., Niedermayr et al., 1993). The most recent observations on the internal features of this material were provided by Henn and Milisenda (1994). The present study supports the findings of these previous researchers, and adds both new characteristics and specific source information to these earlier reports.

LOCATION AND ACCESS

The corundum deposits occur on the southwest flank of the Ganesh Himal (a high mountain massif consisting of several major peaks clustered together), 68 km north-northwest of the capital city of Katmandu, and 40 km west of Trisuli Bazar. An overview of the region reveals rice paddies in the lowlands, with primarily corn and barley crops in the hills. Above approximately 1,830 m (6,000 feet), one finds forests of rhododendron trees, then grass, and, eventually, bare rock. The landscape at the deposits is that of extremely steep, cliff-like domes of dolomitic marble about 150 m (500 feet) high lying in lenticular bodies that are surrounded by steep slopes of schist. There are deeply entrenched, rocky gorges, choked with dense vegetation that

reaches almost to the corundum deposits, which crop out in the dangerously craggy cliffs.

Travel to the deposits from Katmandu usually takes about six days. The trek begins with a circuitous bus ride from Katmandu to Trisuli Bazar, and then five days of rather strenuous hiking up the Ankhu River Valley and its tributaries. Travel to the deposits is hampered not only by the high elevations, remote locations, and rugged terrain, but also by the severe seasonal weather conditions. Winter snow usually covers the higher trails from mid-November to the end of April, and monsoons buffet the countryside from mid-June through September. Therefore, the best times to reach the deposits are usually from early May to mid-June and from early October to mid-November. A knowledgeable guide is essential.

Both the Chumar and Ruyil deposits lie within what was formerly known as the Laba Panchayat of the northern Dhading District, Bagmati Zone, in central Nepal (figure 2). The Chumar deposit lies at 28° 13' 20" N, 84° 58' 52" E, at an altitude of 3,800 m (12,500 feet); it is approximately 1.2 km south of the Mandra Danda mountain peak (elevation 4,358 m/14,300 feet), near the Tamang village of Burang. The Ruyil deposit lies about 6 km northeast of Chumar, at 28° 15' 05" N, 85° 02' 07" E, and an elevation of about 4,200 m (13,800 feet).

GEOLOGY AND OCCURRENCE

The geology of Nepal is dominated by the Himalayan Mountains, which formed as a result of the collision between the northward-drifting Indian plate and the Asian plate starting about 30 to 50 million years ago. The initial line of collision (called the Indus Suture Zone) is now in Tibet. The Indian plate continued in a northward drift, pushing beneath the Asian plate, whereupon the Indian plate broke into northern and southern segments, as the southern segment was forced beneath the northern segment. This major structural breakage is known as the Main Central Thrust (MCT) and extends east-west, the full length of Nepal (figure 3). At least twice subsequently, the continuing northward drift of the Indian plate caused a major breakage along progressively younger and more southerly thrusts, known as the Mahabharat Thrust and the Main Boundary Thrust (MBT). Each continental slice was pushed beneath the higher and more northerly slices of the Indian plate to form the imbricate (shingle-like) stack that is responsible for the elevation of the Himalayan Mountains. Each of these various continental slices has a different lithology and grade of metamorphism; yet they are all roughly the same geologic age (Precambrian and lower Paleozoic), with the highest grade above the MCT and lower grades below the MCT (there is no metamorphism below the MBT). This sequence is inverted from what is normally encountered, because of the subduction thrusts.

The Ganesh Himal corundum occurs near the top of the lower-grade metasediments of the Nawakot Series (again, see figure 3), below the MCT. The gems are found in what was a limestone formation (the Malekhu Limestone, lower Paleozoic) that has

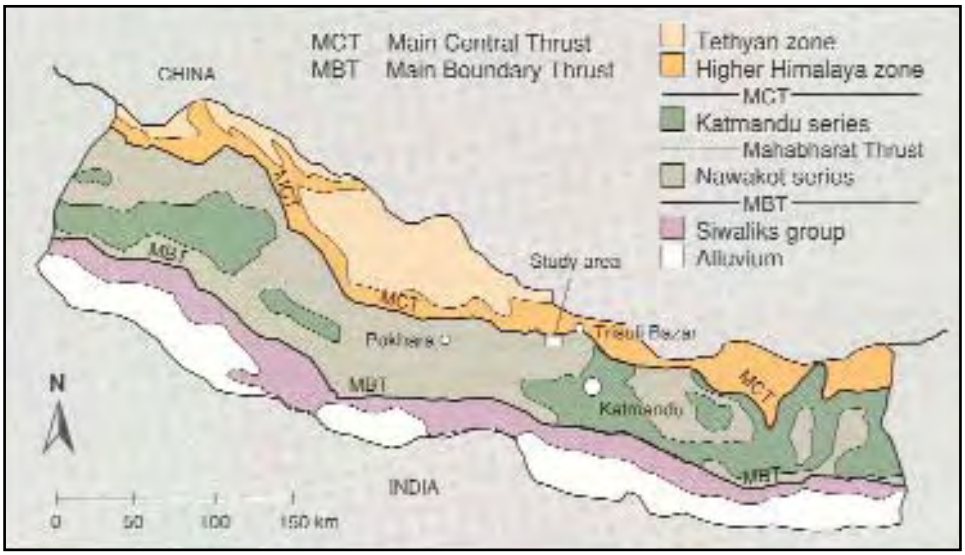

Figure 3. This simplified geotectonic map of Nepal indicates the main geologic structures (tectonic zones) and the main rock-forming series and groups in Nepal. The study area is near the top of the Nawakot series, below the MCT. Source: Mineral Resources Map of Nepal, United Nations publication, 1993.

Figure 4. The remote Chumar ruby deposits are visible along the steep slopes of the Himalayas, where the white marble outcrops overlook the valley below. Photo by Ted Daeschler.

been converted to a dolomite marble because of its proximity to the tectonic forces of the MCT. This once-continuous dolomite marble layer has been torn into a dozen isolated bodies, about 1 km from one another. These dolomite bodies occur as thickened beds and isolated pods 60–150 m thick and up to a kilometer long. The bodies are separated by black schist with quartzite interlayers.

Within these isolated dolomite pods are mineral seams that were originally aluminous clay interlayers in the limestone,- these have been converted, again due to the intense shearing pressures of the MCT, into a suite of metamorphic minerals that includes corundum. Each seam has a slightly different suite of minerals, depending on variations in the original composition of the clay interlayers. In one notable variation (the Ruyil deposit), abundant graphite has formed, presumably due to a local abundance of marine organic material in the original interlayer. The dolomite marble host rock is consistent throughout the dozen pods.

At the western end of these dozen dolomite bodies, which extend for 15 km, they are more distinctively pod-like lenses,- in the central section, the dolomite bodies are more like a thickened stratigraphic bed with parallel walls less than 100 m thick. The continuation eastward has not been explored in the very deep, densely forested chasms, but corundum is known to occur at the Sublay claim at the far eastern end. Of the dozen dolomite bodies, the westernmost four—Pola, Chumar, Shongla, and Shelghar—have produced corundum, only Ruyil in the central part, and only Sublay at the eastern end, are corundum bearing. Of these six corundum-bearing bodies, Chumar and Ruyil have been the most productive, with Shongla and Shelghar only recently developed and Pola and Sublay not yet consistently worked. This study focuses primarily on the Chumar and Ruyil deposits.

Chumar Deposit. First studied in 1984 by AMB, the Chumar deposit extends east-west for about 550 m, with a central thickness of approximately 150 m (figure 4). At the west end, the dolomitic body is bounded by a sharp fault trending N60°W, dipping steeply to the northeast. The east end of the body tapers down to a tail, with no fault line at the boundary. Distinct bedding in the dolomite body, which now consists of large eroded domes, strikes east-west throughout all but the extremities, where it is bent to the northwest, creating a sigmoid shape. The seams, which are about 8 m apart and dip 32°, vary widely in thickness but average about 20 cm; they are sometimes folded on a small scale.

Ruyil Deposit. The first studies of the Ruyil deposit were conducted in 1985 by AMB. This deposit extends east-west for approximately 128 m, with a general thickness of 60 m. The western portion of the dolomite body appears to end abruptly in a curved outline of shattered dolomite without distinct bedding; yet there is no discernible fault line. No corundum has been found in the continuous outcrops of bedded dolomite on the eastern side of this body.

ASSOCIATED MINERALS OF THE CORUNDUM DEPOSITS

Six specimens of corundum in host rock from the Chumar mine (ranging from 2.3 × 1.3 × 1.8 cm to 7.3 × 3.5 × 4.6 cm) were examined. We identified the seam material as primarily calcite and dolomite. Associated minerals include blue tabular blades of kyanite, small brownish orange euhedral crystals of rutile, different micas (stacked sheets of transparent green fuchsite, orange-brown phlogopite, and whitish margarite), and colorless apatite and scapolite, in addition to the violetish blue-to-red crystals of corundum (figure 5). One of the authors also identified brucite, tremolite, talc, pyrite, and sphalerite during his geologic studies at the Chumar mine (Bassett, 1985a). This list expands on the ones published previously; other researchers have additionally identified zoisite, epidote, muscovite, and anor-thite in mineral samples containing corundum from Nepal (Harding and Scarratt, 1986). Mineral specimens from this locality are often very colorful, with green fuchsite, orange phlogopite, blue kyanite, and red corundum, all occurring together in a white calcite matrix.

Rubies from the Ruyil deposit, unlike those from Chumar and the other deposits in Ganesh Himal, are embedded in abundant graphite with a less complete suite of associated minerals. In all other respects, though, they appear to be similar to the rubies from elsewhere in the district. Wel-formed gem-quality corundum crystals are more common from Ruyil than from Chumar.

MINING METHODS

The actual mining for gemstones is usually performed by local Tamang villagers using crowbars, picks, and shovels (figure 6), with occasional blasting. Blasting followed by hammering is used more commonly at the Chumar deposit than at Ruyil, and incline tunnels have been started at the latter deposit (Chakrabarti, 1994). All of the ruby and fancy-color sapphire deposits are primary (i.e., the stones are found in the host rock); no secondary deposits have been located to date. The miners usually excavate where the marble outcrops can be seen at the surface; the corundum itself is the prime indicator mineral for new deposits.

PRODUCTION, QUALITY, AND SIZES

It is very difficult to estimate how many tens of thousands of carats of corundum have been produced from these deposits over the past 15 years or so. Except for the brief period that Himalayan Gems Nepal officially controlled the mining efforts, most mining has been unofficial and uncontrolled, so no

Figure 5. The Nepalese corundum deposits have an interesting assemblage of mineral occurrences, including tabular stacks of green fuchsite, orange-brown phlogopite, and colorless to white margarite micas, as well as blades of blue kyanite and dipyramidal forms of corundum in shades of red or pink (some containing large blue color zones). The host rock is white calcite and dolomite. Photo by Dr. H. A. Hänni.

Figure 6. At the Chumar deposit, local farmers use basic hand tools to remove the corundum crystals from the host rock. Photo by Allen M. Bassett.

Figure 7. Many well-formed crystals have been recovered from the corundum deposits in east-central Nepal. While most crystals are small or medium (usually 5 ct or less) in size, some-such as this 106.42 ct crystal-exceed 100 ct. Photo by Shane F. McClure.

complete records are available. On the basis of our experience in Nepal and the material we have seen in Katmandu, we estimate that current yearly production is less than 1,000 kg. Most of the corundum crystals are small to medium in size (typically 5 ct or less). However, crystals over 100 ct are occasionally recovered (figure 7). The vast majority of the production is in the low-to-medium "commercial quality" range, which is best suited for polishing *en cabochon.* Only a small portion of the material is of fine to very fine "gem quality," which is appropriate for faceting (figure 8).

MATERIALS AND METHODS

All of the samples in this study were collected by two of the authors (MNM and AMB) in Nepal, from independent miners and the mines managed directly by Himalayan Gems Nepal. We originally selected a total of 29 polished gemstones (22faceted and seven cut *en cabochon*) that were fashioned from rough at the cutting factory of Himalayan Gems Nepal. Two faceted samples were subsequently removed from the study. We identified one as a flame-fusion synthetic ruby, and the second yielded properties and characteristics that were not totally consistent with the other samples. Thus, this article presents the results of testing 27 polished samples (0.21 to 9.47 ct), none of which had been heat treated. Seven of these were from the Chumar deposit and 11 were from Ruyil; the exact deposits for the remaining nine are not known. Also included in this study were 13 crystals and crystal fragments, ranging from 0.35 to 106.42 ct, and the six Chumar mineral specimens described earlier. This collection of gemstones and crystals represents the full range of colors—tone and saturation, as well as hue—observed in Nepalese corundums to date.

We used standard gemological instrumentation to record the refractive indices, birefringence, optic character, pleochroism, optical absorption spectra (desk-model spectroscope), and reaction to ultraviolet radiation (365 nm long-wave, 254 nm shortwave) on all fashioned samples. Specific gravity was determined by hydrostatic weighing with an electronic balance equipped with the appropriate attachments. A binocular microscope, incorporating fiber-optic and other lighting techniques, was used to document the internal features of all fashioned samples and single crystals. The results are given in table 1. We used a Perkin Elmer Lambda 9 spectrometer, with a beam condenser and polarizing filters, for polarized spectroscopy in the UV-visible

Figure 8. The Nepal deposits have produced some very high quality rubies, such as the fine 1.40 ct faceted ruby and 3.08 ct ruby crystal shown here. The crystal has a habit of c, r, n *and* z *crystal faces. Also note the narrow, blade-like form which is characteristic of much of the rough from these unique deposits. Photo by Shane F. McClure.*

TABLE 1. Gemological characteristics of the rubies and fancy-color sapphires from Nepal.

Propererties	No. samples	Observations
Color	27 polished	Ranging from red to pink to purplish pink, often with visible violetish blue color banding
Clarity	27 polished 13 crystals	Very clean to heavily included, most in the range slightly to heavily included
Refractive	20 faceted	n_e = 1.760-1.762
Index		n_o = 1.769-1.770
	7 cabochon	n = 1.76-1.77 (spot method)
Birefringence	20	0.008-0.009
Optic	20	uniaxial negative
character		
Specific gravity	27 polished	3.94-4.01
	13 crystals	
Pleochroism	27	Moderate to strong dichroism
		Red zones: yellowish orange to orangy red parallel to the c-axis, and reddish purple to purple-red, or purplish pink to purple-pink, perpendicular to the c-axis *Violetish blue zones:* greenish blue to blue parallel to the c-axis, and violetish blue to violet-blue per pendicular to the c-axis.
UV luminescence	27	*Red to pink zones.* Long-wave (365 nm): Moderate to very strong red Short-wave (254 nm): Faint to moderate red
		Violetish blue zones: Generally inert
Optical absorption spectrum (nm)	27	General absorption up to approximately 450 nm, 468 (sharp, narrow), 475 nm (sharp, weak to moderate), 476 nm (sharp, narrow), 525-585 nm (broad band), 659 nm (faint, nar row), 668 nm (faint, narrow), 675 nm (very faint, narrow; when present), 692 nm (sharp, narrow), 694 nm (sharp, narrow)
Internal features	27	Short rutile needles, various cloud patterns, stringer formations, strong color zoning, weak to prominent growth structures, laminate twinning and parting, "fingerprints," negative crystals and crystalline inclusions of (with elements identified and mode of identification in parentheses): margarite mica (Al, Si, Ca; SEM-EDS and XRD)[a] apatite (Ca, P; SEM-EDS, XRD and Raman)[a] rutile (Ti; SEM-EDS) diaspore (XRD, Raman, and FTIR)[a] dolomite (Raman) phlogopite mica (K, Mg, Al, Si, Fe; SEM-EDS and XRD)[a] calcite (Ca, C; SEM-EDS and FTIR) uvite tourmaline (XRD) anorthite feldspar (Raman) boehmite (FTIR)

[a]*Often containing black inclusions that presumably are graphite.*

through near-infrared region (between 280 and 880 nm) on 17 fashioned samples. For the region between 400 and 6000 wavenumbers (cm^{-1}), we used a Pye-Unicam Fourier-transform infrared (FTIR) 9624 spectrometer with a diffuse reflectance unit for sample measurement. We performed a total of 49 analyses on different regions, color zones, and orientations of 27 samples. Energy-dispersive X-ray fluorescence (EDXRF) chemical analyses were performed on 25 samples (and on different color zones on some samples, for a total of 34 analyses) on a Spectrace TN5000 system, using a program specially developed by Prof. W. B. Stern for the semi-quantitative analysis of corundum. Prof. Stern's program uses chemically pure element standards and three spectra focusing on the light, medium, and heavy elements, so that the results can be interpreted to three decimal places (i.e., 0.001). He also used a beam condenser to measure small areas or zones of an individual stone.

To analyze the internal growth structures of the polished stones, we used a horizontal microscope, a specially designed stone holder, and a mini-goniometer attached to one of the oculars on the microscope, employing the methods described by Schmetzer (1986a and b), Kiefert and Schmetzer (1991), and Smith (1996). We analyzed more than 45 inclusions using a scanning electron microscope with an energy-dispersive X-ray spectrometer (SEM-EDS), X-ray diffraction analysis, and a Raman micro-spectrometer. Some of the inclusions were identified by a single method and others by a combination of techniques (see table 1).

GEMOLOGICAL CHARACTERISTICS OF THE RUBIES AND FANCY-COLOR SAPPHIRES FROM NEPAL

The data revealed no significant differences from one sample to the next-including those samples identified as originating from Chumar and Ruyil—

in terms of standard gemological properties, crystal morphology, inclusion patterns, UV-Vis-NIR spectra, or chemical composition. Therefore, the complete data collected on all of the samples—those with specific deposit designations, as well as those without—will be presented as a single group.

Crystal Morphology. The rough crystals were predominantly euhedral, with little or no evidence of chemical dissolution on their surfaces. Two main crystal forms dominate the morphology of the corundum found in Nepal (figure 9). The first are dipyramidal crystal habits composed of larger, dominant hexagonal dipyramid z (2241) faces and smaller, subordinate basal pinacoid c (0001) and positive rhombohedron r (1011) faces. The second is a modification of this basic habit, where there is an addition of subordinate hexagonal dipyramid n (2243) faces. Rarely, crystal forms consisting of dominant hexagonal dipyramid **?** (14 14 28 3) faces, with subordinate c (0001), *r* (1011), and occasionally n (2243) faces, were also encountered.

Many of the crystals had a blade-like appearance when viewed parallel to the c-axis (again, see figure 8). Groups of intergrown crystals were also frequently encountered.

Figure 9. Two crystal habits were most typical in the rabies and fancy-color sapphires from Nepal. (A) The primary crystal form was dominated by dipyramid z (2241) crystal faces, with more subordinate basal pinacoid c (0001) and positive rhombohedron r (1011) crystal faces also present. (B) This primary crystal form was frequently modified by subordinate to intermediate dipyramid n (2243) crystal faces.

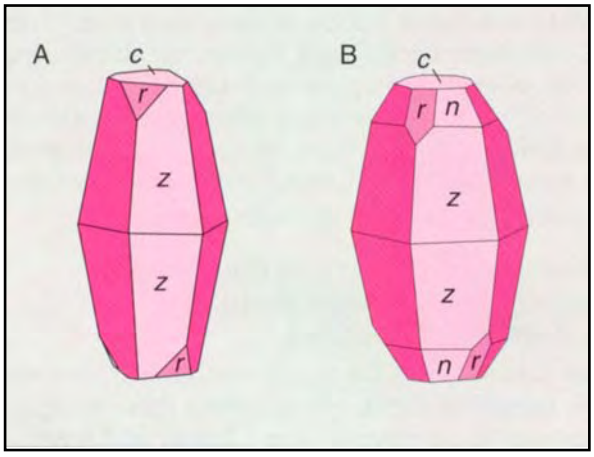

Visual Appearance. Face up, most of the polished samples ranged from a "pure" red or pink to a purplish pink. Both the rough and polished samples commonly had strong, eye-visible color zoning (see Growth Characteristics below). A few could even be better described as bicolored (red and very dark violetish blue) corundum; some had additional colorless or pink zones (figure 10). The diaphaneity of the crystals and polished samples ranged from transparent to translucent, depending on the nature and number of inclusions present, as well as on the color saturation and tone of the violetish blue zones.

Refractive Indices, Birefringence, Optic Character, and Specific Gravity. These standard gemological properties were found to be consistent with corundum in general (see, e.g., Webster, 1983; Liddicoat, 1989; Hughes, 1990; Hurlbut and Kammerling, 1991) and, more specifically, with the rubies and fancy-color sapphires from Nepal described by past researchers (Harding and Scarratt, 1986; Kiefert and Schmetzer, 1986, 1987; Henn and Milisenda, 1994; see table 1).

Reaction to Ultraviolet Radiation. The various color zones of the sample corundums had different reactions to UV radiation. The red to pink zones fluoresced red to both long-wave (moderate to very strong intensity) and short-wave (faint to moderate intensity) UV. The dark violetish blue zones were generally inert to both long- and short-wave UV radiation.

Pleochroism. All samples exhibited moderate to strong dichroism when viewed perpendicular to the c-axis with a dichroscope. Within the red-to-pink color zones, we observed yellowish orange to orangy red or pink parallel to the c-axis and reddish purple to purple-red or purplish pink to purple-pink (i.e., for rubies or pink sapphires, respectively) perpendicular to the c-axis. In the dark violetish blue color zones, we noted greenish blue to blue parallel to the c-axis and violetish blue to violet-blue perpendicular to the c-axis.

Growth Characteristics. Internal Growth Structures. Weak-to-prominent growth structures were seen in essentially all the polished gemstones examined. Most common were straight and angular sequences of the dipyramid *z* planes (figure 11). Less common were sequences of the dipyramids *n* or **?**, as well as the basal pinacoid *c* and the positive rhombohedron *r*.

Observation of the gem perpendicular to the c-axis often enabled us to trace the progression of crystal-habit formation (figure 12).

Color Zoning. Chemical fluctuations in the growth environment produced obvious color zoning in most of the samples examined. Oscillations between consecutive periods of crystal growth, as well as a preferential crystallographic orientation of the color-causing mechanisms Cr^{3+} (ruby) or Fe^{2+} ? Ti^{4+} (blue sapphire), are responsible for the inhomo-geneity of color observed in the samples (also refer to UV-Vis-NIR Spectroscopy). When the color was not homogeneous, red-to-pink and near-colorless zones were typically noted parallel to the dipyramid *z* planes, whereas the dark violetish blue zones were concentrated along the dipyramid *z, n,* or **?** planes, in addition to the positive rhombohedron *r* (again, see figure 12).

The most distinctive color-zoning characteristics were related to the dark violetish blue zones. The dark appearance of these zones is attributed to the presence of red (i.e., chromium) and blue (i.e., iron and titanium) chromophores in the same growth phases. These color zones could be very narrow or very thick; the latter were observed only parallel to the dipyramid z planes (see figures 11 and 13). They also appeared as distinct "wedges" cutting into the gemstone or even dominating it to the point of a bicolor (again, see figure 13). In these zones, we also observed a texture that might best be described as wispy or smoke-like. In some samples, an irregular color concentration had an undulating nature that resulted from near-colorless areas, or halos, surrounding very small, black-appearing mineral grains of presumably rutile (figure 14). In the case of rutile (TiO2) inclusions, Ti would be absorbed from the host corundum, thereby depleting an essential component of the Fe2+ ?Ti4+ charge-transfer necessary for the blue coloration..

Twinning. We saw twinning parallel to the positive rhombohedron r (1011) in several of the stones. Typically, we noted only one direction of laminated twinning, parallel to a single series of r (1011) planes; occasionally, however, there were as many as three twinning systems, parallel to additional positive rhombohedral planes. Parting parallel to r (1011) was also prominent in a few samples (figure 15).

Inclusions. A rich diversity of inclusions were noted in the sample rubies and fancy-color sapphire.

Figure 10. A wide range of gem-quality rubies and fancy-color sapphires have been recovered from Nepal. Distinctly bicolored—red or pink and violetish blue—stones illustrate some of the unusual zoning in this material. The non-heat-treated Nepalese rubies and sapphires shown here range from 0.87 to 3.86 ct. Photo by Shane F. McClure.

Figure 11. Weak to prominent internal growth structures were frequently observed in the sample rubies and sapphires. This 4.81 ct ruby reveals moderate zonal structures parallel to two series of dipyramid z (2241) planes, along with distinct blue color banding. Immersion, magnified 8 ×.

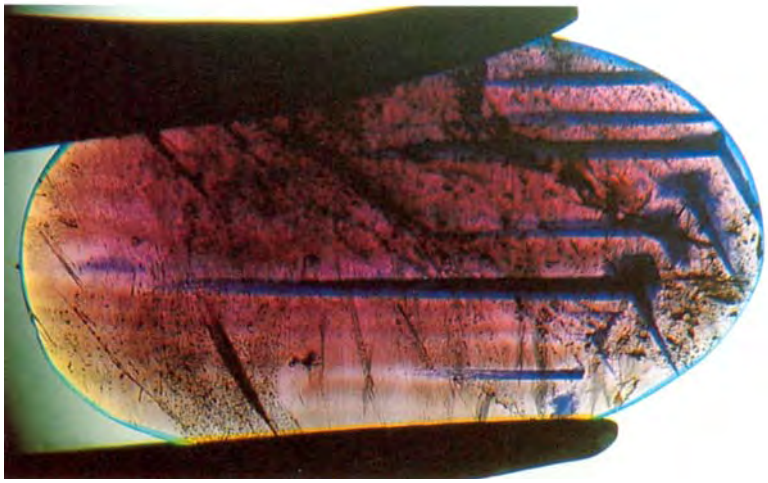

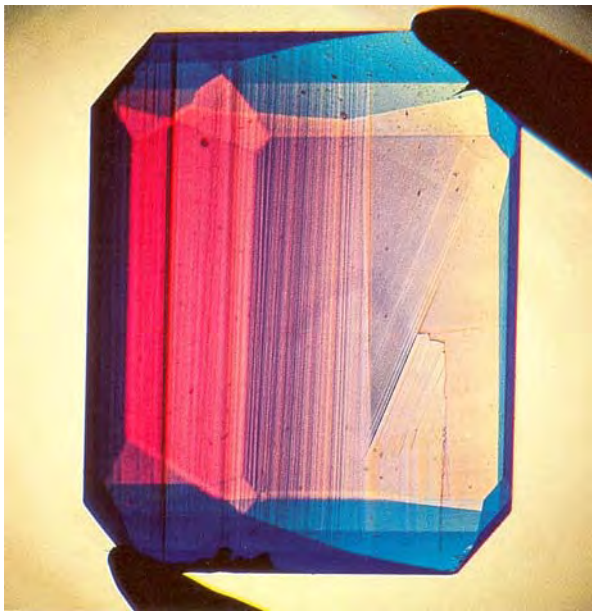

Figure 12. When viewed perpendicular to the c-axis, several samples revealed a great deal about the sequence of crystallographic growth. This Nepalese ruby shows a crystal habit composed of the basal pinacoid c (the faint horizontal growth planes), the dipyramid n (the angled growth planes), and the dipyramid z (the vertical growth planes). Immersion, magnified 12×.

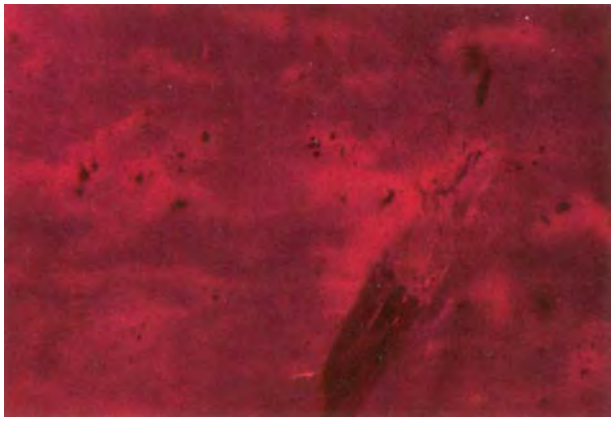

Figure 14. Some Nepalese rubies revealed irregular blue color zones that had paler patches or halos. At 66× magnification, it can be seen that these halos actually surround small mineral grains of what are presumed to be rutile. Darkfield illumination; photomicrograph by Edward f. Gübelin.

Most commonly, clouds of very fine, short rutile needles, present throughout, gave some of the gemstones a slightly "hazy" appearance to the unaided eye (figure 16). Bright orange-to-black crystals of rutile were observed singly or in small irregular clusters (figure 17); these displayed a metallic luster when they were polished at the surface. Other stringer-type inclusion patterns consisted of nearly parallel, slightly diverging "sprays," extending essentially perpendicular to growth planes or in an antenna-like pattern (figure 18).

Apatite took on a variety of forms, including euhedral hexagonal columns (figure 19, left) and slightly curved rods (figure 19, right). Although not commonly noted in apatite, basal cleavage was

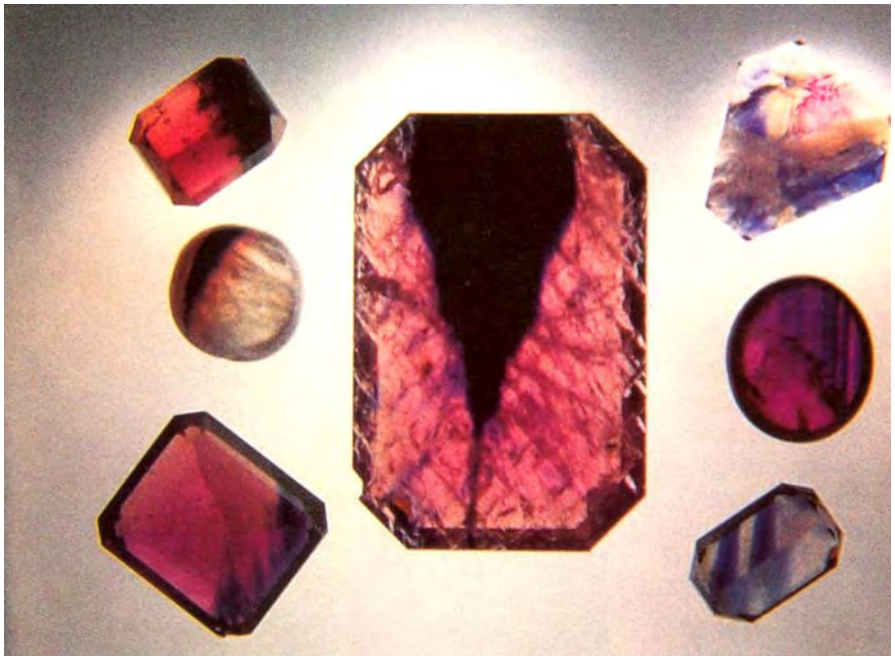

Figure 13. Distinct color zoning was present in most of the sample rubies and sapphires from Nepal. Colorless, red/pink, and dark violetish blue zones filled large sections of the stones, traversed them in bands, or appeared as large wedge-like forms. Such color-zoning characteristics gave many of the gemstones a bicolored appearance.

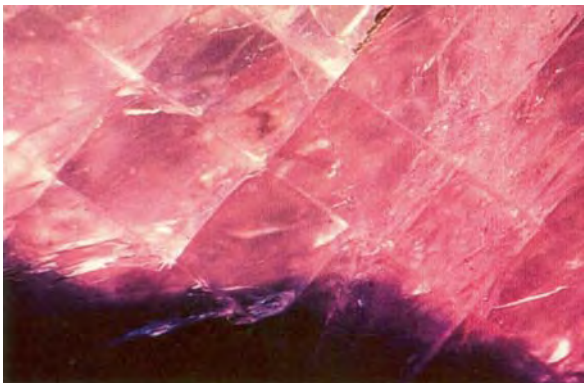

Figure 15. Parting planes parallel to one, two, or three series of positive rhombohedron r (1011) crystal faces, were seen in a few samples. In this stone, the parting planes-which form a checkerboard pattern-were lined with the aluminum oxy-hydroxide boehmite, AIO(OH). Fiber-optic illumination, magnified 20×.

Figure 16. Clouds of very fine, short rutile needles were present in nearly all of the rubies and fancy-color sapphires from Nepal. However, none of these stones revealed the nest-like concentrations that are typical of rubies from Mogok. Fiber-optic illumination, magnified 22×.

observed in several of the apatites we identified, especially in the rod-shaped forms. The calcium-rich mica margarite was often present in irregular masses within which additional inclusions were noted, such as individual crystals of apatite or rutile, or masses of graphite, sometimes forming one complex mineral assemblage (figure 20). Light brown crystals of phlogopite mica occurred in small, mostly irregular, rounded forms (figure 21). Transparent colorless crystals of calcite and dolomite were seen infrequently (most of the transparent colorless crystals in these stones proved to be apatite or margarite). Although rare, black uvite tourmaline (figure 22) and transparent colorless anorthite feldspar (figure 23) were identified. Also unusual was the "halo" of minute rutile needles surrounding an unidentified small black mineral grain (figure 24).

We observed a wide range of fingerprint-like inclusions, all involved in various stages of the "healing" process. Two-phase (liquid and gas) inclusions were common. "Intersection tubules" at the junction of two or three twin planes were frequently penetrated by alteration products such as boehmite. Boehmite was also identified lining the parting planes. Irregular "veins" of AlO(OH)—mostly boehmite, but also diaspore—were also noted traversing several of the polished gemstones. In reflected light, the reduced luster of the AlO(OH) "vein," as compared to the higher luster of the host corundum, could be mistaken for the glass-like

Figure 17. Clusters of small rutile crystals were also common in the rubies from Nepal. Typically, they were bright orange to black and displayed a metallic luster where polished at the surface. Fiber-optic illumination, magnified 50×.

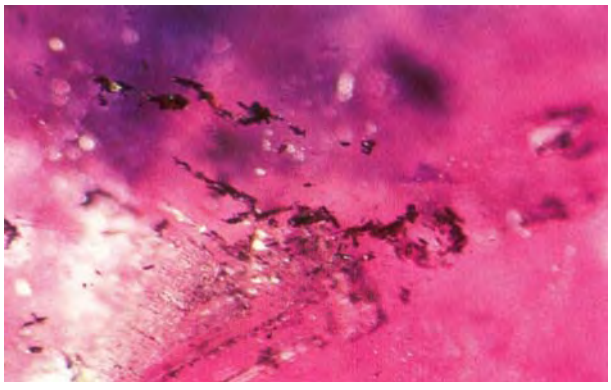

Figure 18. Antenna-hke stringer formations were frequently seen in the Nepalese samples. Although such inclusions have been noted in rubies from Luc Yen (Vietnam) and Mong Hsu (Myanmar), they tended to be more densely concentrated in the Nepalese samples. Fiber-optic illumination, magnified 32×.

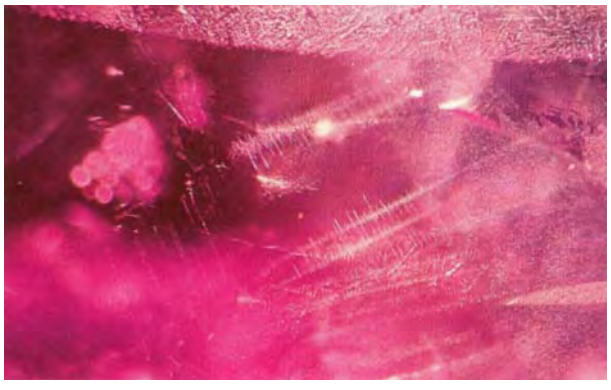

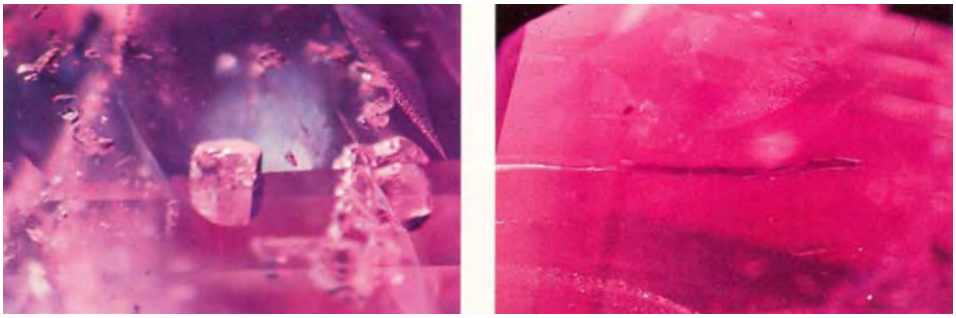

Figure 19. Common in the Nepalese samples, apatite took on several forms, including euhedral, hexagonal columns (left, magnified 50 ×) and slightly curved "rods" (right, 32×). In most cases, these inclusions displayed basal cleavage, a property infrequently seen in apatite. Fiber-optic illumination.

fillings observed in some heat-treated rubies, but careful examination will establish that the gem has not been heated.

Absorption Spectra. All spectra were dominated by Cr^{3}+ absorption features, with the bands being weaker in the lighter red (i.e., pinkish) stones and more intense in the deeper red stones. Occasionally a secondary absorption influence was seen as a result of the Fe^{2}+ ? Ti^{4}+ intervalence charge transfer responsible for the blue color component in the dark violetish blue zones. These results are consistent with those reported earlier by Kiefert and Schmetzer(1986, 1987).

Desk-Model Spectroscope. In the visible range, a general absorption to approximately 450 nm was apparent, along with weak to distinct lines at 468 nm and at 475 and 476 nm (a doublet). The width of a moderate-to-distinct absorption band from approximately 525 to 585 nm was related to the chromium content of the gemstone. We also noted faint lines at 659 and 668 nm, plus two strong lines at 692 and 694 nm, which appear as a bright emission line at 693 nm.

UV-Vis-NIR Spectroscopy. The general shape of the spectral curve also varied considerably depending on the chromium content of the zones measured. The two broad bands at about 405 and 550 nm, as well as the weak to distinct sharp peaks recorded at 468, 475, 476, 659, 668, 692 and 694, are all ascribed to Cr^{3}+. A faint absorption peak observed at 675 nm in some stones has also been recorded in rubies from other sources (e.g., Mong Hsu, Myanmar, and certain deposits in east Africa), but the cause is still unclear (Peretti et al., 1995).

Infrared Spectroscopy. In addition to the dominant absorption characteristics of corundum, between 300 and 1000 cm^{-1} (peak positions at about 760, 642, 602, and 450 cm^{-1}; Wefers and Bell, 1972), the rubies

Figure 20. Complex inclusion assemblages presented some intriguing identification challenges. In this Nepalese ruby, a large mass of the calcium-rich mica margarite (M) played host to other mineral inclusions of its own. The larger, granular-appearing mass proved to be a graphite and margarite combination (G/M), while several of the brighter spots were identified as apatite (A) and rutile (R). SEM photo courtesy of SUVA, Lucerne, Switzerland.

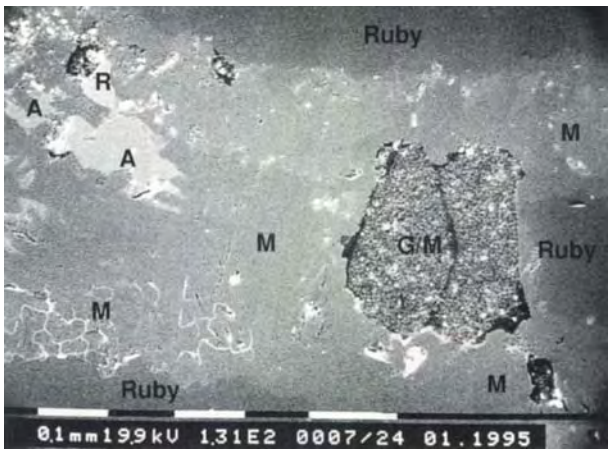

Figure 21. Predominantly small, rounded light brown crystals of phlogopite mica also were seen frequently in the Nepalese rubies. Fiber-optic illumination, magnified 45×.

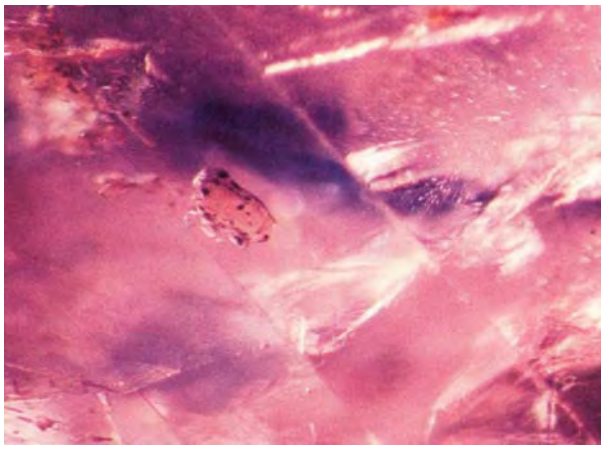

Figure 22. A series of unusual granular masses were identified as uvite tourmaline, which has not been documented as an inclusion in rubies from any other source. It thus provides a useful indication of Nepalese origin. Fiber-optic illumination, magnified 35×.

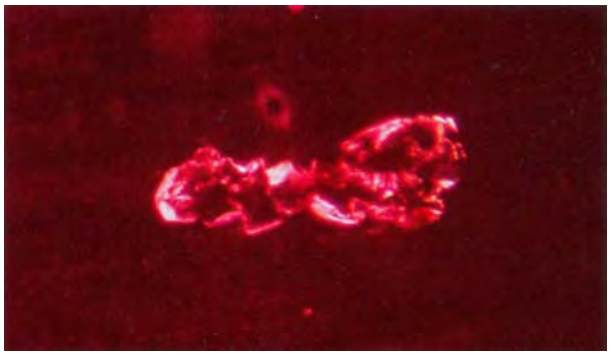

Figure 23. Raman micro-spectroscopy identified this mineral aggregate in a Nepalese ruby as anorthite feldspar. This is the first report of this mineral in ruby from any source. Photomicrograph by Edward J. Gübelin; darkfield illumination, magnified 66×.

and sapphires in this study revealed two dominant bands at about 3320 cm^{-1} and 3085 cnr^{-1}, with an additional pair of weaker bands at 2100 and 1980 cm"1 (figure 25). These absorption bands are related to OH stretching frequencies and identify the presence of boehmite (Farmer, 1974; Wefers and Misra, 1987). Although different color zones did not reveal any statistical differences in the presence or absence of boehmite, different areas and orientations of the same stone did show variations in the absolute and relative intensities of the absorption bands, as well as a slight shift in the position of the absorption maximum. To a much lesser degree, diaspore was also indicated in the infrared spectra of some samples, with bands at approximately 1990, 2040, 2885, and 3025 cm^{-1} (Farmer, 1974; Wefers and Misra, 1987; Smith, 1995).

The presence of AlO(OH)—boehmite and diaspore—was generally traced to locations along parting planes or irregular seams. Not all samples showed AlO(OH)-related absorption bands, while several displayed such strong AlO(OH) absorption features that a distinction between boehmite and diaspore was not possible. Absorption bands associated with mica and calcite were also occasionally recorded.

Chemical Analysis. The most significant variations were recorded in Cr concentration, which again correlated to the depth of red-to-pink color in the area measured. Titanium (Ti) and iron (Fe) were the next most significant trace elements recorded, followed by measurable amounts of vanadium (V) and gallium (Ga), as shown in table 2.

One interesting observation related to the trace-element concentrations of areas that were "pure" red as opposed to ones that were "pure" dark violetish blue. In every instance, the concentrations in absolute and relative values showed no consistent variation between Cr, Fe, or Ti within the two color zones.

DISCUSSION

Corundum from Nepal has received sporadic mention in the gemological literature over the past decade or so (see, e.g., Harding and Scarratt, 1986; Kiefert and Schmetzer, 1986 and 1987; Bank et al., 1988; Niedermayr et al., 1993). The results of this current investigation support and expand on the findings of such earlier researchers and, for the first time, provide detailed locality information. We identified three inclusions in the rubies from Nepal that had not been described before—uvite tourmaline, anorthite feldspar, and diaspore—as well as several distinctive inclusion and color-zoning patterns. However, we did not observe the three-phase inclusions described by Kiefert and Schmetzer (1986, 1987) in any of our samples. Also, we did not encounter the identification difficulties experienced by Bank et al. (1988); that is, all of our samples were easily identified as natural corundum.

In general, the rubies and fancy-color sapphires from Nepal are similar to corundum from other marble-type sources found around the world, including Myanmar (Burma), Vietnam, Afghanistan, Pakistan, and Tanzania. The most distinctive features of these Nepalese corundums are their inclusions.

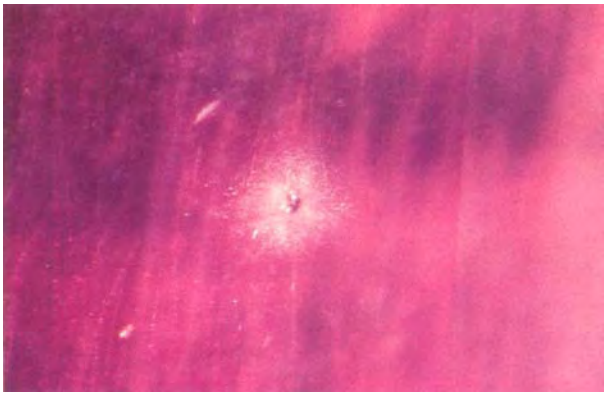

Figure 24. Still another feature that has not been noted in rubies from other sources was present in many of the rubies and fancy-color sapphires from Nepal: small black mineral grains surrounded by halos of very fine, minute rutile needles. Fiber-optic illumination, magnified 50×.

The dense concentrations of very fine, short rutile needles are unlike the long, highly iridescent rutile needles observed in most rubies from marble-type deposits. Dense "nests" of short rutile needles, so typical of rubies from the historic Mogok stone tract in upper Myanmar, were not seen in our Nepalese study samples. The various stringer patterns we saw in these Nepalese stones have also been seen in rubies from other deposits, including Mong Hsu in Myanmar (Smith and Surdez, 1994; Peretti et al., 1995) and Vietnam (Kane et al., 1991; Smith, 1996). However, the Nepalese stones appeared to have much denser concentrations of such patterns.

Apatite crystals of various forms may be seen in rubies from many sources, including Mogok (e.g., Gübelin and Koivula, 1986), Vietnam (Kane et al., 1991), and various deposits in East Africa. However, the rod-shaped apatites observed in the samples from Nepal have not been described in rubies or fancy-color sapphires from any other source. Kane et al. (1991) described similar transparent colorless rod-shaped minerals in rubies from Vietnam, but these were identified as calcite. A common mineral inclusion in rubies from marble-type deposits, calcite was encountered only rarely in the rubies from Nepal.

Mica is common in corundum from other deposits (e.g., Myanmar, Sri Lanka, and Tanzania), but the sheer number of inclusions of the variety margarite in our test samples is unlike anything we have seen in rubies from other sources. Anorthite feldspar and uvite tourmaline, which were observed in a few of our sample rubies and fancy-color sapphires, have not been identified in rubies from any other locality. Therefore, they may also be instrumental in establishing Nepalese origin. Nor have the authors seen inclusion patterns such as the small black mineral surrounded by a spherical "halo" of minute rutile needles in rubies from other sources. On the other hand, inclusions such as pyrrhotite, zircon, pyrite, and spinel have not been identified to date in rubies from Nepal; these are frequently seen in rubies from East Africa, Vietnam, and Myanmar, as well as other sources.

In their natural (not heat-treated) state, these rubies, pink sapphires, and bicolored sapphires should not be difficult to distinguish from rubies, including those with blue color zones, from other sources. No heat-treatment studies were conducted on these samples. However, when such stones are heat treated, the inclusion features and color zoning will be greatly altered, making it more difficult to identify corundum from Nepal (see, e.g., Peretti et al., 1995). Although it is usually difficult to detect a gemstone's source by the inclusion features, observation of any of the above-described mineral inclusions will clearly separate a natural ruby or fancy-color sapphire from a synthetic counterpart produced by any of the known manufacturing processes.

The linear and angular sequences of non-color-zoned growth structures in our samples—following the crystal planes *z, n,* ?, *r,* and *c*—did not reveal any unique or diagnostic features or patterns. Similar sequences of growth structures have been observed by one of the authors (CPS) in natural rubies from other sources (e.g., Vietnam or East Africa). However, they can be useful in separating

TABLE 2. Semi-quantitative EDXRF chemical analyses of major-to-trace elements in the rubies and fancy-color sapphires from Nepal.

Oxide	Wt.%
Al_2O_3	98.9-99.8
Cr_2O_3	0.013-0.383
TiO_2	0.016-0.224
Fe_2O_3	0.004-0.069
V_2O_5	0.004-0.034
Ga_2O_3	0.010-0.023

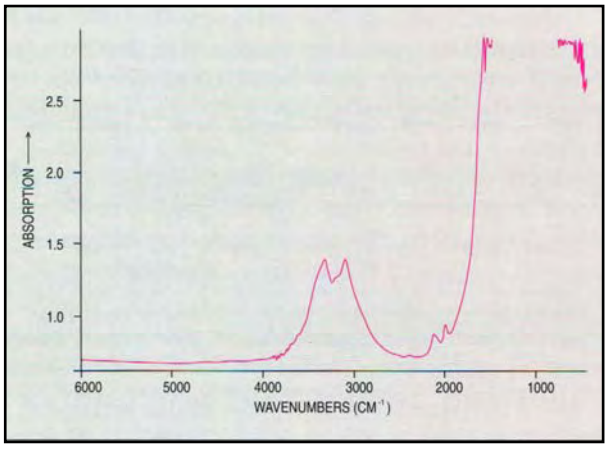

Figure 25. The non-heat-treated rubies and fancy-color sapphires from Nepal revealed additional absorption features in the infrared region of the spectrum. Distinct absorption bands at 3320 and 3085 cm^{-1}, and weaker peaks at 2100 and 1980 cm^{-1}, indicated the presence of boehmite, which was seen concentrated along veins or lining parting planes. Such absorption characteristics are helpful not only in identifying foreign mineral phases that may be present, but also for indicating that the gem has not been heat treated.

natural from synthetic rubies (Schmetzer, 1986a and b; Kiefert and Schmetzer, 1991; Smith, 1996). Kiefert and Schmetzer (1986, 1987) also identified growth planes consisting of the second-order hexagonal prism a (1120) and hexagonal dipyramid *v* (4481). Bank et al. (1988) described an unusual sequence with these two growth planes that also was not encountered during our study. This unusual sequence appears to relate directly to the blade-like forms of some rough crystals. Our samples did not reveal any "swirled" growth structures, such as those seen in rubies from Mogok (e.g., Gübelin and Koivula, 1986) or Vietnam (Kane et al., 1991). Nor did they have centralized "cores," such as those present in rubies from Mong Hsu (Smith and Surdez, 1994; Peretti et al., 1995).

Blue color zones and color banding have been noted in rubies from several sources, including Afghanistan (Bowersox, 1985; Bowersox and Chamberlin, 1995), Myanmar (Mong Hsu: Smith and Surdez, 1994; Kammerling et al., 1994; Smith, 1995; Peretti et al., 1995), Vietnam (Kane et al., 1991), as well as Sri Lanka and Tanzania (Tunduru), by one of the authors (CPS). However, the blue color zones and banding in Nepal rubies have some distinctive characteristics. These include the successions of straight and angular, thin-to-thick bands parallel to the dipyramid *z* (2241) planes; the large red and dark violetish blue zones (i.e., bicolored stones); the "wedge-shaped" color zones,- and the wispy to smoke-like textures observed in the color bands and "halos" of nonblue zoning surrounding mineral inclusions.

Chemically, these rubies and fancy-color sapphires are also similar to their counterparts from other marble-type sources (Tang et al., 1988; Hughes, 1990). Nevertheless, their chemistry will provide a ready means of separating them from high-iron natural rubies from sources such as Thailand (Tang et al., 1988), Cambodia (Jobbins and Berrange, 1981), Madagascar (Smith, 1996), and certain deposits in East Africa (see, e.g., Hänni and Schmetzer, 1991). In addition, the collection of chemical data is also valuable in separating natural from synthetic corundum (e.g., Stern and Hänni, 1982; Muhlmeister and Devouard, 1991).

Infrared spectroscopy may provide additional proof that the gemstone was not heat treated, when AlO(OH) is present, as well as a very good indication of whether it is natural or synthetic (Volynets et al., 1972; Beran, 1991; Smith, 1995, pp. 326–328). One of the authors (CPS) has observed that rubies from other natural sources, such as certain deposits in Vietnam or East Africa, sometimes also reveal dominant absorption features relating to boehmite, as well as other minerals.

No consistent variations were noted in the samples from Chumar as compared to those from Ruyil, with respect to their standard gemological properties, UV-Vis-NIR and FTIR spectral characteristics, crystal morphology, chemical make-up, or the inclusions identified. One inclusion feature, however, that may indicate that a ruby came from the Ruyil mine is the presence of graphite (in association with certain mineral inclusions), which appears to be much more prevalent in the corundum from this deposit.

It is interesting to note that "trapiche" corundum, with six "arms" extending from a central core, has been found at the Ruyil deposit (figure 26). Trapiche-like rubies and pink sapphires have been reported from Vietnam and Mong Hsu (Müllenmeister, 1995; Schmetzer et al., 1996). However, the arms in the Nepalese samples are very different in composition—predominantly phlogopite, apatite, calcite, and graphite—from that identified in samples from other sources.

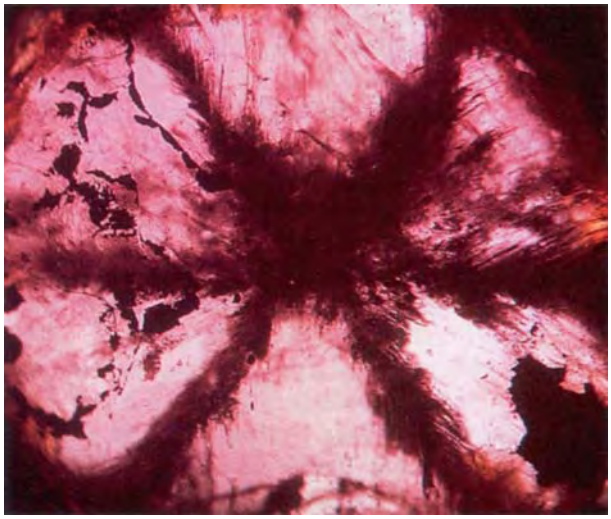

Figure 26. Reminiscent of trapiche emeralds, a very small number of rubies from the Ruyil deposit display a series of rays that intersect at the center of the crystal, along the three-fold axis and parallel to the prism crystal faces. Each ray consists of a linear concentration primarily of phlogopite, apatite, calcite, and graphite. Such unusual forms of "trapiche" corundum have also been recovered from Vietnam and Myanmar. Photo by Eva Strauss-Paillard.

CONCLUSION

In recent years, a number of ruby and sapphire deposits have been discovered in a wide variety of sources around the world. While Nepal is neither the newest nor most significant corundum source in the trade today, it offers an interesting array of ruby and fancy-color sapphires for jewelers, gemologists, and consumers alike. These gems from the Ganesh Himal appear to be concentrated along a single geologic "belt" within the northern Dhading District of east-central Nepal, and in two mines in particular, Chumar and Ruyil. Since they were first discovered in the early 1980s, these gemstones have been entering the world markets. The isolated locations, high altitudes, harsh seasonal weather conditions, and other difficulties have contributed to the sporadic mining activities and the relatively small amounts of gem material produced to date. However, research by two of the authors (MNM and AMB) indicates that larger reserves of these rubies and fancy-color sapphires are yet to be discovered. Modernized mining equipment and methods (including tunneling or "benching" techniques) will be necessary for these deposits to reach their full potential.

Although similar in general to rubies and fancy-color sapphires from other marble-type deposits, the Nepal corundums may be distinguished on the basis of the entire collection of the gem's individual properties and characteristics. Certain features that may prove helpful in the identification include dense concentrations of very fine, short rutile needles throughout the stone; rod-shaped forms of apatite; masses of transparent colorless margarite,-opaque black masses of uvite tourmaline; transparent colorless anorthite feldspar; and small black mineral grains surrounded by "halos" of minute rutile needles. Nepal may also be indicated for a particular ruby if any of the transparent mineral inclusions are associated with black masses of graphite. Nepal rubies and fancy-color sapphires may also have distinctive color-zoning characteristics, such as large red and dark violetish blue portions in a single stone (i.e., bicolor), or dark violetish blue zones in thick bands or wedge shapes. Especially distinctive is the presence of a wispy or smoke-like texture or near-colorless "halos" surrounding a mineral inclusion.

Such an ensemble of internal features also will help separate a Nepalese corundum from a synthetic corundum of any of the various production techniques. As a reminder, even in the remotest regions of the world, one should never take for granted that a gemstone is natural, as the synthetic ruby crystal fragment purchased in Nepal by one of the authors (MNM) illustrates.

Nepal's mineral wealth—consisting of tourmaline, beryl, garnet, quartz, spinel, danburite, kyanite, apatite, sodalite, zircon, sphalerite, epidote, diopside, iolite, and andalusite, among others—is already recognized widely in the trade. Now rubies, pink sapphires, and bicolored corundum can also be added to the list.

Acknowledgments: The authors are grateful to Dr. L. Kiefert and Dr. H. A. Hänni of the Swiss Gemmological Institute (SSEF), Basel, Switzerland, for performing Raman spectral analyses; to Dr. H.-D. Von Schulz of SUVA, Lucerne, Switzerland, for performing scanning electron microscopic analyses; to Professor S. Graeser of the Institute of Mineralogy and Petrography, University of Basel, for X-ray diffraction analyses; and to Prof. W. B. Stern of the Institute of Mineralogy and Petrography, University of Basel, Switzerland and Ms. N. Surdez of the Gübelin Gemmological Laboratory, Lucerne, for providing the semi-quantitative chemical analyses. Unless otherwise noted, photomicrographs are by Christopher P. Smith.

REFERENCES

Baba T. (1982) A gemstone trip to Nepal. *Gemmological Review,* Vol. 4, No. 12, pp. 2–5.

Bank H.; Gübelin E., Harding H.H., Henn U., Scarratt K., Schmctzer K. (1988) An unusual ruby from Nepal. *Journal of Gemmology,* Vol. 21, No. 4, pp. 222–226.

Bassett A.M. (1979) Hunting for gemstones in the Himalayas of Nepal. *Lapidary Journal,* Vol. 33, No. 7, pp. 1492–1520.

Bassett A.M. (1984) Rubies in the Himalayas of Nepal. Report submitted to the Nepal Department of Mines and Geology, Katmandu, 19 pp.

Bassett A.M. (1985a) Application for mining license. Submitted to the Nepal Department of Mines and Geology, Katmandu, 14 pp. Bassett A.M. (1985b) The tourmalines of Nepal. *Mineralogical Record,* Vol. 16, No. 5, pp. 413–418.

Bassett A.M. (1987) Nepal gem tourmalines. *Journal of Nepal Geological Society,* Vol. 4, No. 1–2, pp. 31–41.

Beran A. (1991) Trace hydrogen in Verneuil-grown corundum and its colour varieties-an IR spectroscopic study. *European Journal of Mineralogy,* Vol. 3, pp. 971–975.

Bowersox G.W. (1985) A status report on gemstones from Afghanistan. *Gems & Gemology,* Vol. 21, No. 4, pp. 192–204.

Bowersox G.W., Chamberlin B.E. (1995) *Gemstones of Afghanistan.* Geoscience Press, Tucson, AZ.

Chakrabarti C.K. (1994) A preliminary report on the Ganesh Himal ruby occurrences. Submitted to the Nepal Department of Mines and Geology, Katmandu, 8 pp.

Farmer V.C. (1974) The infrared spectra of minerals. *Mineralogical Society Monograph 4,* Mineralogical Society, London.

Gübelin E.J., Koivula J.I. (1986) *Photoatlas of Inclusions in Gemstones.* ABC Edition, Zurich, Switzerland.

Hänni H.A., Schmetzer K. (1991) New rubies from the Morogoro area, Tanzania. *Gems & Gemology,* Vol. 27, No. 3, pp. 156–167.

Harding R.R., Scarratt K. (1986) A description of ruby from Nepal. *Journal of Gemmology,* Vol. 20, No. 1, pp. 3–10.

Henn U., Milisenda C.C. (1994) A microscopical study of Nepalese ruby and sapphire. *Journal of the Gemmological Association of Hong Kong,* Vol. 17, pp. 82–84.

Hughes R.W. (1990) *Corundum,* 1st ed. Butterworths Gem Books, Butterworth-Heinemann, London.

Hurlbut C.S., Kammerling R.C. (1991) Gemology, 2nd ed. Wiley Interscience, New York.

Jobbins E.A., Berrangé J.P. (1981) The Pailin ruby and sapphire gemfield, Cambodia. *Journal of Gemmology,* Vol. 17, No. 8, pp. 555–567.

Kammerling R.C, Scarratt K., Bosshart G., Jobbins E.A., Kane R.E., Gübelin E.J., Levinson A.A. (1994) Myanmar and its gems-An update. *Journal of Gemmology,* Vol. 24, No. 1, pp. 3–40.

Kane R.E., McClure S.F., Kammerling R.C, Khoa N.D., Mora C, Repetto S., Khai N.D., Koivula J.I. (1991) Rubies and fancy sapphires from Vietnam. *Gems & Gemology,* Vol. 27, No. 3, pp. 136-155.

Kiefert L., Schmetzer K. (1986) Rosafarbene und violette Sapphire aus Nepal. *Zeitschrift der Deutschen Gemmologischen Gesellschaft,* Vol. 35, pp. 113–125.

Kiefert L., Schmetzer K. (1987) Pink and violet sapphires from Nepal. *Australian Gemmologist,* Vol. 16, No. 6, pp. 225–230.

Kiefert L., Schmetzer K. (1991) The microscopic determination of structural properties for the characterization of optical uniaxial natural and synthetic gemstones, part 1: General considerations and description of the methods. *Journal of Gemmology,* Vol. 22, No. 6, pp. 344–354.

Liddicoat R.T. (1989) *Handbook of Gem Identification,* 12th ed. Gemological Institute of America, Santa Monica, CA.

Muhlmeister S., Dcvouard B. (1991) Determining the natural or synthetic origin of rubies using energy-dispersive X-ray fluorescence (EDXRF). In A.S. Keller, Ed., *Proceedings of the International Gemological Symposium,* Gemological Institute of America, Santa Monica, CA, pp. 139–140.

Müllenmeister H.J. (1995) Ein Trapiche-Rubin aus Myanmar (Burma). Lapis, Vol. 12, No. 95, pp. 50.

Niedermayr G., Brandstätter P., Hammer V.M.F. (1993) Edelund Schmucksteinvorkommen in Nepal. *Zeitschrift der Deutschen Gemmologischen Gesellschaft,* Vol. 42, No. 2–3, pp. 69–89.

Peretti A., Schmetzer K., Bernhardt H.J., Mouawad F. (1995) Rubies from Mong Hsu. *Gems & Gemology,* Vol. 31, No. 1, pp. 2–26.

Robinson G.W., King V.T., Asselbom E., Cureton F., Tschernich R., Sielecki R. (1992) What's new in minerals? *Mineralogical Record,* Vol. 23, No. 5, pp. 423–437.

Schmetzer K. (1986a) An improved sample holder and its use in the distinction of natural and synthetic ruby as well as natural and synthetic amethyst. *Journal of Gemmology,* Vol. 20, No. 1, pp. 20–33.

Schmetzer K. (1986b) *Natürliche und synthetische Rubine–Eigenschaften und Bestimmung.* Schweizerbart, Stuttgart, Germany.

Schmetzer K., Hänni H.A., Bernhardt H-J., Schwartz D. (1996) Trapiche rubies. *Gems & Gemology,* Vol. 32, No. 4, pp. 242–250.

Smith C.P., Surdez N. (1994) The Mong Hsu ruby: A new type of Burmese ruby. *JewelSiam,* Vol. 4, No. 6, pp. 82–98.

Smith C.P. (1995) Contribution to the nature of the infrared spectrum for Mong Hsu rubies. *Journal of Gemmology,* Vol. 24, No. 5, pp. 321–335.

Smith C.P. (1996) Introduction to analyzing internal growth structures: Identification of the negative d plane in natural ruby. *Gems & Gemology,* Vol. 32, No. 3, pp. 170–184.

Stern W.B., Hänni H.A. (1982) Energy dispersive X-ray spectrometry: a non-destructive tool in gemmology. *Journal of Gemmology,* Vol. 18, No. 4, pp. 285–296.

Tang S.M., Tang S.H., Tay H.S., Retty A.T. (1988) Analysis of Burmese and Thai rubies by PIXE. *Applied Spectroscopy,* Vol. 42, No. 1, pp. 44–18.

Volynets F.K., Sidrova E.A., Stsepuro N.A. (1972) OH-groups in corundum crystals which were grown with the Verneuil technique. *Journal of Applied Spectroscopy,* Vol. 17, pp. 1088–1091.

Webster R. (1983) *Gems: Their Sources, Descriptions and Identification,* 4th ed. Butterworths, London.

Wefers K., Bell G.M. (1972) *Oxides and Hydroxides of Alumina, Alcoa Research Laboratories Technical Paper No. 19.* Alcoa Research Laboratories, St. Louis, MO.

Wefers K., Misra C. (1987) *Oxides and Hydroxides of Alumina, Alcoa Research Laboratories Technical Paper No. 19,* Revised. Alcoa Research Laboratories, St. Louis, MO.

GEMOLOGICAL PROPERTIES OF NEAR-COLORLESS SYNTHETIC DIAMONDS

By James E. Shigley, Thomas M. Moses, Ilene Reinitz, Shane Elen, Shane F. McClure, and Emmanuel Fritsch

Examination of 51 colorless to near-colorless synthetic diamonds from all known sources of production confirms that they can be distinguished from similar-appearing natural diamonds on the basis of their gemological properties. Although some may contain opaque mtallic inclusions, the most distinctive feature of near-colorless synthetic diamonds is their luminescence to ultraviolet radiation and to an electron beam (cathodoluminescence). In particular, almost all fluoresce yellow or yellow-green to short-wave UV and, when the ultraviolet lamp is turned off, they continue to phosphorese for 60 seconds or more. These distinctive reactions to ultraviolet radiation are very useful in identification, because many diamonds can be checked at one time.

ABOUT THE AUTHOR

Dr. Shigley is director of GIA Research, Carlsbad, California; Mr. Moses is vice president of Identification Services, and Dr. Reinitz is a research scientist, at the GIA Gem Trade Laboratory, New York; Mr. Elen is a research associate in GIA Research, Carlsbad; and Mr. McClure is supervisor of Identification Services in the GIA Gem Trade Laboratory, at the Gemological Laboratory, Physics Department, University of Nantes, France.

Gems & Gemology, *Vol. 33 No. 1, pp. 42–53*

The past few years have witnessed the entry into the trade of synthetic diamonds (mainly yellow) from various research institutes in Russia and elsewhere (Shigley et al., 1993a; Scarratt et al., 1994). In 1993, however, Thomas Chatham, of Chatham Created Gemstones, made the first of several public announcements of his intention to market Russian-grown synthetic diamonds, including "colorless" ones, for jewelry purposes ("Chatham to sell 'created' diamonds," 1993; Nassau, 1993). So far, however, there are only a few documented cases of faceted "colorless" synthetic diamonds in the jewelry trade. In 1996, a near-colorless 0.16 ct round-brilliant-cut synthetic diamond was submitted to the GIA Gem Trade Laboratory in New York by a local diamond dealer, and was quickly identified by laboratory staff. Nevertheless, gem-testing laboratories, individual diamond dealers, and jewelers need to prepare for the appearance of small amounts of this material in the market, possibly represented as natural stones.

A brief description of the distinctive features of colorless to near-colorless synthetic diamonds was provided in a chart and article by Shigley et al. (1995). However, the information in that chart was based on the examination of only 22 near-colorless synthetic diamonds, the total data base at the time the chart was prepared. The present article expands on that description by presenting detailed information on these 22 synthetic diamonds plus 29 examined since then (see, e.g., figure 1), for a total of 51 colorless to near-colorless synthetic diamonds tested by GIA researchers from 1984 through 1996 (see the list in table 1). All known manufacturers are represented.

BACKGROUND

In 1971, Robert Crowningshield published the first gemological description of the faceting-quality synthetic

Figure 1. These near-colorless synthetic diamonds (0.41 to 0.91 ct) were fashioned from crystals grown for experimental purposes at the De Beers Diamond Research Laboratory in Johannesburg, South Africa. Examination of these and many other near-colorless synthetic diamonds, representing all known methods of production, has revealed several distinctive gemological properties that allow then identification by standard gem-testing methods.

diamonds that had been grown by General Electric (G.E.) scientists. Among the samples he examined were two faceted synthetic diamonds that were nearly colorless (0.305 ct and 0.260 ct; "J" and "G" color grades, respectively).

Although a number of diamond simulants (such as strontium titanate, yttrium aluminum garnet [YAG], and synthetic spinel) were available in the jewelry trade at that time (Nassau, 1980; Hobbs, 1981), these could be easily and readily distinguished from diamond on the basis of their thermal conductivity and other gemological features. In contrast, the possibility of faceted "colorless" synthetic diamonds entering the gem market caused great concern among diamond dealers at both wholesale and retail levels. If these synthetics could not be identified readily and practically with simple gem-testing equipment (since thermal conductivity meters would read the same for both natural and synthetic diamond), they could undermine consumer confidence in natural gem diamonds.

Following the article by Crowningshield (1971) and an update on the G.E. synthetics by Koivula and Fryer (1984), we know of only a few other gemological articles that mention "colorless" synthetic diamonds. In the early 1990s, we reported on two experimental, isotopically pure carbon-12, diamond crystals (1.04 and 0.91 ct) grown at General Electric Superabrasives (Anthony et al., 1990; Shigley et al., 1993b). Shigley et al. (1992) described a 5.09 ct synthetic diamond crystal produced by Sumitomo researchers that was yellow and blue at the outer portions, and colorless in the center. Rooney et al. (1993) described a small, experimental, boron-doped, near-colorless (slightly gray) De Beers synthetic diamond that weighed 0.049 ct. In their Fall 1996 Gems *&* Gemology article, Welbourn et al. describe two diamond-verification instruments developed by De Beers scientists, the DiamondSure™ and the DiamondView™. The DiamondSure, which is based largely on a spectral feature inherent to most near-colorless type la natural diamonds, but not their colorless to near-colorless synthetic counterparts, will refer near-colorless synthetic diamonds for further tests. However, the Diamond View uses the pattern of ultraviolet fluorescence, which is very different for natural as compared to synthetic diamonds, as the basis for separating both near-colorless and colored diamonds.

MATERIALS AND METHODS

Synthetic Diamonds Examined. Table 1 lists the 51 near-colorless synthetic diamond samples seen by GIA researchers from 1984 to the present and some of our observations: 11 from General Electric, three produced by Sumitomo Electric Industries, six Russian synthetic diamonds (the research facility where they were produced has not been identified by the distributor, Chatham Created Gems), 22 manufactured by De Beers researchers in South Africa, eight of unidentified manufacture (loaned by Starcorp Inc., of Goleta, California), and the 0.16 ct round brilliant mentioned above, which was submitted to the GIA Gem Trade Laboratory by a client in the trade. Most of these 51 samples (specifically, the G.E., Sumitomo, and De Beers

TABLE 1. Properties of near-colorless synthetic diamonds examined by GIA. 1984–1996.

Ref. no.	Discription	Color grade[a]	Date of study	Mfr.[d]	Ultraviloet luminescence[e]		Cathodo-Inclusions	Inclusions	Attraction to a magnet	Electrical conductivity (intensity)	Other features
					Short-wave UV fluorescence	Phosphorescence (duration)					
10210	0.30 ct round brilliant	n.t.[b]	1984	G.E.	Weak yellow	Yellowish white	n.t.	n.t	n.t.	n.t.	
10211	0.31 ct crystal	n.a.[c]	1984	G.E.	Yellow	Yes (color not reported)	n.t.	n.t.	n.t.	n.t.	
20121	0.20 ct crystal	na.	1986	G.E.	Moderate yellowish white	Strong blue, persistent[f]	n.t.	Opaque metallic flux	n.t	n.t	
20226	0.50 ct crystal	n.a.	1986	Sumitomo	Moderate yellow	Strong yellow, persistent	Strong green-blue; blue phosphorescence	Opaque metallic flux	n.t.	Yes (variable)	
20805	0.75 ct crystal	n.a.	1988	G.E.	Moderate yellow, zoned	Strong yellow, persistent	Strong blue, zoned; blue phosphorescence	Opaque metallic flux	n.t.	Yes	Blue electrolumines cence
20808	0.39 ct round brilliant	J-K	1988	G.E.	Moderate yellow, zoned	Moderate yellow, persistent	Strong blue, zoned	Opague metallic flux	n.t.	Yes (weak)	
781	0.91 ct crystal	n.a.	1991	G.E.	Weak orange-yellow	Moderate green-yellow, persistent	Strong blue, zoned	Clouds of gray platelets	Yes	n.d.[g]	Yellow luminescence to X-rays
782	1.04 ct crystal	n.a.	1991	G.E.	Weak orange-yellow	Moderate green-yellow, persistent	Moderate yellow-green, zoned	Triangular platelets and opaque metallic flux	n.d.	n.d.	Yellow luminescence to X-rays
21282	0.78 ct round brilliant	F-G	1991	G.E.	Moderate green-yellow, zoned	Moderate green-yellow, persistent	n.t.	Opaque metallic flux	Yes	Yes (variable)	Blue electroluminescence
21283	0.29 ct oval brilliant	H	1991	G.E.	Moderate green-yellow, zoned	Moderate green-yellow, persistent	n.t.	Pinpoint	Yes	Yes (variable)	Blue electroluminescence
21399	0.05 ct round brilliant	K	1991	De Beers	Strong yellow, zoned	Strong yellow, persistent	Strong yellow, zoned	Opaque metallic flux	n.d.	n.d.	Faint yellow and blue color zones
21620	0.16 ct crystal	n.a.	1993	De Beers	Moderate green-yellow	Moderate yellow, persistent	Yellow-green, zoned	Triangular platelets and opaque metallic flux	n.d.	Yes (variable)	Faint blue color zone
21621	0.15 ct crystal	n.a.	1993	De Beers	Moderate green-yellow	Moderate yellow, persistent	Yellow-green, zoned	Pinpoint attraction	Weak	n.d.	
21622	0.15 ct crystal	n.a.	1993	De Beers	Moderate green-yellow	Moderate yellow, persistent	Yellow-green, zoned	Opague metallic flux	Moderate attraction	n.d.	
21705	1.25 ct crystal	n.a.	1994	Sumitomo	Moderate orange-yellow, zoned	Orange-yellow	Weak blue, zoned	Opaque metallic flux	Moderate attraction	Yes (variable)	Zoned: blue and red electroluminescence, with blue phospho rescence; orange thermoluminescence; weak orange fluores cence to long-wave UV
21706	0.23 ct crystal	n.a.	1994	Sumitomo	Weak green, zoned	Greenish blue, persistent	Strong blue	Opaque metallic flux	n.d.	n.d.	
21617	0.19 ct crystal	n.a.	1994	De Beers	Moderate greenish yellow, zoned	Moderate yellow, persistent	Yellow-green, zoned	Opaque metallic flux	Weak attraction	Yes (variable)	Faint blue and yellow color zones
21619	0.17 ct crystal	n.a.	1994	De Beers	Moderate greenish yellow, zoned	Moderate yellow, persistent	Yellow-green, zoned	Opaque metallic flux	Weak attraction	Yes (variable)	Faint blue and yellow color zones
21618	0.22 ct crystal	n.a.	1994	De Beers	Moderate greenish yellow, zoned	Moderate yellow, persistent	Yellow-green, zoned	Pinpoint	n.d.	Yes (variable)	Faint blue and yellow color zones
21686	0.42 ct crystal	n.a.	1994	Unidentified Russian co. (Chatham)	Very weak yellow	Weak yellow, persistent	n.t.	Opaque metallic flux	n.d.	Yes (variable)	
30089	0.11 ct crystal	n.a.	1995	Unidentified Russian co. (Chatham)	Weak yellow	Moderate yellow, persistent	n.t.	Opaque metallic flux	Yes	Yes (variable)	
30099	0.01 ct round brilliant	I	1996	Unknown (Starcorp)	Inert	Inert	n.t.	None visible	Too small to test	Too small to test	
30094	0.09 ct trill iant	I	1996	Unknown (Starcorp)	Weak yellow, zoned	Weak yellow, persistent	n.t.	Opaque metallic flux	Yes	n.d.	
30091	0.11 ct rectangle	K	1996	Unknown (Starcorp)	Weak yellow, zoned	Weak yellow, persistent	n.t.	Opaque metallic flux	Yes	Yes (variable)	Blue electroluminesc ence, zoned, withblue phosphorescence
30096	0.22 ct crystal	n.a.	1996	Unknown (Starcorp)	Moderate yellow	Moderate green-blue, persistent	n.t.	Opaque metallic flux	Yes	Yes (variable)	Blue electrolumines cence, zoned, with blue phosphores cence; fluoresced weak yellow to long-wave UV
30092	0.07 rectangle	I	1996	Unknown (Starcorp)	Weak yellow, zoned	Strong yellow, persistent	n.t.	Opaque metallic flux	Yes	Yes (variable)	Blue electrolumines cence, zoned, with blue phosphores cence
30095	0.25 ct crystal	n.a.	1996	Unknown (Starcorp)	Weak yellow, zoned	Strong yellow, persistent	n.t.	Opaque metallic flux	n.d	Yes (variable)	Blue electrolumines cence, zoned, with blue phosphores cence

Ref. no.	Discription	Color grade[a]	Date of study	Mfr.[d]	Ultraviloet luminescence[e]		Cathodo-Inclusions	Inclusions	Attraction to a magnet	Electrical conductivity (intensity)	Other features
					Short-wave UV fluorescence	Phosphorescence (duration)					
30098	0.02 ct round brilliant	H	1996	Unknown (Starcorp)	Weak yellow	Strong yellow, persistent	n.t.	None visible	Too small to test	Too small to test	
30097	0.02 ct round brilliant	H	1996	Unknown (Starcorp)	Weak yellow	Strong yellow, persistent	n.t.	None visible	Too small to test	Too small to test	
30103	0.41 ct round brilliant	G	1996	De Beers	Weak yellow-green, zoned	Strong green-yellow	Strong blue	Opaque metallic flux	n.d.	n.d.	Blue thermolumines cence
30102	0.52 ct round brilliant	I	1996	De Beers	Weak yellow-green, zoned	Strong green-yellow	Strong blue	Opaque metallic flux, with a reddish appearance	Moderate attraction	n.d.	Blue thermolumines cence
35018	0.16 ct round brilliant	F to G	1996	Unknown	Weak yellow-green	Weak green changing to blue	Moderate blue, zoned	None visible	n.d.	n.d.	
35017	0.72 ct round brilliant	H to J	1996	G.E.	Moderate yellow	Strong yellow-green	n.t.	Pinpoint	n.d.	nd	
30100	0.61 ct round brilliant	H	1996	De Beers	Weak yellow, zoned	Strong green-yellow	Strong blue, zoned	Blue, triangular platelets	n.d.	n.d.	Blue thermolumines cence
30101	0.91 ct round brilliant	I	1996	De Beers	Weak yellow, zoned	Strong green-yellow	Strong blue	Opaque metallic flux	n.d.	n.d.	Blue thermolumines cence
21966	0.56 ct round brilliant	H	1996	De Beers	Moderate yellow-green, zoned	Moderate yellow-green	n.t.	Platelet, pinpoint, and opaque metallic flux	Moderate attraction	n.d.	
21965	0.58 ct round brilliant	I	1996	De Beers	Moderate yellow-green, zoned	Moderate yellow-green	n.t.	Triangular platelets	Weak attraction	n.d.	
21962	0.37 ct round brilliant	H	1996	De Beers	Moderate yellow-green, zoned	Moderate yellow-green	n.t.	Platelet, pinpoint, and opaque metallic flux	n.d.	n.d.	
21961	0.26 ct round brilliant	H	1996	De Beers	Moderate yellow-green, zoned	Moderate yellow-green	n.t.	Pinpoint and opaque metallic flux	n.d.	n.d.	
21960	0.37 ct round brilliant	H	1996	De Beers	Moderate yellow-green, zoned	Moderate yellow-green	n.t.	Pinpoint and opaque metallic flux	n.d.	n.d.	
21959	0.32 ct round brilliant	H	1996	De Beers	Moderate yellow-green, zoned	Moderate yellow-green	n.t.	Platelet, pinpoint, and opaque metallic flux	n.d.	n.d.	
21970	0.42 ct round brilliant	H	1996	De Beers	Moderate yellow-green, zoned	Moderate yellow-green	n.t.	Pinpoint and opaque metallic flux	Weak attraction	n.d.	
21969	0.67 ct round brilliant	I	1996	De Beers	Moderate yellow-green, zoned	Moderate yellow-green	n.t.	Pinpoint and opaque metallic flux	Strong attraction	n.d.	
21967	0.57 ct round brilliant	H	1996	De Beers	Moderate yellow-green, zoned	Moderate yellow-green	n.t.	Platelet, pinpoint, and opaque metallic flux	n.d.	n.d.	
21956	0.36 ct round brilliant	H	1996	De Beers	Moderate yellow-green, zoned	Moderate yellow-green	n.t.	Pinpoint and opaque metallic flux	n.d	nd	
30105	0.51 ct crystal	n.a.	1996	Unidentified Russian co. (Chatham)	Very weak orange	Weak yellow	n.t.	Opaque metallic flux	Yes	Yes	
30106	0.50 ct crystal	n.a.	1996	Unidentified Russian co. (Chatham)	Strong yellow	Strong yellow, persistent	n.a.	Opaque metallic flux	Yes	Yes	
30107	0.41 ct crystal	n.a.	1996	Unidentified) Russian co. (Chatham)	Strong yellow	Strong yellow, persistent	n.t.	Opaque metallic flux	Yes	Yes	
30108	0.42 ct crystal	n.a.	1996	Unidentified) Russian co. (Chatham)	Very weak orange	Weak yellow	n.t.	Opaque metallic flux	Yes	Yes	
30109	round brilliant	n.a.	1996	G.E.	Moderate yellow-green	Very strong green	n.t.	Pinpoint	n.t.	n.a.	
22007	0.27 ct round brilliant	n.t.	1996	De Beers	Moderate yellow-green, zoned	Moderate yellow-green	n.t	Opaque metallic flux	n.d.	n.d.	

[a]Color grades are for discussion purposes only. GIA-GTL does not grade synthetic diamonds. No grades are given for unfashioned samples.

[b]n.t. = Not tested.

[c]n.a. = Not applicable.

[d]GE. = General Electric Company: Sumitomo = Sumitomo Electric Industries; De Beers = De Beers Diamond Research Laboratory.

[e]All but two samples were inert to long-wave UV. The two samples that fluoresced to long-wave UV were ret. nos. 21705 (weak orange, zoned) and 30096 (weak yellow).

[f] Persistent=Phosphorescence that lasted 15 seconds or longer.

[g]n.d. = Tested but no reaction detected.

synthetic diamonds) represent experimental, rather than commercial, products. Color-grade equivalents on most of the faceted samples were determined by the staff of the GIA Gem Trade Laboratory, using standard grading procedures, for research purposes only. (GIA GTL does not provide color or clarity grading services for synthetic diamonds.)

A large portion of this sample consists of the 15 faceted near-colorless experimental synthetic diamonds, produced by De Beers scientists during 1995, that were loaned to GIA for examination in the spring of 1996 (see, again, figure 1 here and also figure 1 in Welbourn et al., 1996, which illustrates similar material). The largest of these samples weighed 0.91 ct, and the color grades of this group all fell within the "G" to "I" range.

In May 1994, Thomas Chatham loaned GIA Research a 0.42 ct near-colorless synthetic diamond crystal that he reported was of Russian origin (for a photo and brief description of this crystal, see Koivula and Kammerling, 1994, pp. 123–124). Two years later, in May 1996, Mr. Chatham also made available to us about 100 small (as large as 0.7 ct, but most weighing 0.25 ct or less) near-colorless synthetic diamond crystals from Russia, which he later offered for sale at the 1996 JCK jewelry show in Las Vegas. Although these crystals appeared colorless, for the most part they were distorted in shape, contained numerous metal inclusions, and were very small; as such, they were not well-suited for jewelry. Because we had very little time to examine these samples, we selected only four of the larger crystals for testing.

The majority of the samples we examined for this study would be considered near-colorless on the GIA color-grading scale.

Characterization Techniques. To observe the color, relative intensity (described as *none, very weak, weak, moderate, strong,* and *very strong*), and distribution pattern, if any, of the ultraviolet fluorescence in all of the samples, we used a long-wave (366 nm) and short-wave (254 nm) GIA Gem Instruments UV lamp unit in a darkened room with contrast-control glasses. When the UV lamp was turned off, a notation was made of the color, relative intensity, and duration (by means of an electronic timer) of any phosphorescence emitted by each sample. Whenever possible, we took photos of these UV luminescence reactions to help illustrate the diagnostic value of these features. Some of the samples acquired in 1996 were examined with the De Beers Diamond View, which was loaned to GIA in September 1996. Fluorescence images captured with the Diamond View were stored electronically.

Relative transparency to ultraviolet radiation was observed in all samples examined since 1991 by placing the sample between the short-wave UV lamp and a piece of synthetic scheelite (a material that luminesces blue to short-wave UV). The extent of the UV transparency could then be estimated by judging the relative intensity of the scheelite's fluorescence.

We looked for luminescence to an electron beam (cathodoluminescence) in 21 samples with a Nuclide ELM-2B luminoscope (currently manufactured by Premier American Technologies, Bellefonte, Pennsylvania), again noting the color and distribution pattern, if any. Photographs of all the types of luminescence were captured whenever possible.

We used a binocular gemological microscope to examine all but the two earliest G.E. samples for inclusions and other features. (A Nikon SMZ-U photomicroscope was used to prepare photomicrographs of distinctive visual features for those samples seen since spring 1995.)

Magnetism (caused by the presence of transition metal inclusions, such as iron) has been shown to be a valuable test for recognizing some synthetic diamonds (Koivula and Fryer, 1984; Shigley et al., 1986, 1987, 1993a,- Hodgkinson, 1995). We judged magnetic attraction (none, weak, moderate, or strong) for 41 samples by observing the amount of movement or rotation when a rare-earth iron magnet (as suggested by H. Oates and W. Hanneman,-see Hodgkinson, 1995) was brought close to a synthetic diamond that had been suspended in air by means of a thin plastic thread. (We did not use this specific test on the early G.E. samples or those that were too small to be suspended from the thread.)

Forty-four samples were tested for electrical conductivity with a standard gemological conductometer. We also looked for visible luminescence produced by an electrical current (electroluminescence) in these 44 samples. We used a darkened room with the sample placed between the metal probes of the conductometer.

In five of the samples examined in 1996, we detected some interesting thermoluminescence by placing the synthetic diamond in hot water (about 140°F/60°C) after exposure to the ultraviolet lamp. Again, a subjective visual judgment was made of the emitted color.

We used either a Beck prism or a Discan digital-scanning diffraction-grating spectroscope to observe the optical absorption spectra of all of our samples. Pye-Unicam 8800 and Hitachi U-4001 spectrophotometers were also used to record visible-range absorption spectra over the wavelength range 250–850 nm (with the sample held at liquid-nitrogen temperatures in an evacuated chamber) for 25 samples. A Nicolet 60SX Fourier-transform infrared spectrometer was used to record room-temperature infrared absorption spectra over the wavelength range 400–25000 cm^{-1} for 24 samples.

RESULTS

We determined that all of these synthetic diamond samples were type Ha on the basis of a combination of their infrared absorption spectra and their greater transparency to ultraviolet radiation. As table 1 indicates, some of these were electrically conductive or had a faint yellow or faint blue component to their color. In those samples for which we had infrared spectra, we typically saw evidence of boron- and/or nitrogen-related absorption features.

Characteristics of the Crystals. As with other synthetic diamond crystals (Shigley et al., 1986, 1987, 1993a), all of the near-colorless crystals in this study had a very distinct shape that consisted of a portion of a cuboctahedron with a flat base. Octahedral {111} and cube {100} faces were most common in both abundance and surface area (size) on these synthetic diamond crystals, but smaller dodecahedral {110} and trapezohedral {113}—and, occasionally, {115}—faces were also seen. In general, these crystals had relatively flat faces, with sharp edges and corners between adjacent faces (figure 2). The flat base was not a true crystal face but a growth surface, where the tiny seed crystal was located (figure 3).

The evidence of extensive mechanical abrasion or chemical etching that is seen on many natural (octahedral) diamond crystals was absent on our synthetic samples. Nevertheless, many of these synthetic diamond crystals had interesting surface markings that, if retained after faceting, might be of diagnostic value. Such diagnostic markings include dendritic or striated patterns (figures 2 and 4). However, features that appear identical to the well-known trigons seen on natural diamond crystals may also be found on some synthetic diamonds (figure 5), so it is important not to conclude that a diamond is natural based on the presence of these triangular markings.

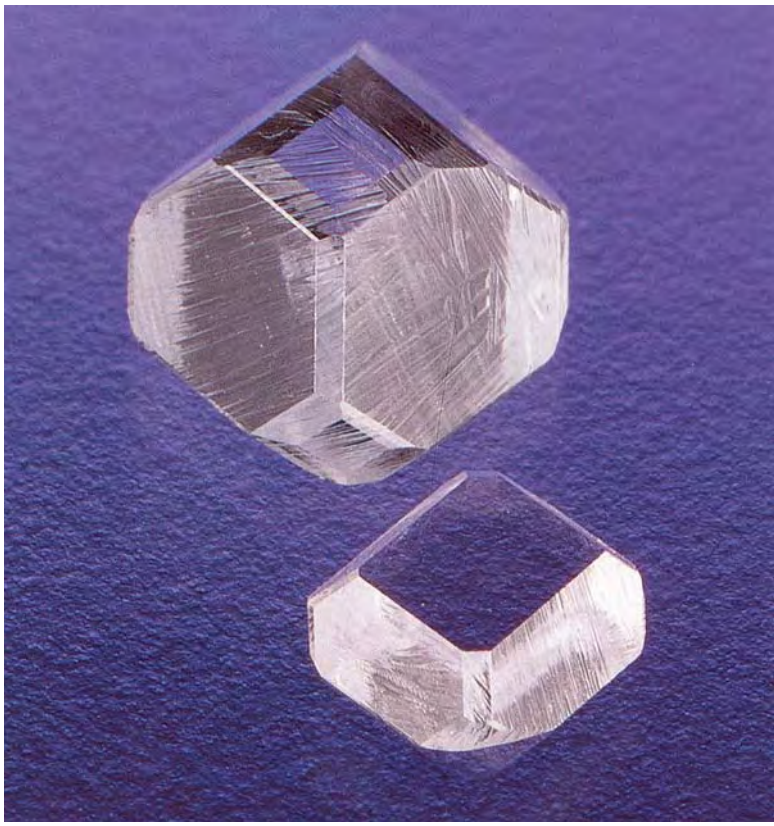

Figure 2. The cuboctahedral form exhibited by these two experimental Sumitomo synthetic diamond crystals (0.23 and 1.25 ct; reference nos. 21706 and 21705, respectively) is typical of synthetic diamonds from all known manufacturers. The 1.25 ct crystal shows the larger octahedral faces and smaller cube, dodecahedral, and trapezohedral faces that are characteristic of this material. Note also the striations covering the surface, which are not seen in natural diamonds. Photo © GIA and Tino Hammid.

Ultraviolet Fluorescence and Phosphorescence. All but two samples showed no fluorescence to long-wave UV radiation. No response to either long- or short-wave UV was observed in sample no. 30099. However, all other samples did fluoresce yellow to orange-yellow or yellow-green to short-wave UV (see, e.g., figure 6). The intensity of this reaction varied from very weak to moderate. Because the very weak short-wave fluorescence observed in some of these synthetic diamonds could be mistaken for no fluorescence reaction, care must be taken

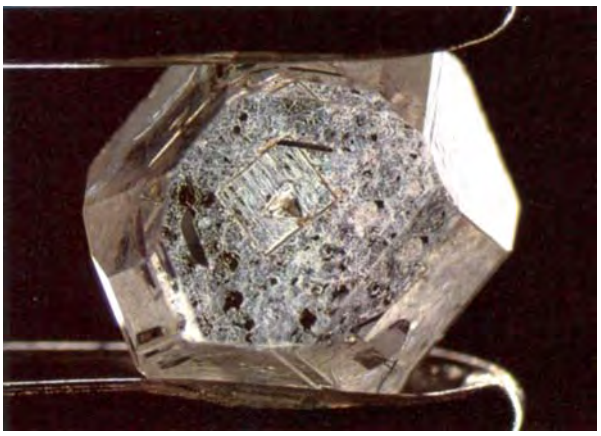

Figure 3. The flat base of this 0.22 ct Starcorp synthetic diamond crystal (reference no. 30096) shows the square imprint of the seed from which the crystal grew. Photomicrograph by Shane Elen; magnified 5×.

in making these observations. This is why fluorescence should be tested in a *completely darkened room,* and only when one's eyes have had time to adjust to those viewing conditions (at least several minutes).

In many of our study samples, the short-wave UV fluorescence was unevenly distributed, with certain internal growth sectors (sometimes in the form of a black, cross-shaped pattern; again, see figure 6) exhibiting no fluorescence. An example of the UV fluorescence pattern obtained with the new De Beers DiamondView instrument is shown in figure 7 (see also Welbourn et al., 1996). Note that the color of the UV fluorescence as seen with the DiamondView is different from that seen with a standard UV lamp unit. In either case, it is the fluorescence pattern that is of greatest diagnostic importance.

In addition, when the UV lamp was turned off, most of our study samples continued to phosphoresce a weak to strong yellow, yellow-green, or blue for 15–60 seconds or longer. In some cases, this phosphorescence was so intense that the glowing synthetic diamond could be seen from a distance of several feet in a darkened room.

Cathodoluminescence. Of the samples tested, 19 (representing all sources of production) exhibited blue (figure 8), yellow, or green-yellow Cathodoluminescence. This was unevenly distributed in a pattern (again, often cross-shaped) that differs from those patterns seen in a natural diamond.

Magnification. When viewed with a binocular gemological microscope, the study samples revealed a few distinctive features. Most prominent were fluxmetal inclusions, which usually appeared opaque in transmitted light and metallic in reflected light. The flux inclusions were usually elongate with rounded edges, and could be seen singly or in small groups,-some had a dendritic appearance (figure 9). The elongate metallic inclusions were present in most of the samples (see table 1). In general, however, they

Figure 4. Magnification (12×) reveals the distinctive striation pattern on this Sumitomo synthetic diamond crystal (reference no. 21706). Photomicrograph by John I. Koivula.

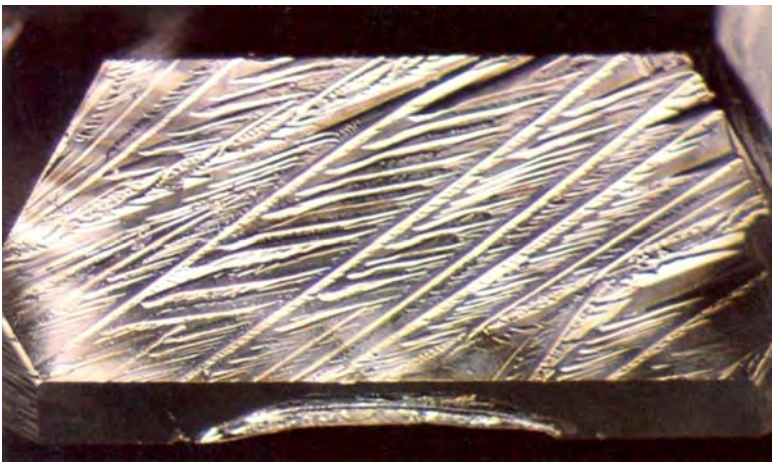

Figure 5. The triangular, pyramid-like markings on an octahedral crystal face of this near-colorless De Beers synthetic diamond (reference no. 21618) strongly resemble the trigons seen on natural diamonds. Photomicrograph by John Koivula; magnified 10 ×.

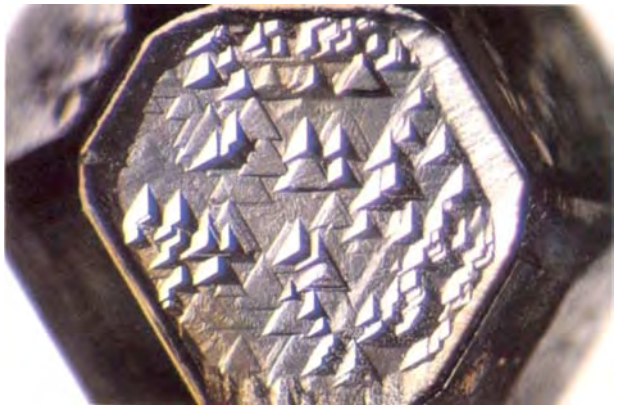

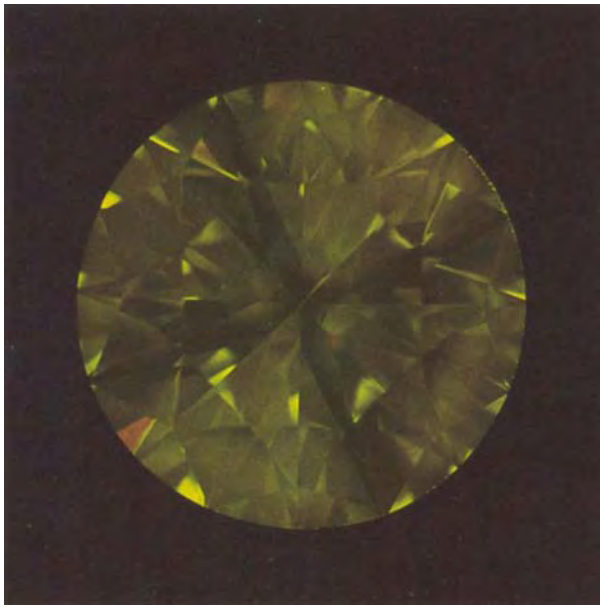

Figure 6. This 0.91 ct De Beers synthetic diamond (reference no. 30101) displays the zoned fluorescence to short-wave UV that is commonly seen in synthetic diamonds. The black, cross-shaped areas where there is no fluorescence correspond to internal growth sectors that lack the impurities responsible for the UV fluorescence emitted by the other growth sectors. Photo by Shane Elen.

seemed to be more numerous in the Russian synthetic diamonds. In some cases, the synthetic diamond was attracted by a magnet because of these metallic inclusions. In approximately onethird of our samples, we saw tiny pinpoint inclusions that probably also were metallic flux.

In eight of the De Beers synthetic diamonds, we saw groups of thin, translucent, oriented, triangular inclusions of uncertain identity (figure 10). These inclusions, often associated with weak strain (anomalous birefringence), were translucent and blue in transmitted or polarized light (figure 11, left), and less translucent and reddish brown in reflected light (figure 11, right). These triangular inclusions often were apparent only in certain orientations of the sample (with respect to the direction of the light source); otherwise, they were nearly transparent and could easily go unnoticed during observation with a gemological microscope. Close inspection of these features revealed surface details similar to the large tetrahedral stacking faults observed using X-ray topography (as illustrated in Field, 1979, p. 442).

We did not see intersecting graining patterns in any of the samples; these patterns are an important identification feature in colored synthetic diamonds (Shigley et al., 1995). Even the most strong-

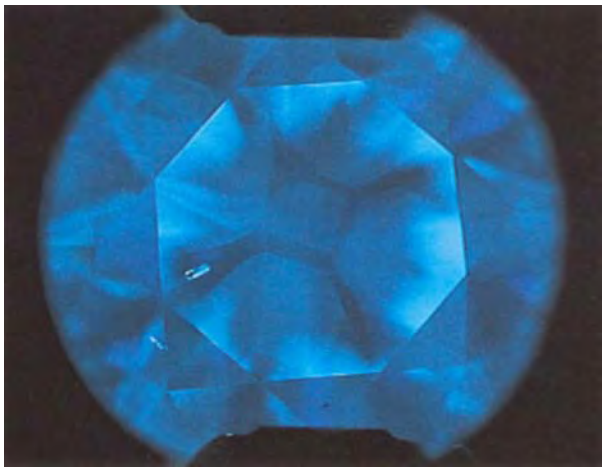

Figure 7. The uneven pattern of fluorescence typical of synthetic diamonds-here, in a cross shape-is readily apparent in this reference photo taken with the De Beers DiamondView verification instrument. Note that because two very different excitation sources are used, the color of fluorescence as seen with the DiamondView is very different from that seen with a standard UV unit (e.g., figure 6). Photo by Shane Elen.

colored sample (no. 30095) exhibited no obvious internal color zoning. (In several instances, though, a very faint color zone was seen with magnification; table 1.)

Figure 8. Like fluorescence, cathodoluminescence in near-colorless synthetic diamonds is also typically uneven and very different from the patterns seen in natural diamonds. A faint cross shape is visible in this 0.61 ct near-colorless De Beers synthetic diamond (reference no. 30100). Photo by Shane Elen.

Figure 9. An unusual dendritic inclusion accompanies the elongate inclusions in this 1.25 ct Sumitomo synthetic diamond crystal (reference no. 21705). Photomicrograph by John I. Koivula; transmitted light, magnified 20×.

Birefringence. When observed between crossed polarizing filters with the microscope, the synthetic diamonds typically displayed weak anomalous birefringence ("strain"; see, e.g., figure 6 in Shigley et al., 1993b, p. 194), as was the case for many of the colored synthetic diamonds we examined. This weak "strain" is indicated by low-order interference colors (typically just black, gray, or white, and frequently in a cross-shaped pattern).

Magnetism. About one-half of the study samples exhibited some attraction to a magnet. Samples with more metallic inclusions seemed to display a stronger attraction.

Electrical Conductivity. In 20 of the 45 samples tested, we noted some electrical conductivity with a strength that varied depending on the point on the sample that we tested with the conductometer probes. For the crystals, this electrical conductivity could be seen to vary depending on which pair of crystal faces were selected for testing with the probes (although it was not possible to determine exactly which faces were conductive because of their small size and the difficulty of ensuring that we were touching just one face with the probe).

Electroluminescence. Of the samples that showed some electrical conductivity, six also displayed aninteresting blue luminescence (usually sporadic and weak) when the sample was touched with the conductometer probes (figure 12). To our observers, this luminescence did not appear to be emitted by the entire sample. Rather, it appeared to be localized, and to extend between the points on the sample touched by the two probes (somewhat like a flash of lightning). Because this reaction is similar to that seen in many natural diamonds, this test usually is not useful to identify the synthetic stones. However, one Sumitomo crystal displayed both *blue* and *red* electroluminescence, depending on where it was touched with the probes; when the probes were removed, the diamond continued to phosphoresce blue for several seconds.

As was the case with electrical conductivity, we could not relate the visible electroluminescence in the unfashioned samples to the particular crystal faces being touched by the conductometer probes (although the impurities causing the conductivity were presumed to be distributed unevenly between the internal growth sectors of the synthetic diamond).

Thermoluminescence. When immersed in hot water after exposure to UV radiation, all five samples tested were seen to emit luminescence (which continued briefly when the still-warm sample was removed from the water). Four emitted blue and one (reference no. 21705) emitted orange. We have not observed this reaction in natural diamonds.

Figure 10. Groups of tiny, translucent, oriented, triangular inclusions of uncertain identity can be seen in this 0.61 ct De Beers synthetic diamond (research no. 30100). Photomicrograph by Shane Eleri; unpolarized reflected light, magnified 15×.

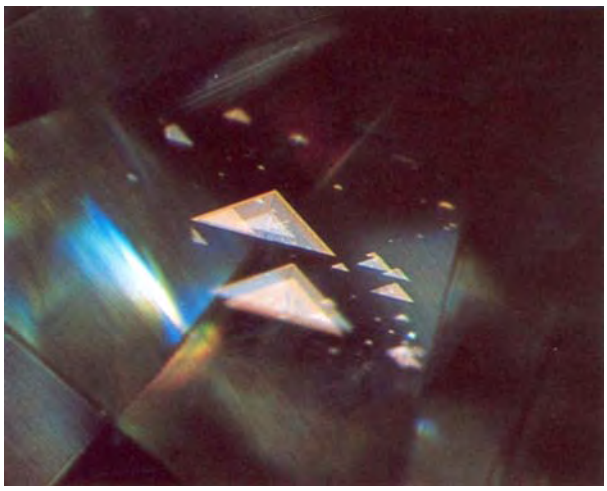

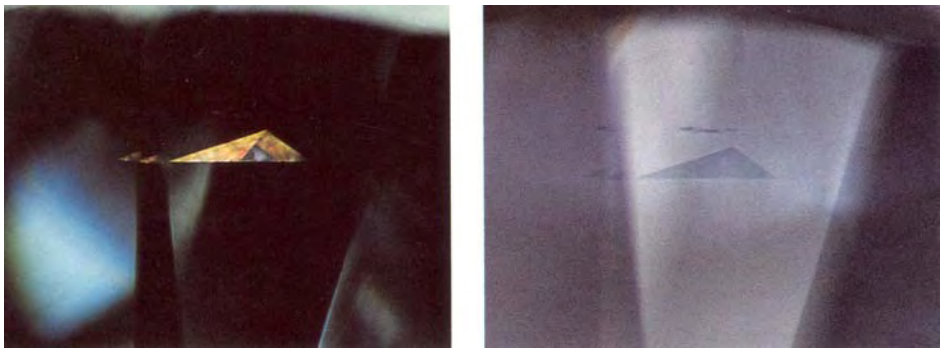

Figure 11. In polarized transmitted light (left), the triangular growth features appeared translucent blue and often had localized strain. In unpolarized reflected light (right), they appeared less translucent and reddish brown. Sample no. 21967 (De Beers); photomicrographs by Shane Elen, magnified 12.5×.

Absorption Spectrum. The vast majority of the synthetic diamonds in this study did not reveal any significant absorption bands with either the spectrophotometer or the handheld spectroscope. (Although a well-defined band at 270 nm has been identified in near-colorless synthetic diamonds [C. Welbourn, pers. comm., 1997], it was not resolvable with our instruments.) However, the two G.E. synthetic near-colorless diamonds we examined in 1984 displayed a very weak band at about 732 nm in the spectra recorded with the Pye-Unicam spectrophotometer (a feature discussed by Lawson and Kanda, 1993). Since we have not seen this band in synthetic diamonds produced more recently, we do not consider it to be significant.

Although the infrared spectra allowed us to establish that all of our samples were type IIa diamonds (and, as mentioned earlier, that some had weak boron- and/or nitrogen-related absorption features), they contained no features by which we could separate a natural type IIa diamond from a synthetic type IIa stone.

Figuie 12. Blue electroluminescence was emitted by some of the samples when they were touched with the conductometer probes. Sample no. 30096 (Starcorp); photomicrograph by Shane Elen, magnified 2.5×.

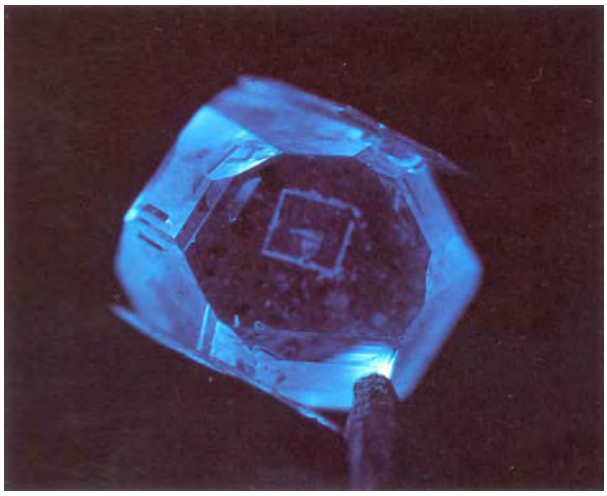

DISCUSSION

Natural near-colorless diamonds are usually type Ia; those that contain little or no nitrogen are referred to as type IIa (for a brief discussion of diamond types, see Box A in Fritsch and Scarratt, 1992, pp. 38–39). The synthetic diamonds described here are all type IIa, although some have a small type lib or type IaB component. To date, we have not seen a type la near-colorless gem synthetic diamond; nor, to our knowledge, has one ever been reported. Near-colorless type IIa diamonds have a greater degree of transparency from the blue end of the visible spectrum into the near-ultraviolet region than do near-colorless type la diamonds.

In addition, type IIa diamonds do not display the nitrogen-related sharp absorption peaks in their absorption spectra ("Cape lines," with the strongest peak at 415 nm and additional peaks between 415 and 478 nm) that are seen in type la diamonds. This is the principal behind the new De Beers DiamondSure instrument (Welbourn et al., 1996). Once it is established that the diamond in question is a type IIa, other tests such as UV fluorescence or cathodoluminescence can be used to determine whether it is natural or synthetic.

Natural diamond crystals are typically in the shape of an octahedron or dodecahedron, where growth has taken place outward in all directions from a central core to give an equant crystal (see figure 7 in Welbourn et al., 1996 p. 163). Many natural diamond crystals have rounded surfaces that are due to chemical dissolution (etching) of the diamonds while they were still in the Earth, or to mechanical abrasion during transport from the host rock in a stream or river. Synthetic diamonds have a very different crystal morphology (again, see figure 5 in the

article by Welbourn et al., 1996, p. 162). Unlike natural diamonds, growth only takes place outward and upward from the seed location at the flat base.

In his description of the early G.E. synthetic diamonds, Crowningshield (1971) reported that the two near-colorless samples had an unusual reaction to ultraviolet radiation. They did not fluoresce to long-wave UV, but did fluoresce to short-wave UV, with a yellow color that continued, in his words, "for a long time" even after the UV lamp had been turned off (phosphorescence). He mentioned how different this reaction was to that of natural near-colorless diamonds, and how observation of both fluorescence and phosphorescence to short-wave UV would be imperative for synthetic diamond verification. Thus, at this early date, he established what has become a practical means by which synthetic diamonds can be recognized by the gemologist.

Observations of the fluorescent and phosphorescent reactions to UV radiation among our study samples confirm Crowningshield's results. Specifically, strong short-wave UV fluorescence (relative to long-wave UV) and, in some cases, phosphorescence are very distinctive of synthetic diamonds (Shigley et al., 1995). Almost all the near-colorless synthetic diamonds we have examined to date exhibited these phenomena. Weak or absent long-wave UV fluorescence, and the presence of stronger short-wave UV fluorescence and phosphorescence, do not immediately prove that a "colorless" diamond is a synthetic. However, any diamond that displays these reactions should be considered suspect and should be examined by other gem-testing methods. The typical form of zoned fluorescence seen in synthetic diamonds is not found in natural diamonds. When present, fluorescence in a natural near-colorless diamond is typically blue (rarely, it is yellow) to both long- and short-wave UV radiation, with the reaction almost always being more intense to long-wave UV.

Cathodoluminescence is an important additional means of identifying a diamond as being synthetic, since the pattern of luminescence from the different internal growth sectors is even more visible with this technique than with conventional observation of UV fluorescence (Ponahlo, 1992; Shigley et al., 1995). This equipment has become more standard at gem-testing laboratories, although the availability of the new De Beers DiamondView may make the need for cathodoluminescence instrumentation less-critical.

Strong magnetism in a diamond suggests that it is synthetic. However, because some synthetic diamonds (including a number examined during this study) contain few if any metallic inclusions, magnetism is not an effective test for all stones.

Our latest findings, reported here, support previous indications that the most diagnostic gemological features for distinguishing near-colorless type Ha synthetic diamonds (so far, from any source) are still those summarized by Shigley et al. (1995):

- The cuboctahedral crystal shape, and the possibil ity of striations and other unusual patterns on the surfaces of the crystal faces.
- Metallic inclusions, which seem to be relatively abundant in the near-colorless Russian-grown synthetic diamonds we have examined so far.
- Attraction of the synthetic diamond to a magnet.
- The short-wave ultraviolet fluorescence and phosphorescence.
- The greater UV transparency, which is indicative of a type IIa diamond (most natural near-color diamonds are type la).
- Weak or absent anomalous birefringence ("strain").
- Electrical conductivity.

In contrast to the situation with colored synthetic diamonds, our near-colorless synthetic samples lacked color zoning, graining patterns, and, in most cases, distinctive absorption bands in the visible and infrared spectra. Thus, these features are of little if any diagnostic value for the separation of natural from synthetic near-colorless diamonds.

CONCLUSION

A few polished synthetic diamonds have been seen in the jewelry industry, but we know of only one confirmed instance of a near-colorless sample of unknown origin appearing in the trade without being represented as synthetic (the 0.16 ct round brilliant mentioned earlier). Because of technical challenges and the high cost of production, we question the likelihood that fashioned near-colorless synthetic diamonds over 25 points will enter the jewelry industry in commercial quantities. In our opinion, the greatest possibility is the availability of near-colorless melee, because at these small sizes synthetic diamonds can be grown relatively fast and efficiently.

The group of near-colorless type IIa synthetic diamonds described in this article is the largest known to have been examined by standard and advanced gem-testing techniques for the express purpose of establishing practical identification criteria. The most useful identification clues for synthetic diamond crystals are the crystal shape and surface features. For a polished stone, key identification features include metallic inclusions and the related possibility of attraction to a magnet, the possibility of electrical conductivity, and the characteristic short-wave UV fluorescence and phosphorescence. These gemological properties appear to be diagnostic of near-colorless type IIa synthetic diamonds, and are very different from near-colorless natural type la and type IIa diamonds.

Diamond dealers, jewelers, and gemologists must be prepared to handle the identification of jewelry-quality near-colorless synthetic diamonds if they become more widely available. Testing will require a more careful gemological examination of near-colorless diamonds. The synthetic nature of a diamond must be disclosed at the time of sale or appraisal. The GIA Gem Trade Laboratory will continue its policy of issuing only identification reports, reports, on synthetic diamonds.

Acknowledgments: The following individuals and organizations provided synthetic diamonds and, in some cases, information for this study: Rick D 'Angela and Dr. William Banholzer of General Electric Superabrasives, Worthington, Ohio; Dr. Thomas Anthony of General Electric Research &Development, Schenectady, New York; Dr. Shuji Yazu and his colleagues at Sumitomo Electric Industries, Itami, Japan; Thomas Chatham of Chatham Created Gems, San Francisco, California; and Marion Matthews of Starcorp, Goleta, California. The largest group of samples in this study were produced by Dr. Robert Burns and his colleagues at the De Beers Diamond Research Laboratory in Johannesburg, South Africa; they were made available through Martin Cooper of the Diamond Trading Company (DTC) Research Centre in Maidenhead, United Kingdom.

REFERENCES

Anthony T.R., Banholzer W.F., Fleischer J.F., Wei L, Kuo P.K., Thomas R.L., Prycr R.W. (1990) Thermal diffusivity of isotopically enriched ^{12}C diamond. *Physical Review B (Condensed Matter),* Vol. 42, Third Series, No. 2, pp. 1104-1111.

Chatham to sell "created" diamonds (1993). *New York Diamonds,* No. 22, Autumn, pp. 44, 46.

Crowningshield R. (1971) General Electric's cuttable synthetic diamonds. *Gems & Gemology,* Vol. 13, No. 10, pp. 302-314.

Field J.E. (1979) *Properties of Diamond.* Academic Press, New York.

Fritsch E., Scarratt K. (1992) Natural-color nonconductive gray-to-blue diamonds. *Gems & Gemology,* Vol. 28, No. 1, pp. 35–42.

Hobbs J. (1981) A simple approach to detecting diamond simulants. *Gems & Gemology,* Vol. 17, No. 1, pp. 20–33.

Hodgkinson A. (1995) Magnetic wand-Synthetic gem diamond detector. *Rapaport Diamond Report,* May 5, pp. 34-35.

Koivula J.I., Fryer C.W. (1984) Identifying gem-quality synthetic diamonds: An update. *Gems & Gemology,* Vol. 20, No. 3, pp. 146–158.

Koivula J.I., Kammerling R.C. (1994) Gem news: Near-colorless Russian synthetic diamond examined. *Gems & Gemology,* Vol. 30, No. 2, pp. 123–124.

Lawson S.C., Kanda H. (1993) An annealing study of nickel point defects in high-pressure synthetic diamond. *Journal of Applied Physics,* Vol. 73, No. 8, pp. 3967–3973.

Nassau K. (1980) *Gems Made by Man,* Chilton Book Co., Radnor, PA.

Nassau K. (1993) Are synthetic diamonds from Russia a threat? *Rapaport Repoit,* November 5, pp. 29–32.

Ponahlo J. (1992) Cathodoluminescence (CL) and CL spectra of De Beers' experimental synthetic diamonds. *Journal of Gemmology,* Vol. 23, No. 1, pp. 3–17.

Rooney M-L.T., Welboum CM., Shigley J.E., Fritsch E., Reinitz I. (1993) De Beers near colorless-to-blue experimental gem-quality synthetic diamonds. *Gems & Gemology,* Vol. 29, No. 1, pp. 38–45.

Scarratt K., Du Toit G., Sersen W. (1994) Russian synthetics examined. *Diamond International,* No. 28 (March/April), pp. 45–52.

Shigley J.E., Fritsch E., Stockton CM., Koivula J.I., Fryer C.W., Kane R.E. (1986) The gemological properties of the Sumitomo gem-quality synthetic diamonds. *Gems & Gemology,* Vol. 22, No. 4, pp. 192–208.

Shigley J.E., Fritsch E., Stockton CM., Koivula J.I., Fryer C.W., Kane R.E., Hargett D.R., Welch C.W. (1987) The gemological properties of the De Beers gem-quality synthetic diamonds. *Gems & Gemology,* Vol. 23, No. 4, pp. 187–206.

Shigley J.E., Fritsch E., Reinitz I., Moon M. (1992) An update on Sumitomo gem-quality synthetic diamonds. *Gems & Gemology,* Vol. 28, No. 2, pp. 116–122.

Shigley J.E., Fritsch E., Koivula J.I., Sobolev N.V., Malinovsky I.Y., Pal'yanov Y.N. (1993a) The gemological properties of Russian gem-quality synthetic yellow diamonds. *Gems & Gemology,* Vol. 29, No. 4, pp. 228–248.

Shigley J.E., Fritsch E., Reinitz I. (1993b) Two near-colorless General Electric type IIa synthetic diamond crystals. *Gems & Gemology,* Vol. 29, No. 3, pp. 191–197.

Shigley I.E., Fritsch E., Reinitz I, Moses T.M. (1995) A chart for the separation of natural and synthetic diamonds. *Gems & Gemology,* Vol. 31, No. 4, pp. 256–264.

Welboum CM., Cooper M., Spear P.M. (1996) De Beers natural versus synthetic diamond verification instruments. *Gems & Gemology,* Vol. 32, No. 3, pp. 156–169.

GIA GEM TRADE
LAB NOTES

DIAMOND

Two Noteworthy Stones from the Americas

The October 11, 1996, *Rapaport Diamond Report* included an article on the purchase of a 28.3 ct rough diamond, recently recovered from the Kelsey Lake mine in Colorado (see also Winter 1996 Gem News, pp. 282–283). The highly etched brownish yellow crystal yielded a 5.39 ct pear-shaped brilliant (figure 1). A rather deep, etched feather was seen in the pavilion of the finished stone (figure 2). Althoughthis stone was submitted to the laboratory for an Identification and Origin of Color Report only, we would have graded the clarity in the SI range; the color was graded as Fancy Deep Brownish Yellow.

Fluorescence to long-wave ultraviolet radiation was strong in intensity and predominantly blue with small zones of strong yellow. The diamond fluoresced a weaker yellow to shortwave UV. The absorption spectrum, seen at low temperature using a desk-model spectroscope, showed a strong "Cape series" and weak sharp bands at about 545 and 563 nm. These properties are consistent with hydrogen-rich diamonds (see E. Fritsch and K. Scarratt, *Journal of Gemmology,* "Gemmological Properties of Type la Diamonds with an Unusually High Hydrogen Content," Vol. 23, No. 8, 1993, pp. 451–60). Although the distinctive properties of this class of diamond were observed decades ago, hydrogen's role in causing the color was only recognized in the last five years. These hydrogen-rich diamonds have also occurred in other recently

Figure 1. This 5.39 ct Fancy Deep Brownish Yellow diamond was cut from a 28.3 ct piece of rough recovered from the Kelsey Lake mine in Colorado.

Figure 2. An etched feather can be seen in the pavilion of the Kelsey Lake diamond shown in figure 1. Magnified 57×.

Editor's note: The initials at the end of each item identify the contributing editor(s) who provided that item.

Gems & Gemology, *Vol. 33, No. 1, pp. 54-59*

developed sources, such as in Australia, Russia, and the Jwaneng mine in Botswana.

Only a few days after we saw the Kelsey Lake stone, a long-time GTL client submitted a 2.15 ct old-minecut diamond (figure 3) that was reportedly from Brazil. Graded Fancy Intense Greenish Yellow, this stone revealed gemological properties common to stones with strong "green transmission" luminescence. The H3 optical center that is associated with this effect gives rise to absorption bands at about 494 and 503 nm. Diamonds with this optical center not only routinely fluoresce strongly to UV radiation, but they also are excited by visible light—often appearing quite green when exposed to a strong incandescent light source (figure 4). This strong luminescence may influence the color grade of such diamonds, as it did with this one. In our experience, some diamonds with these properties do originate from Brazil and Venezuela, thus lending support to this stone's reported provenance (see also J. F. Cottrant and G. Calas, "Étude de la coloration de quelques diamants du Muséum National d'Histoire Naturelle," *Revue de Gemmologie,* No. 67, 1981, pp. 2–8).

According to our client, the stone was reportedly given by Pedro II (emperor of Brazil from 1831 to 1889) to his niece. A member of the Braganza royal family, which ruled Portugal from 1640 until 1910, Pedro II was purportedly greatly interested in diamonds and mineral specimens.

The submission of diamonds of known or well substantiated provenance provides the laboratory with the opportunity not only to document the properties of such stones, but also to help answer ongoing questions related to the origin of color in diamonds. *TM*

Figure 3. This 2.15 ct old-minecut diamond was graded Fancy Intense Greenish Yellow.

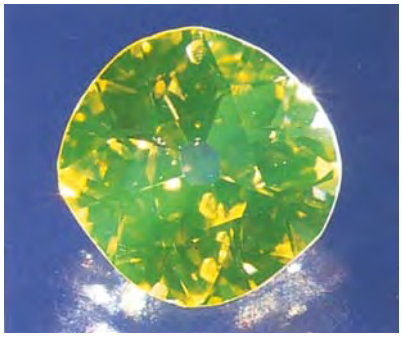

Figure 4. The green transmission luminescence in the diamond in figure 3 is best seen when the stone is excited with a strong incandescent light source, such as fiber-optic illumination.

Damaged from Wear

When appropriate, GIA GTL diamond grading reports on round brilliants contain a comment that the average crown angles are less than 30° or exceed 35°. These comments are intended to alert the reader of the report that the crown angles deviate seriously from industry norms and, in the case of shallow angles, warn of a threat to the stone's durability.

The East Coast lab recently issued a report on just such a stone—a 2.66 ct yellow diamond that had been removed from a four-prong ring setting. As can be seen in figure 5, the unusually thin girdle was chipped in many places. When the stone was viewed from the side (figure 6), the crown angles appeared to be very shallow. Just how shallow was seen when the stone was viewed in a GIA Proportion Scope (figure 7): The angles averaged less than 25°. In addition, the pavilion anglewere less than

Figure 5. Many chips can be seen on the girdle of this 2.66 ct round-brilliant-cut diamond, which was originally set in a four-prong lady's ring.

Figure 6. Damage to the diamond in figure 5 is related to the combination of a thin girdle and shallow crown angles, as can be seen in this profile view.

Figure 7. A GIA Proportion Scope revealed that the diamond in figures 5 and 6 had crown angles of about 25°.

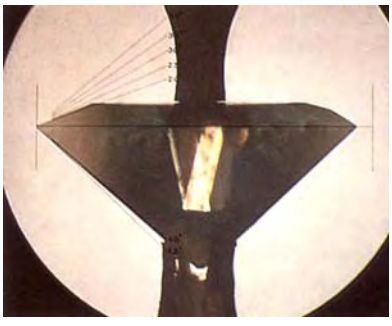

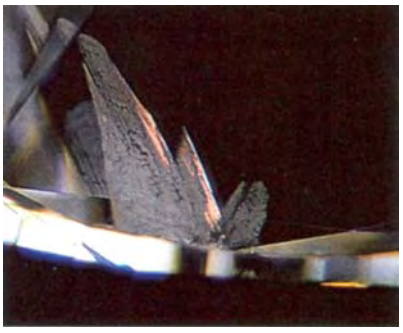

Figure 8. Only a muted pink flash color could be seen in this filled fracture in a 1.05 ct oval diamond. Magnified 30 ×.

Figure 9. At higher (63 ×) magnification, the dendritic pattern of the flow structure and cloudiness of the fracture shown in figure 8 con firmed that it was filled.

41°. This combination of cutting faults usually leads to damage during normal wear. The potential for damage to such a stone can be minimized by choosing mountings, such as gypsy or bezel settings, that protect the girdle area.

GRC and TM

Identifying Filled Fractures: New Challenges

Over the last six months, the East Coast lab examined four diamonds with unusual-appearing fractures. These stones gave us an advanced lesson in distinguishing filled fractures from unusual-appearing fractures that are unfilled, a lesson that required checking for all the features summarized by McClure and Kammerling in "A Visual Guide to the Identification of Filled Diamonds" (Summer 1995 *Gems & Gemology,* pp.114–119, plus chart).

A 1.05 ct oval modified brilliant showed muted, subtle flash-effect colors (figure 8), similar to those observed in filled diamonds that had been heated (see Kammerling et al, "An Update on Filled Diamonds: Identification and Durability," Fall 1994 *Gems & Gemology,* pp. 142–177, especially figure 27). This prompted us to examine the fracture closely at higher magnification, which revealed a dendritic pattern typical of filled fractures, together with flow structure and cloudiness in the fracture plane (figure 9).

A contrasting unfilled example was provided by a cleavage in a 1.23 ct round brilliant (figure 10). Although large in area, this break was nearly invisible from most angles. Higher magnification, with a variety of lighting techniques, revealed neither flash colors nor any internal structure—all of which indicated that the cleavage was not filled. An X-radiograph confirmed this conclusion. The entire stone, including the fracture, was transparent to X-rays, whereas fracture-filling material would have been opaque.

An unusual inclusion that proved to be fracture-filled was seen in the 1.01 ct round brilliant shown in figure 11. A laser drill hole led to a crystal inclusion centered in a large fracture. The walls of the drill hole showed a rough texture, as did the fracture at the p oint of drill-hole contact. At the point of contact, the surface of the fracture appeared burned. The rest of the fracture was smoother and showed flow structures. We observed flash colors only in the areas of the fracture that surrounded the crystal; these ranged from orange to pink and blue.

The complicated group of fractures in figure 12 illustrate the importance of viewing angle in identifying filled fractures. From most sides, this 1.48 ct marquise showed both the characteristic flash colors of filled fractures and the natural iridescence of unfilled fractures. The profile view of this diamond (figure 13) showed one unfilled fracture that displayed a whole rainbow of interference colors, and another fracture, nearly perpendicular to the first, with a blue flash color. This diamond illustrates the importance of not halting the examination of a stone before it is viewed from all sides, as not all fractures in a filled stone can or will absorb the filling. The

Figure 10. This large cleavage in a 1.23 ct round brilliant diamond stretches from the pavilion to the table. Although not filled, the cleavage was only visible from a few viewing angles. Magnified 15×.

Figure 11. Flash colors and flow structure characteristic of fracture filling are visiable in parts of this complex inclusion in a 1.01 ct round brilliant diamond. Magnified 45×.

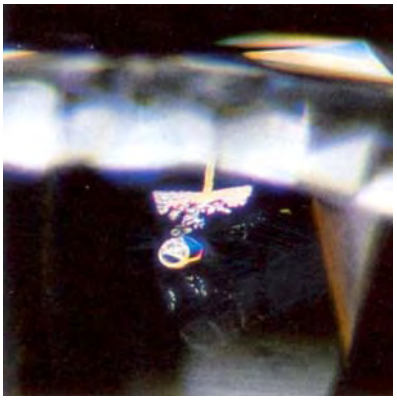

Figure 12. Some of the fractures in this 1.48 ct marquise are filled and others are unfilled.

many fractures and their reflections in this diamond made the presence of fracture filling unusually difficult to identify.

IR and Vincent Cracco

Imitation

From time to time, mineral specimens—loose crystals or pieces of rough—are submitted to GIA GTL for identification. Transparent-to-translucent, near-colorless specimens arc usually submitted in the hope that they will turn out to be diamond. Sometimes these specimens have been doctored to resemble diamond crystals. Although occasionally minerals other than diamond are used for this purpose, the most common imitation diamond rough that we see is fashioned from cubic zirconia (see, for instance, Lab Notes, Winter 1988, pp. 241–242, and Fall 1996, p. 205; Gem News, Spring 1994, p. 47).

Standard gemological testing alone was sufficient to identify a specimen of near-colorless rough that was submitted to the East Coast lab last winter. The rough had triangular engravings, resembling trigons, on part of its surface (figure 14). The specific gravity was also approximately that of diamond—and very different from that of CZ. However, one flat

Figure 13. In profile, the stone in figure 12 can be seen to contain naturally iridescent unfilled fractures (to the right of the tweezer) as well as a blue flash effect (visible throughout the region to the left) from reflections of filled fractures. Magnified 20×.

(cleaved or polished) surface gave refractive indices of about 1.61–1.63. The fact that the material was doubly refractive meant that it clearly could not be either diamond or CZ. With magnification, we observed fluid inclusions, which also typically are not encountered in diamond.

This combination of properties identified the rough as topaz. The markings were probably added to simulate "trigons," to better convince the unwitting buyer that this was a diamond. Although the term is a misnomer and rarely used today, colorless topaz was once called "slave's diamond" because of its resemblance to diamond (see M. Bauer, *Precious Stones,* Charles E. Tuttle & Co., Rutland, Vermont, 1969, p. 330).

Figure 14. Trigons were engraved on this 17.56 ct colorless topaz rough to make it look like a diamond.

Nicholas DelRe

HORNBILL "IVORY"

An elaborate yellow metal brooch (figure 15) was sent to our East Coast lab for identification of its large center carving. Accented by two large pearls, this semi-translucent red and yellow portrait of Buddha measured about 70 × 47 × 12.5 mm.

Only very limited gemological tests could be performed because of the mounting. However, we did get a vague spot refractive index reading, in the low 1.50s, from a small, fairly well-polished area on one side. The carving fluoresced a faint bluish white to short-wave ultraviolet radiation, which is similar to the response of some dentine ivories as well as of hornbill "ivory," a nondentine material that is among the rarest of gem rriaterials.

Observation with a microscope at about 10× magnification revealed numerous thin, parallel fibers in the yellow part of the carving, with a few small dark-pigmented granules scattered throughout. These structural characteristics are typical of an organic material such as ivory. The thin layer around the main carving was uniformly red, with no internal features apparent. The transition from the red to yellow areas was gradual, with no obvious demarcation separating the different colors. These characteristics proved that the carving was a single piece and not assembled. We concluded from these properties, especially the distinctive red and yellow coloring and the structure seen with magnification, that this carving was fashioned from hornbill "ivory."

Figure 15. This portrait of Buddha is carved from rare hornbill "ivory."

Hornbill "ivory" is obtained from the casque (the large protuberance covering a portion of the head and bill) of the helmeted hornbill, an exotic bird *(Rhinoplax vigil)* native to southeast Asia and Borneo. (Because this material is not fashioned from teeth or tooth modifications, such as tusks, it is not considered a true ivory.) Comprehensive articles have appeared in *Gems & Gemology* (A. S. Munsuri, "Hornbill Ho-Ting," Fall 1973, pp. 208–211; R. E. Kane, "Hornbill Ivory," Summer 1981, pp. 96–97) and in the *Journal of Gemmology* (G. Brown and A. J. Moule, "Hornbill Ivory," January 1982, pp. 8-19). The distinctive bright red border of the yellow helmet makes this material easy to identify despite its rarity. *KH*

Editor's Note: The helmeted hornbill has been declared endangered throughout the region where it lives. Commerce in recent hornbill "ivory" is now illegal in most countries, including the United States. However, hornbill-" ivory" pieces 100 years old or older may be legal to own and import, provided they have not been repaired recently.

MOGUL TALISMANS

An interesting set of three large baroque beads, which reportedly once belonged to the Mogul emperor Akbar Shah (1542–1605), were submitted to the East Coast laboratory for testing. The set (figure 16) consisted of a natural pink spinel, a natural blue sapphire, and an aquamarine. Standard gemological testing readily identified the materials from which each bead was fashioned.

The spinel's gemological properties were within normal published values. Mineral inclusions established that the stone was natural. It fluoresced strong red to long-wave UV radiation and moderate red to short-wave UV. As expected from the fluorescence, the stone showed several sharp "organ pipe" lines beyond 650 nm in the red end of the spectrum, which are due to the presence of chromium. The sapphire fluoresced weak red to long-wave UV. It had a moderately strong 450 nm line with weak "chrome lines" in its absorption spectrum. Long, fine needles, pristine crystals, and fluid-filled "fingerprint" inclusions were visible with magnification, indicating that the stone had not been heat treated.

The aquamarine had a "spot" refractive index of 1.57 and a rather strong iron line at 427 nm. The most distinctive feature was its color. Before the now-common

Figure 16. A set of beads, which reportedly once belonged to a Mogul emperor, consists of a 114.38 ct spinel, a 106.57 ct sapphire, and an 87.72 ct aquamarine

Figure 17. The spinel bead in figure 16 is inscribed with the names "Akbar Shah" and Jehangir," as well as with the (Moslem calendar) date "971."

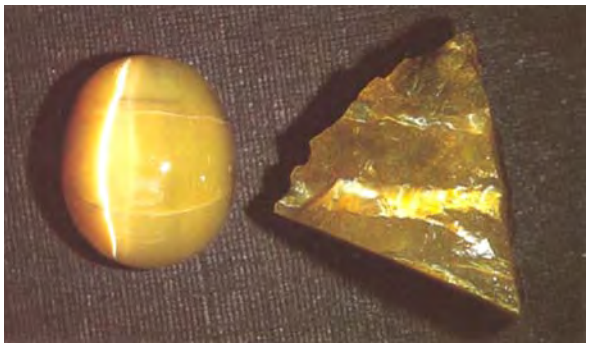

Figure 18. This 4.86 ct cat's-eye opal cabochon was cut from a band similar to those in the accompanying 8.59 ct piece of rough

Figure 19. Chatoyancy in this 2.92 ct quartz cabochon is caused by reflection of light from the parallel array of coarse rutile needles.

practice of heat treating aquamarines to make them blue, the green color was actually considered more desirable (see, e.g., K. Nassau's *Gemstone Enhancement,* 1st ed., Butterworth, Oxford, England, 1984, p. 98). The aquamarine bead is this green color.

Because it is often difficult to validate historical information, we were unable to verify the age(s) of the beads. However, careful observation can sometimes provide indications of authenticity. The green color of the aquamarine bead is one such indication. In addition, all the beads had crude conical drill holes, which indicates that they were drilled with hand tools and not by machine. Further, the names Akbar Shah and Jehangir (his son), together with the date 971 (on the Moslem calendar, which is 1565 on the Gregorian calendar) are inscribed on the spinel (figure 17). These inscriptions are in keeping with a tradition of engraving gemstones with the names of rulers in India. An inscribed Mogul spinel from the time of Jehangir is in the collection of the Victoria & Albert Museum in London (Benjamin Zucker, pers. comm., 1996).

TM and GRC

OPAL, with True Chatoyancy

In 1983, a piece of greenish yellow banded rough—identified as opal—was donated to the GIA collection. Later that year, we were shown a 1.5 ct brownish orange chatoyant stone that was purportedly cut from one of the bands of this type of material (see Spring 1983 Lab Notes, pp. 45–46). Although this cabochon was also identified as opal, it was very different in color from the rough specimen in our collection. The Fall 1990 Gem News section (pp. 232–233) reported on a 0.76 ct opal that had a sharp "eye" and showed an excellent "milk and honey" effect. Because such chatoyancy is relatively rare in opal, the laboratory was not able at that time to determine the reason for this phenomenon. (A different type of chatoyancy—and even asterism—is seen in opals with chatoyant play-of-color, including some stones from Jalisco, Mexico [see, e.g., Winter 1990 Gem News, p. 304], and especially Idaho.)

Earlier this year, staff members at the East Coast lab remembered the greenish banded rough while identifying a 4.86 ct cat's-eye opal. When this cabochon and the rough piece were examined side by side (figure 18), the similarity in color of the two specimens was evident; now it was easier to believe that the previous examples had been cut from similar rough. This material is unusual in that it shows chatoyancy caused by linear inclusions—that is, "true" chatoyancy. Such inclusions are uncommon in opal, which is primarily composed of small spheres of silica.

TM and GRC

QUARTZ, Cat's-eye Effect Caused by Large Rutile Needles

The cat's-eye phenomenon in gemstones is usually caused by either of two forms of fine parallel inclusions. One form involves hollow tubes, as in cat's-eye emeralds and tourmalines (see, for instance, Winter 1990 Gem News, pp. 306–307). The other involves needle-like inclusions, as in the cat's-eye apatite illustrated in the Fall 1995 Gem News (pp. 205–206). In many samples of cat's-eye and star quartz, the inclusions that cause this phenomenon are very fine rutile needles. This was not the case, however, with a 2.92 ct cabochon submitted to the West Coast laboratory in summer 1996: The rutile inclusions responsible for the cat's-eye effect were large and prominent (figure 19). In fact, had this stone not demonstrated chatoyancy, we would have simply called it rutilated quartz. However, because this stone fit the criteria for both cat's-eye quartz and rutilated quartz, our conclusion stated that it was cat's-eye rutilated quartz.

MLJ and SFM

PHOTO CREDITS

Nicholas DelRe supplied the pictures used in figures 1,2, 14, 15, and 18. Figures 3 4, and 19 were taken by Maha DeMaggio. The photos in figures 5–13 were taken by Vincent Cracco. Figures 16 and 17 are courtesy of Dr. Gary Hansen, St. Louis, Missouri.

GEM N.E.W.S

Editors • Mary L. Johnson and John I. Koivula

Contributing Editors
Dino DeGhionno and Shane F. McClure,
GIA GTL, Carlsbad, California
Emmanuel Fritsch, University of Nantes,
France Henry A. Hänni, SSEF, Basel, Switzerland

TUCSON '97

For the colored stone market, the new year begins not on January 1, but in late January to early February, at the many shows in Tucson, Arizona. The Gem News staff visited 17 of the 23 "official" shows—of gems, minerals, beads, and finished goods. We also combed the blocks-long bazaar of open-air booths and tents that paralleled the Interstate 10 highway.

This year, a one-week gap separated two of the biggest shows, the American Gem Trade Association (AGTA) show and the retail segment of the Tucson Gem and Mineral Society (TGMS) show, both held at the Tucson Convention Center, so the overall "Tucson experience" lasted just over three weeks (from January 26 through February 16). Several of the more interesting materials and individual stones that we uncovered are discussed here, and more will be profiled throughout the year. Special thanks go to GIA Gem Trade Laboratory gemologists Maha DeMaggio (who also photographed many of the specimens), Cheryl Wentzell, Nick DelRe, and Phillip Owens for their tireless questing after the new, the unusual, and the downright odd.

DIAMONDS

"Opalescent" and other unusual diamonds. Although the Tucson shows primarily showcase colored stones, some interesting diamonds were also available, including black diamonds, treated-color green and blue diamonds, and naturally "colored" (by cloud-like inclusions) "white" diamonds. These "white" diamonds are sometimes called "opalescent" because flashes of spectral colors, caused by dispersion from the back facets, resemble play-of-color when viewed through their milky white body color. One such diamond is shown in figure 1: In the table-down position, it has a "J" color grade and is faintly brown. Similar diamonds were also discussed in the Spring 1992 Gem News section (p. 58).

Diamond crystals were prominent at the TGMS show. David New, of Anacortes, Washington, showed diamond crystals from many localities, including five from the new Kelsey Lake mine in Colorado and a "Star-of-David" twinned made from South Africa. (A similar crystal is described and illustrated on pp. 117–118 of the Summer 1991 Gem News section).

Diamond "pearls." For some time, one editor (MLJ) has been intrigued by the idea of a cabochon diamond. This year, at the booth of Crystal Classics, Okehampton, Devon, England, she found the next best thing: diamond "pearls" (figure 2). Dr. Heinz Malzahn, of Berlin, Germany, has adapted the technique for making round pearlescent diamonds from one used by De Beers around 1970 to process industrial diamonds. According to Dr. Malzahn, rough diamonds with roundish shapes are ground to rough spheres and then "'cooked" in sodium carbonate, in an inert atmosphere at about 800°C, to produce the pearly surface. This process is sometimes referred to as chemical polishing by selective

Figure 1. This 0.03 ct "opalescent" diamond was among several marketed by Malhotra Inc., New York City. Photo by Maha DeMaggio.

Figure 2. These 1.66 and 0.28 ct diamond "pearls" were polished by selective dissolution in hot sodium carbonate. The larger "pearl" measures about 5.76 ×5.58 mm. Photo by Maha DeMaggio.

dissolution: Comer sites on the surface of the diamonds etch faster than edge sites, and edges dissolve faster than flat or curved surfaces, resulting in a smoothly polished round stone. Because the process is destructive, we have only seen the results of treating "industrial" (non-gem) diamond crystals.

Custodiam, a Brussels firm, is also marketing "diamond pearls," according to the December 1996 issue of *Antwerp Facets* (pp. 37, 39). They also grind rough diamonds into spheres, which they then "polish" by chemical etching. Belgian designers—such as Christiguey and Jan Pycke—are using these "pearls" in jewelry.

COLORED STONES AND ORGANIC MATERIALS

Andradite from Arizona. Mineral collectors are familiar with the clusters of brownish green andradite crystals, some with iridescent surfaces, that have been found for many years at Stanley Butte in Graham County, Arizona. Although these specimens typically have bright surfaces and sharp crystal faces, they are not transparent enough to facet. This year at Tucson, however, Charles Vargas of Apache Gems, San Carlos, Arizona, was offering gem andradites (figure 3) from a new locality near Apache Camp on the San Carlos Apache Reservation,- this is about 10 miles (17 km) from the Stanley Butte locality.

These garnets come from a contact zone between carbonate-rich basement rocks and basalt lava flows, according to Mr. Vargas. The garnet deposit was discovered only recently, in June 1996, and there was no evidence that it had been worked earlier. The garnets occur as dodecahedral crystals, with calcite, in pockets in multiple decomposing dikes within a 15 square-mile (about 40 km2) area; up to 18 inches (about 45 cm) of topsoil covers the dikes. As of early April 1997, Mr. Vargas reports, the largest fashioned andradite weighed about 4 ct; production was a few kilos per month of faceted stones, ranging in size from melee to just over 1 ct.

We examined 10 andradites (see, e.g., figure 3), which weighed 0.10 to 1.51 ct. All had properties typical for andradite garnet: brownish greenish yellow to yellow- brown color, singly refractive optic character, R.I. greater than 1.81 (over the limit of a standard refractometer), and no reaction (inert) to both long- and short-wave ultraviolet radiation. Specific gravity values—determined hydro—statically-averaged 3.92 (18 readings on nine stones). All 10 samples had a line at 440 nm in a desk-model spectroscope. Visible through the microscope were healed fractures, "fingerprints," growth banding, a few dark crystals (in two stones), and two-phase inclusions (in four stones). The growth banding was visible as linear or roiled features in plane-polarized light and showed first- to low-second-order interference colors between crossed polarizers. No "horsetail" inclusions were seen.

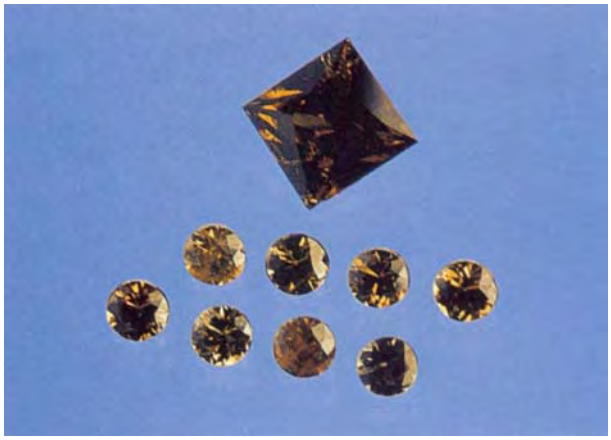

Figure 3. These nine faceted andradites (0.10–1.51 ct) are from a newly discovered contact metamorphic deposit on the San Carlos Apache Reservation in Arizona. Stones courtesy of Apache Gems-, photo by Maha DeMaggio.

Carved aquamarine with natural crystal faces. In the Winter 1996 Gem News section (p. 283), we reported on faceted stones that had incorporated naturally etched faces of the original crystal. The stones illustrated were gem varieties of beryl; this mineral, occurring as it does in late-stage pegmatites, often shows shattered or dissolved surfaces that have healed into well-defined crystal faces. Mark Herschede Jr., of Turmali and Herschede, Sanibel, Florida, showed one of the editors another variation on this same idea using aquamarine from the Ukraine. Not only did the approximately 45 ct stone include part of the natural crystal, but carver Glenn Lehrer (Lehrer Designs, San Raphael, California) had also fashioned the bail as part of the pendant (figure 4).

Cat's-eye chrysoberyl. One of the notable stones at the AGTA show was a large, fine cat's-eye chrysoberyl (figure 5), shown by Evan Caplan of Los Angeles, California. The 72.68 ct cabochon is reportedly from the Faisca area in northeastern Minas Gerais, Brazil, which has been producing relatively large quantities of fine chrysoberyl since 1939 (see, e.g., K. Proctor, "Chrysoberyl and Alexandrite from the Pegmatite Districts of Minas Gerais, Brazil," *Gems & Gemology,* Spring 1988, pp.16–32). Two flat sur faces on the back

Figure 4. This approximately 45 ct aquamarine pendant, shown here as viewed from the side, was carved both to include faces from the original crystal and to provide its own bail. Carving by Glenn Lehrer, courtesy of Turmali and Herschede-, photo by Maha DeMaggio.

Figure 5. Some particularly fine cat's-eye chrysoberyl from Brazil was shown in Tucson this year, including this 72.68 ct cabochon and the accompanying 317.7 ct piece of rough. Courtesy of Evan Caplan; photo by Robert Weldon.

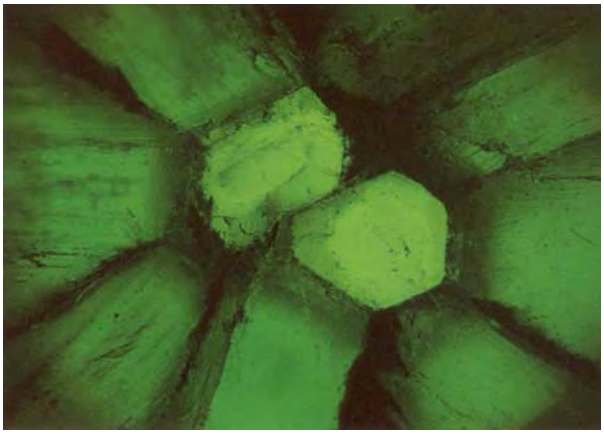

Figure 6. The double center in this 3.50 ct trapiche emerald is most unusual. Photomicrograph by John I. Koivula; magnified 5×

of the stone marked where two pieces had been removed to cut two smaller cabochons. Mr. Caplan the also had a large (317.7 ct) piece of rough chatoyant chrysoberyl that also reportedly originated from the Faísca area.

Unusual trapiche emerald. Ron Ringsrud of Constellation Colombian Emeralds, Saratoga, California, displayed a variety of trapiche emeralds from Colombia at his booth in the AGTA show. One cabochon was particularly unusual, in that it had two central columns, each with the black "spokes" typical of trapiche emeralds (figure 6). The 3.50 ct oval cabochon measured 10.24 × 8.95 × 5.97 mm. The double-column structure extended completely through the stone and appeared to taper only slightly from the dome to the base of the cabochon. Perhaps the double center resulted from parallel growth of two individual crystals that were later incorporated into one piece as growth continued. This double-center trapiche emerald was the first that Mr. Ringsrud or any of the Gem News editors had encountered (although K. Nassau and K. A. Jackson showed a trapiche emerald slice with two inter-grown crystals in the April 1970 *Lapidary Journal,* p. 82).

The return of jet. The natural hydrocarbon jet became popular in mourning jewelry in the late Victorian era. With the recent interest in black opaque materials (see, for instance, "Some Gemological Challenges in Identifying Black Opaque Gem Materials" by M. L. Johnson et al, Winter 1996 *Gems & Gemology,* pp. 252–261), we noticed more jet at Tucson this year, including bead necklaces from Czechoslovakia. At the Pueblo Inn, Russian dealer Serguei Semikhatov of Lithos, Irkutsk, had blocks of massive jet and a few carvings, including the bear shown in figure 7. The material is being quarried near the village of Matagan, on a river leading into Lake Baikal north of the city of Irkutsk, according to Mr. Semikhatov. The Russian name for this material is "gagate."

"Bicolor" labradorite. So-called "spectrolitc"—

Figure 7. This 71.1 × 42.1 × 41.1 mm bear was carved from the hydrocarbon jet, which is being quarried near Matagan, Russia. Photo by Maha DeMaggio.

labradorite feldspar with iridescent schiller—is by no means a new material, and the locality at Ylämaa, Finland, is also well known. However, this year, G.P.G. Trading of New York City, in conjunction with Jogan Oy, Mikkeli, Finland, was marketing large quantitites of cabochons—in a variety of shapes—that had been cut from this material. Subsequently, one of the editors saw a nicely patterned 9.51 ct rectangular cabochon with a distinct delineation between two colors of sheen (figure 8) at the booth of another firm, the D&R Collection, Los Angeles.

According to Don Pier, of G.P.G. Trading, the leaseholder recently extracted 650 tons of material from this locality, using earth-moving equipment. The Ylämaa deposit is located close to the Russian border and the Arctic circle,- the nearest town is Lappeenranta. Mr. Pier estimates that the deposit is about 5 m wide by 40 m long by 80 m deep; because it is in a permafrost region, mining is possible only three months a year. The labradorite is being fashioned into calibrated goods by cutters in Sri Lanka.

Figure 8. This 9.51 ct labradorite cabochon from Finland (17.65 × 13.75 × 4.01 mm) has blue and orange schiller in a "bicolor" pattern; the center white stripe probably marks the boundary between two adjacent crystals. Photo by Maha DeMaggio.

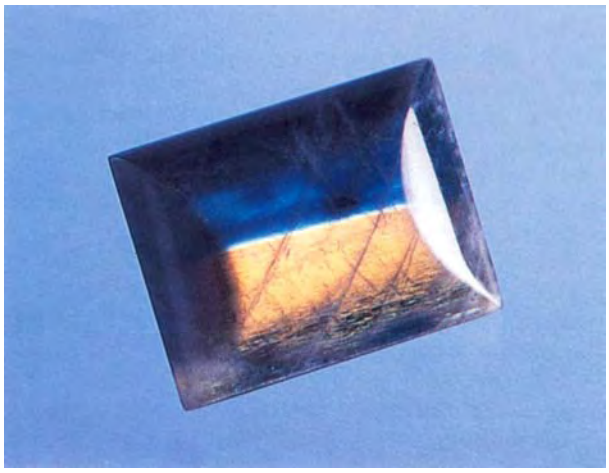

Figure 9. This 20.58 ct "rainbow" obsidian cabochon (19.20 × 16.39 × 10.91 mm) has been carved at its broadest point to produce a heart-shaped pattern of iridescence. Note the hole-visible on the right, where the cabochon has been drilled for easy stringing on a chain or cord. Photo by Maha DeMaggio.

"Rainbow" obsidian hearts. We have reported in the past on "rainbow" obsidian from Mexico, which shows layered schiller in interference colors (see, e.g., Summer 1993 Gem News, p. 133). In 1996, many dealers were showing this material fashioned in a new way: A groove cut into the widest part of an oval or pear-shaped cabochon the size of a paperweight produced a pattern of concentric hearts. This year, Zee's of Tucson, Arizona, added yet another twist: Jewelry-size cabochons with the heart pattern were drilled through their tops, so that a chain or cord could be passed directly through the piece (figure 9).

Botryoidal white opal from Milford, Utah. The botryoidal opal from Milford, Utah, has been known for at least 20 years. Since 1996, William Cox, a gem cutter from Provo, Utah, has been cutting this material into flat-topped free-form cabochons with curved schiller—a result of the botryoidal internal layering. Mr. Cox is marketing these cabochons as Satin Flash opal.

We examined the cabochon shown in figure 10. With magnification, we saw a structure of curved layers throughout this material; some layers showed crazing in reticulated patterns, but cracks were confined to individual layers for the most part and did not extend through the stone. Some small rounded white crystals were also visible,- these were clumped in small patches rather than distributed evenly throughout the material. When examined with crossed polarizers, the stone did not

Figure 10. This 37.18 ct opal fmm Milford, Utah demonstrates schiller from its curved internal surfaces. Stone cut by William Cox, provided courtesy of Richard Shall, Out of Our Mines, Arcata, California; photo by Maha DeMaggio.

show the extremely high strain characteristics of hyalite opals from most localities. The cabochon had a typical opal R.I. of 1.45, and a specific gravity—measured hydrostatically— of 2.14; it was inert to both long- and short-wave UV.

Similar opal from Utah—banded in translucent brown and translucent-to-transparent white—was seen in the booth of Charles R. Richmond, Blountville, Tennessee. Marketed as Candy-Stripe opal, this material could be carved into cameos or striped cabochons, depending on the orientation.

Petrified palm wood as an ornamental material. Women's fashions sometimes affect the popularity of certain gemmaterials. For instance, last year's emphasis on bright orange, yellow, and lime green clothing helped spark interest in "Mandarin" spessartine garnets, peridot from Pakistan, and grossular-andradite garnets from Mali. This year, one fashion trend is a growing interest in "animal prints"—fabrics designed to resemble the hide patterns of leopards, zebras, and other animals. Joe Jelks of the Horizon Mineral Co., Houston, Texas, markets cabochons of certain naturally patterned stones as "animal print" cabochons, including Australian "zebra rock" (sec, e.g., Gem News, Summer 1994, pp. 128–129). Another material that is enjoying increased popularity—in part because of its resemblance to animal patterns—is petrified palm wood from Louisiana, Texas, and Arkansas. Although this is not a new material, custom jewelry makers are beginning to explore its design possibilities. The three pieces of petrified palm wood in figure 11 show some of the colors and patterns in which the material is available. The 45 × 42 mm brooch, by Nature/Man, Lyons, Colorado, contains tan wood with a leopard pattern in black; while the rough samples from Ancient Earth, Hurricane, Utah, are reddish brown with tan patterns and tan with brown patterns.

Figure 11. Petrified palm wood shows a variety of colors and animal patterns. Photo by Maha DeMaggio.

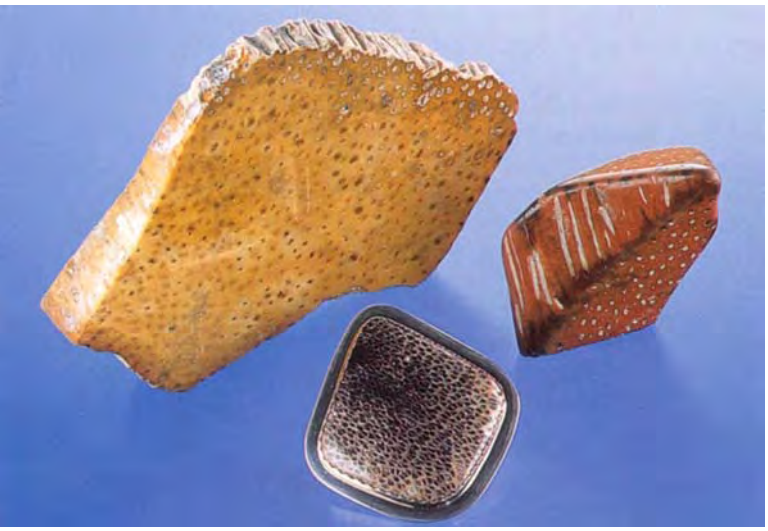

Figure 12. This rough section of a concretion from the Volga River, and the cabs cut from similar material, have surfaces of naturally iridescent drusy pyrite. The largest cab measures 21.73 × 13.02 × 4.61 mm. Stones courtesy of foe Jelks; photo by Maha DeMaggio.

Drusy iridescent pyrite from Russia. The interest in drusy materials continues unabated. One new material this year was drusy pyrite, found as crystals lining concretions in the bed of Russia's Volga River. We borrowed samples of rough and fashioned material (figure 12) from Joe Jelks of the Horizon Mineral Co. The concretions are gathered from one section of the Volga when the water is shallow. The pyrite is naturally iridescent, according to Mr. Jelks, and has not been artificially tarnished. The concretion material itself is sufficiently strong that a separate backing material is not required.

"Wasp-tail" citrine/smoky quartz. Klaus Schafer, a young gem carver from Idar-Oberstein, Germany, cuts exacting stones from humble materials. This year, he showed several bar-shaped faceted stones cut from a

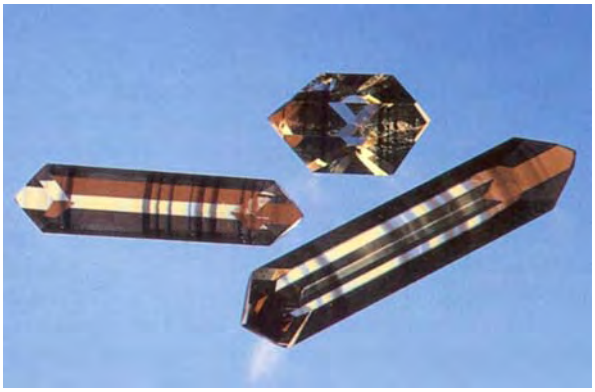

Figuie 13. These quartz "wasp-tails" (4.4 to 9.61 ct) were cut from a chunk of heat-treated citrine/smoky quartz from Brazil. Stones courtesy of Klaus Shäfer; photo by Maha DeMaggio.

single heat-treated piece of banded citrine and smoky quartz (figure 13). The bars had been carefully cut—perpendicular to the growth zoning that paralleled a rhombohedral face—so that the color bands were distinct. Mr. Schäfer calls these pieces "wasp-tail" quartz, but he agreed that they also looked like bar codes. He showed these at the booth of Richard Bernhard and Company, Idar-Oberstein.

Quartz with "rainbow" hematite inclusions . . . We have seen quartz included with red iron oxides from Madagascar (Fall 1995 Gem News, pp. 209–210) and Kazakhstan ("strawberry quartz," Spring 1995 Gem News, pp. 63–64). This year at Tucson, Vladimir Chernavtsev of Charmex, Moscow, was showing quartz included with very thin hexagonal to irregular plates of hematite, showing an iridescent "rainbow" tarnish; this material came from Aldan Mountain in Yakutia. A 25.59 ct polished free-form hexagonal tablet (22.20 ×18.47 × 6.50 mm) is shown in figure 14. The thicker hematite plates look black and opaque, but those that are thin appear transparent red and some plates show regions of both colors.

Figure 14. Thin plates of bright red-to-black hematite, with an iridescent "rainbow" tarnish, are visible in this 25.59 ct polished free-form hexagonal tablet of quartz from Yakutia. Photo by Maha DeMaggio.

... And with pyrite inclusions. Aventurescence in quartz is generally thought to be caused by the presence of many tiny platelets of the chromium-colored variety of mica known as fuchsite. In such quartzes, the inclusions are randomly oriented. Thus, in almost any cutting orientation, a sufficient number of the platelets show essentially the same reflective direction, so that aventurescence occurs in reflected light without a special need to orient the rough before cutting.

However, Gem News editor John Koivula acquired another form of aventurescent quartz from the Gemological Center, Belo Horizonte, Brazil. The host material was a 70.48 ct oval faceted rock crystal quartz that measured 40.01 × 21.44 × 12.67 mm (figure 15). Here, the mineral inclusion causing the aventurescence was pyrite.

The pyrite inclusions creating the distinctive reflectance did not display the isometric crystal habits typical for this mineral. Instead, these crystals grew as disks in a fracture plane in the quartz host. As seen in figure 16, these inclusions strongly resemble the so-

Figure 15. Aventurescence in this 70.48 ct rock crystal quartz is caused by light reflecting off a multitude of pyrite inclusions. Photo by Maha DeMaggio.

Figure 16. The disk-shaped aventurescence-causing pyrite inclusions in the stone shown in figure 15 formed along a single fracture plane. Photomicrograph by John I. Koivula; magnified l0×.

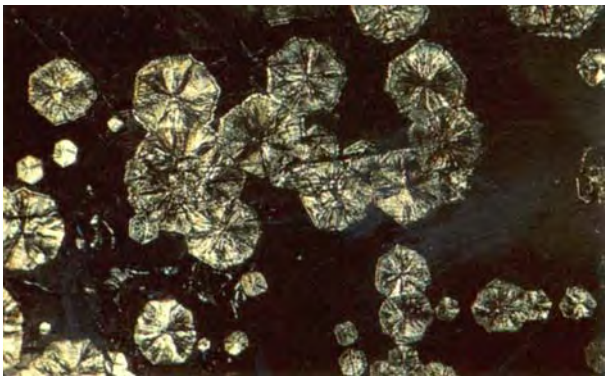

Figure 17. The color in this 2.28 ct Tundura sapphire is exceptionally vivid. Courtesy of Malhotra Inc.; photo by Maha DeMaggio.

called pyrite "sand dollars" or "suns" that are found as concretions between bedding planes in black and gray shale and slate.

To create the unusual aventurescence, the lapidary had to position the layer of pyrite disks at an angle just off-parallel to the table facet. This was done so that the aventurescent effect could be seen without the distraction of light reflections off the table facet surface. This need for specific orientation of the inclusion plane is in direct contrast to the random orientation of cutting quartz in which the aventurescence is caused by fuchsite.

Orange sapphire and other gems from the Tundura region. East Africa continues to produce astounding gems. One example is shown in figure 17: a 2.28 ct bright slightly reddish orange natural sapphire from the Tunduru region of Tanzania, shown by Malhotra Inc., New York City. Mr. Malhotra said that he had not seen a stone of such color in his 40 years in the trade. The stone had been cut in Bangkok and may have been heat treated.

Other unusual materials from Tanzania (seen at the booths of New Era Gems, Grass Valley, California) included: peridot and "mint" (light green) and "honey" (brownish yellow) grossular from Mcrelani; and light-pink and light-purple to "rose pink" spinel from Pokot, near Tunduru. According to Bill Vance of New Era Gems, some blue-to-purple spinels from Tunduru look pink when viewed through the Chelsea filter, so he suspects that they contain cobalt.

Tanzanite in abundance: Gem carvings and "enhydro" crystal section. Tanzanite was readily available in Tucson this year. One possible reason was that-in addition to the "traditional" tanzanite mines (see, e.g., Summer 1996 Gem News, pp. 135–136)—the gem is now being recovered as a byproduct of large-scale graphite mining in the Merelani region, as reported in the *Mineralogical Record* (T. Moore, "What's New in Minerals: Denver Show 1996," Vol. 28, No. 1, 1997, especially p. 60). In addition to plentiful supplies of calibrated goods, we saw some notable individual pieces. New Era Gems showed several examples, including a 255.75 ct terminated blue crystal that contained an obvious fluid inclusion, with a movable gas bubble (figure 18). They also showed contributing editor Shane McClure a trio of tanzanite gem carvings: a rabbit, a frog, and a horse head (figure 19).

Another firm, Affro Gems of Dallas, Texas, had some tanzanites with unusual colors, including a medium-toned grayish blue stone that was similar in color to some blue zircons.

Tourmaline from the Neu Schwaben region, Namibia: A major new player. After an initial offering at the Hong Kong show last September, tourmaline from Indigo Sky Gems of Windhoek, Namibia, made its U.S. debut at Tucson. The Neu Schwaben deposit is alluvial in nature, according to the company's managing director

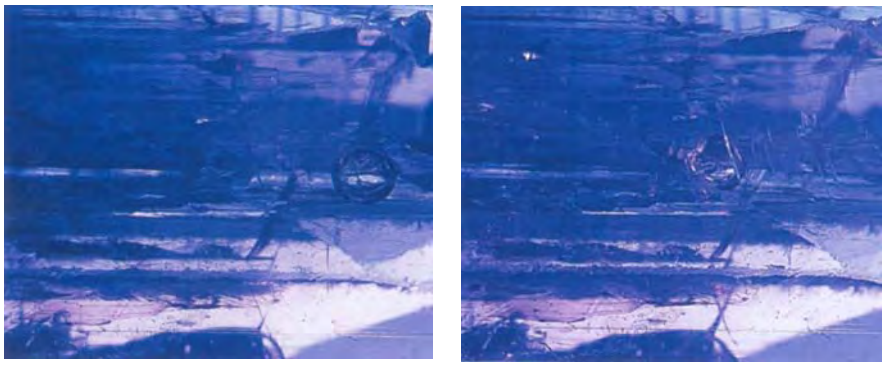

Figure 18. This 255.75 ct tanzanite crystal contains a fluid inclusion with a large gas bubble that, as is evident in these two photos, moves freely within the liquid. Courtesy of New Era Gems; photos by Maha DeMaggio.

Chris Johnston, it is expected to produce fine green, blue, and blue-green tourmalines of all sizes, from calibrated goods to major single gems, for many years to come. Several articles about this deposit have already been published in the trade press, including the November 1996 issue of *Modem Jeweler* ("Neu Schwaben Tourmaline," by David Federman, pp. 17-18); the December 1996 issue of Asia Precious ("Namibian Tourmaline Touches the Sky," by Robin Bower, pp. 96–98); and the January 1997 issue of Colored Stone ("Blue Tourmaline Makes Name for Namibia," by Greg Bartolos, pp. 539, 558–560). Mr. Johnston co nfirmed that the production information in these articles was essentially correct.

The Neu Schwaben deposit has been known to sources in Idar-Oberstein since 1925, but it has been mined by the present company only for the last year or so. Current estimates of the reserves are 12.5 million carats of gem-quality tourmaline (from 500,000 to 750,000 tons of alluvial gravels). The deposit covers a tourmaline-bearing dike—a potential source of additional material—that is about 1 km long. The Indigo Sky Company will only market cut stones, not rough; current production is 10,000 calibrated stones per month, about 10% of which are 1 ct or larger. Several large stones (see, e.g., figure 20) have been cut, with the largest to date approximately 65 ct.

The Indigo Sky Company is operating under Namibia's Export Processing Zone regulations, which are intended to encourage employment of local workers,- the company hopes to employ 150 local miners, with some of the profits being invested in providing regular medical care for workers and their families. According to Mr. Johnston, attempts are being made to mine the deposit in an "ecologically responsible fashion," so that sustainable long-term development over the mine's projected 20-year life will be accompanied or followed by reclamation of the mine site.

Gemological information on this material will appear in a forthcoming issue of *Gems &Gemology.*

TREATMENTS

Gold-electroplated jade and silver ore. Bill Heher of the Rare Earth Mining Company, Trumbull, Connecticut, always brings unusual material to Tucson. New this year were nephrite jade cabochons that had been electroplated with gold (figure 21). According to Mr. Heher, only the green and black nephrite from an old deposit near Victorville, California, responds to this treatment. This material contains magnetite inclusions, to which the gold attaches. Sometimes, only some of the black inclusions accept the gold plate (again, see figure 21). Mr. Heher first saw such treated material (not fashioned into cabochons) many years ago in Idar-Oberstein, and he had been trying to obtain some of this nephrite for many years. Finally, letters he wrote to several West Coast lapidary clubs resulted in the discovery of a few pounds of rough.

Figure 19. These are the first carvings made from gem tanzanite that the editors have seen. This 55 × 22 × 33 mm frog, 62 × 37 × 33 mm rabbit, and 44 × 26 × 12 mm horse head were at the booth of New Era Gems. Photo by Maha DeMaggio.

SYNTHETICS AND SIMULANTS

Assembled stones using inset gem material. It is well known that color concentrated in the culet of a stone will appear to be spread evenly throughout the gem

Figure 20. This 46.48 ct (23 × 18 mm) emerald-cut tourmaline from Neu Schwaben, Namibia, is representative of the fine material that this region produces. Stone faceted by Martin Key, courtesy of Indigo Sky Gems; photo by Maha DeMaggio.

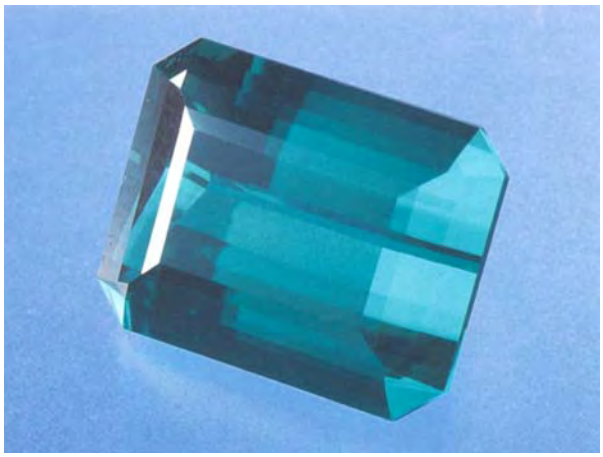

Figure 21. Magnetite inclusions in some nephrite, such as this 56.62 ct crescent-shaped cabochon (65.8 × 17.75 × 4.38 mm), form artistic patterns when electroplated with gold. Photo by Maha DeMaggio.

when that stone is viewed face up. David Brackna, a gem cutter from Germantown, Maryland, told staff gemolo-gist Cheryl Wentzell that he has found another use for this effect. For example, he set an approximately 3 mm cabochon of Australian opal within the culet area of a 14 × 12 mm faceted green beryl from the Ural Mountains in Russia (figure 22, left). Face up, the opal's play-of-color is reflected throughout the larger stone (figure 22, right). Mr. Brackna calls this technique "optical inlay."

To create this effect, Mr. Brackna first fashioned the rough beryl into an antique cushion mixed cut with a step-cut crown ("Harlequin cut"). The culet was cut off, and a concave "divot" was fashioned into the culet area of the main piece. A small opal cabochon was glued into the divot with UV-curing epoxy; the UV content of daylight was sufficient to set this glue in about 15 seconds. A replacement culet was then fashioned from a piece of beryl similar to the main piece. To increase the dispersive effects of the opal's play-of-color, Mr. Brackna carves high crowns on his pieces. The concave facet on the inside of each piece magnifies the effect of the inset material.

In the two months before the Tucson shows, Mr. Brackna cut and assembled 25 such stones. Other shapes are possible, including round and fancy cuts. For the bodies of these assembled stones, Mr. Brackna has used amethyst and citrine, as well as aquamarine and golden beryl.

Red and purple hydrothermal synthetic beryl. Two mysterious emerald cuts were turned over to GIA by the Tucson police in 1996. One, 0.81 ct, was red and the other, 0.90 ct, was red-purple (figure 23). Apparently, they had been found at a show that year and were never claimed by their owner. The red sample (measuring 7.06 × 5.10 × 3.30 mm) was strongly pleochroic—with orange (ordinary ray) and purple-red (extraordinary ray) colors; the pleochroism was so strong that the color of the sample varied from orangy red to purplish red depending on its position and orientation relative to the viewer and the light source. The red-purple emerald cut (7.05 × 5.16 × 3.64 mm) was also strongly pleochroic, with the ordinary ray orangy red and the extraordinary ray red-purple. The two samples were cut in different orientations: The optic axis ran down the length of the 0.81 ct piece, but through the width of the 0.90 ct piece.

Gem properties in common for both samples included: specific gravity (2.68, measured hydrostatically), lack of reaction (inert) to both long- and short-wave ultraviolet radiation, lack of visible luminescence, and an orangy red color when viewed through a "Chelsea" color filter. Features visible with magnification were "chevron" growth zoning (typical for hydrothermal synthetic beryl), pinpoint inclusions,

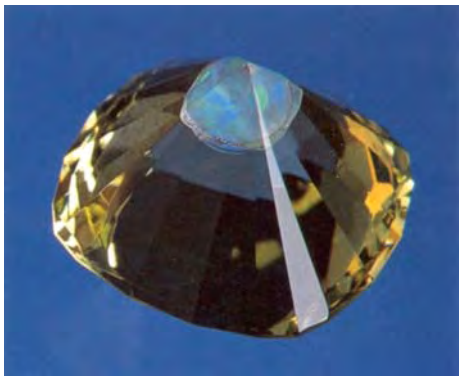

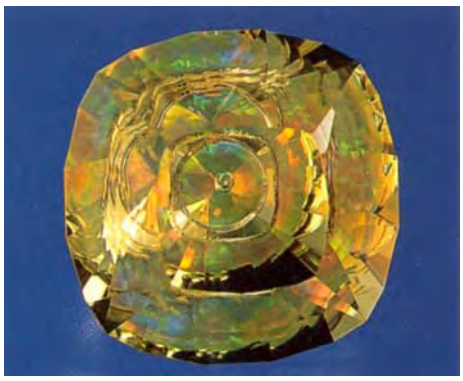

Figure 22. Left, a small opal cabochon was inserted into the culet area of this 11.82 ct assembled stone, and then covered with a replacement culet of green beryl similar to that used for the body. Right, when the stone is viewed face up, the play-of-color from the opal appears throughout. Courtesy of David Brackna; photos by Maha DeMaggio.

and stringers. The samples differed in some properties, however: The 0.81 ct red had refractive indices of 1.568-1.572 (birefringence 0.004) and a complicated absorption spectrum when viewed through the hand-held spectroscope—with a diffuse band at 420 nm, a broad 435-465 nm band, a faint band at 500 nm, a diffuse weak band at 530 nm, a strong 545 nm band, and lines at 560 and 585 nm. In contrast, the red-purple 0.90 ct emerald cut had refractive indices of 1.575–1.581 (birefringence of 0.006) and a simpler absorption spectrum—a diffuse 435 nm band, a diffuse band at 540–580 nm, and weak lines at 650, 660, and 670 nm. EDXRF revealed major amounts of Al and Si in both samples, as well as trace amounts of Mn, Fe, Ni, Cu, Zn, Ga, and Rb; the red-purple 0.90 ct example also contained Ti and Cr. All these properties were consistent with hydrothermal synthetic beryl; the samples' complicated absorption spectra are not surprising, given the many chromophores present.

Dichroic glass as an opal imitation. Nancy Goodenough is an artist from San Francisco, California, who works in glass. She creates dichroic glass cabochons (figure 24) that could be mistaken for white opal, nonphenomenal white opal, and the blue opal from Peru. Another artisan, Susan Slayton of Earthly Enchantments, Covina, California, has been creating free-form cabochons of dichroic glass that she then etches to create a matte surface (again see, figure 24). Neither artist creates these items specifically to imitate opal. However, we saw a display at one show in which such cabochons were scattered among free-form cabochons of boulder opal. They could easily have been mistaken for opals by the unsuspecting.

Figure 24. These cabochons of dichroic glass could be mistaken for opals. The large free-form piece, by Susan Slayton, measures 34.38 × 24.24 × 10.61 mm and weighs 64.82 ct; the round cabochons, by Nancy Goodenough, range from 1.30 to 4.40 ct (the largest is 10.4 mm in diameter). Photo by Maha DeMaggio.

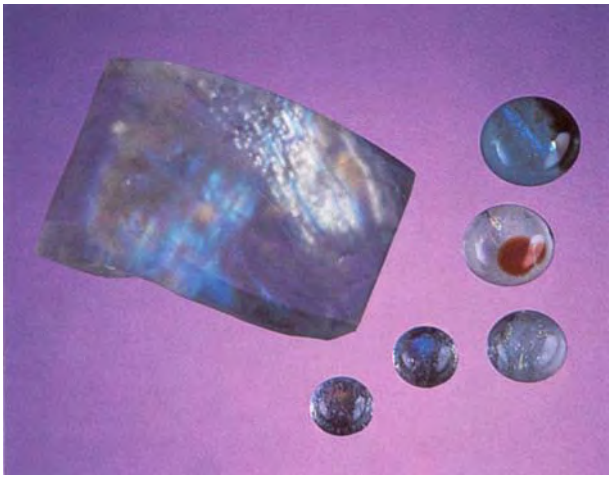

Figure 23. These samples (0.81 and 0.90 ct), left unclaimed after the 1996 Tucson show, turned out to be hydrothermal synthetic beryls. Photo by Maha DeMaggio.

Aventurescent synthetic quartz. In the quest to develop more varieties of synthetic quartz, not all experiments are successful. One exhibitor from the state enterprise VNIISIMS (the Russian Research Institute for the Synthesis of Minerals and Pilot Plant), Alexandrov, Vladimir Region, Russia, showed contributing editor Shane F. McClure two examples of an experiment gone awry. The scientists at VNIISIMS were attempting to synthesize aventurescent quartz by including flakes of copper in their hydrothermal synthesis; however, the copper flakes attached only to the middle seed plane of the synthetic quartz (figure 25).

Synthetic opal in glass. Opal is in some respects an atypical gem material because of its durability problems,- however, the beauty of opal gives it considerable value despite the risks of damage inherent in wearing it. Gilson synthetic opal is actually more durable than most natural opal, in our experience, as it is more heat resistant and does not craze. Using this durability advantage, Gerry Manning of Manning International, New York City, was offering briolettes, hearts, and spheres (figure 26) of glass with Gilson synthetic opal chips in the center, similar to the faceted "Gemulets" mentioned in the 1992 Tucson Gem News report (Spring 1992, p. 65). When examined between crossed polarizers, two spheres showed strain colors up to first-order blue, as well as flow lines and spherical gas bubbles. This implies that the glass was in a molten state when it was poured around the synthetic opal chips. A natural opal probably would not have survived this treatment.

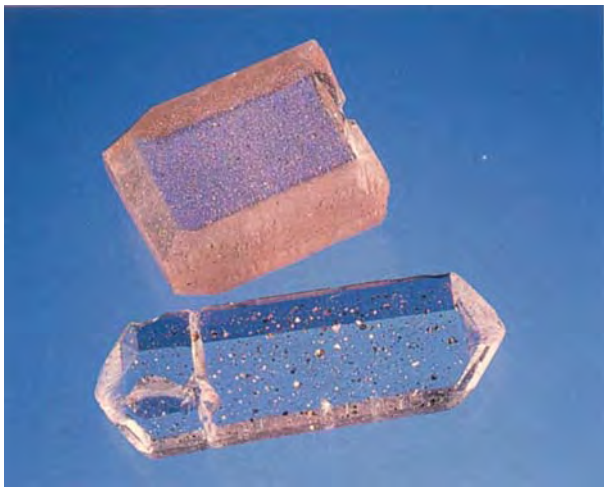

Figure 25. These two crystals of synthetic quartz (44.28 and 15.28 ct, respectively) were produced in an attempt to simulate aventurescent quartz. The spangled inclusions are metallic copper. Samples courtesy of VNIISIMS; photo by Maha DeMaggio.

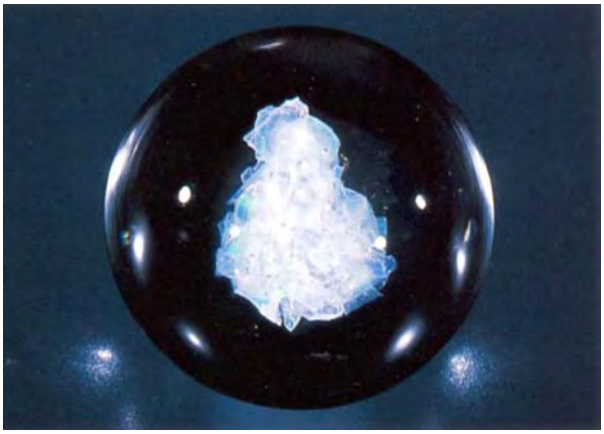

Figure 26. This 26.55-mm-diameter sphere has a center of Gilson synthetic opal. Photo by Maha DeMaggio.

MISCELLANEOUS

"Amphoragems." Many brightly colored gemmy materials are primarily available as small crystals or crystal fragments; they only appear as larger pieces on rare occasions, or at prohibitive prices. While thinking about the design possibilities inherent in a small Paraiba tourmaline crystal, Brian Charles Cook of Nature's Geometry, Graton, California, had the idea of amplifying the effect of its color by enclosing it in a magnifying setting of optical-grade quartz. This idea is the basis of the assemblages that he calls "Amphoragems," in which small euhedral crystals with saturated colors are placed in liquid-filled wells in curved quartz bottles (figure 27). Crystals of more than one material may be used in the same piece, and the cap of the "amphora" may be quartz or another material. The "bottles" may stand alone or be worn as pendants. Among the materials that have been placed in the centers of these "Amphoragems" are spessartine and chrome pyrope garnets, Paraiba tourmalines, red beryls, gold nuggets, diamond crystals, and abalone pearls; materials chosen for the caps include chrysoprase, chrysocolla, rutilated quartz, amethyst, aquamarine, and black jade.

ANNOUNCEMENTS

Gems & Gemology wins three out of five. For the third time in the past five years, *Gems & Gemology* won first place as best journal in the prestigious American Society of Association Executives (ASAE) Gold Circle competition. *Gems & Gemology* has won awards in the competition for five consecutive years, including twice winning first-place trophies for best scientific-educational feature articles. *Gems & Gemology* Technical Editor Carol M. Stockton, of Alexandria, Virginia, accepted the award in early December on behalf of the journal.

Figure 27. The "Amphoragem" assemblage in this necklace contains crystals of (top to bottom): green gahnite, spessartine from Brazil, and red beryl from Utah. The body of the piece is quartz and the cap is rhodochrosite from Tadjikistan. Courtesy of Nature's Geometry; photo by Maha DeMaggio.

GEMS & GEMOLOGY
C·H·A·L·L·E·N·G·E

Anyone who missed even one issue of *Gems & Gemology* in 1996 missed a great deal. Spring started the year with African diamond sources and Russian hydrothermal synthetic emeralds. Summer brought information on Madagascar sapphires, Russian demantoid garnets, and Ethiopian opals. Fall highlighted the new De Beers diamond verification instruments, growth-structure analysis in gem identification, and Russian flux-grown synthetic alexandrites. The Winter issue covered such diverse topics as imitation tanzanite, trapiche rubies, gems from Sri Lanka, black opaque gem materials, and the Capão Imperial topaz mine. Now, we invite you to test your knowledge of these important topics by taking the 1 lth annual *Gems & Gemology* Challenge.

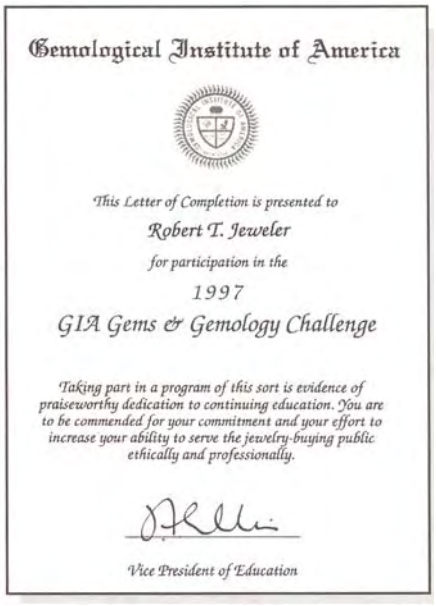
Gemological Institute of America

This Letter of Completion is presented to

Robert T. Jeweler

for participation in the

1997

GIA Gems & Gemology Challenge

Taking part in a program of this sort is evidence of praiseworthy dedication to continuing education. You are to be commended for your commitment and your effort to increase your ability to serve the jewelry-buying public ethically and professionally.

Vice President of Education

The following 25 questions are based on information from the four 1996 issues of *Gems & Gemology*. Refer to the feature articles and Notes and New Techniques in these issues to find the *single best answer* for each question,- then mark your choice with the corresponding letter on the response card provided in this issue (sorry, no photocopies or facsimiles will be accepted; contact the Subscriptions Department if you wish to purchase additional copies of the issue). Mail the card so that we receive it no later than Monday, August 18. Be sure to include your name and address (print legibly, please) All entries will be acknowledged with a letter and an answer key.

Score 75% or better, and you will receive a GIA Continuing Education Certificate. Earn a perfect score, and your name will also be featured in the Fall 1997 issue of *Gems & Gemology*.

1. The rarest color of topaz from the Capao mine is
   A. purple.
   B. "sherry" red.
   C. orange-yellow.
   D. reddish orange.

2. The De Beers DiamondSure™ instrument has been designed for the rapid examination of large numbers of
   A. natural diamonds.
   B. rough diamonds.
   C. polished diamonds.
   D. synthetic diamonds.

3. Of the top 10 diamond-producing countries from antiquity to 1994, Africa is home to
   A. three.
   B. five.
   C. seven.
   D. nine.

4. Before its recent fame as a source of fine blue sapphire, Madagascar was best known for producing beryls, tourmalines, and
   A. rubies.
   B. emeralds.
   C. garnets.
   D. diamonds.

5. Demantoid's usefulness in jewelry is dictated by its hardness, which is just under
   A. 8.
   B. 7.
   C. 6.
   D. 5.

6. Some brownish yellow and orange topazes from Ouro Preto are altered to pink by
   A. dyeing.
   B. heat treatment.
   C. diffusion treatment.
   D. irradiation.

7. One reason that the black members of the spinel mineral group represent an identification challenge is that the group contains

A. species with several morphologies.
B. species with different specific gravities.
C. 21 species
D. Shades of gray.

8. In addition to advanced testing techniques, "Tairus" hydrothermal synthetic emeralds can be separated from natural emeralds on the basis of their

A. internal features.
B. polariscope reactions.
C. reaction to ultraviolet radiation.
D. refractive indices.

9. To date, the negative *d* plane has been observed in natural rubies thought to be from

A. Sri Lanka and Tanzania.
B. Vietnam and Myanmar.
C. Myanmar and Thailand.
D. Thailand and Cambodia.

10. The surest means of separating natural alexandrite from Russian synthetic alexandrite is

A. optic character and specific gravity.
B. UV-visible absorption spectra.
C. characteristic growth patterns.
D. X-ray fluorescence and infrared spectroscopy.

11. Opal mining at Yita Ridge, Ethiopia, is presently

A. highly mechanized.
B. diminishing.
C. near capacity.
D. small in scale.

12. The most prestigious source of natural alexandrites is

A. Mexico.
B. Brazil.
C. Russia.
D. Tanzania.

13. For lapidaries and gem cutters, the most familiar durable black opaque material is probably the variety of quartz called

A. "black jade."
B. "black onyx."
C. "burnt topaz."
D. "black spinel."

14. The negative d plane, as a domi nant feature, is most common in

A. natural rubies.
B. flux-grown synthetic rubies.
C. flame-fusion synthetic rubies
D. none of the above.

15. Trapiche rubies are composed of triangular or trapezoidal sectors formed by the fixed arms of

A. a six-rayed star.
B. a four-rayed star.
C. an eight-rayed star.
D. all of the above.

16. A new, commercial source in Madagascar for fine blue sapphires is

A. Iankaroka.
B. Amboasary.
C. Antananarivo.
D. Andranondambo.

17. Much of the material that enters the gem trade as "tanzanite" is actually

A. irradiated blue iolite.
B. heat-treated colorless spinel.
C. heat-treated brown zoisite.
D. synthetic corundum.

18. Before the introduction of pipe mining in South Africa in 1869, what percentage of the world's annual diamond production came from Brazil?

A. 35%.
B. 50%.
C. 75%.
D. 90%.

19. The first country outside South Africa to have an economic kimberlite pipe was

A. Ghana.
B. Rhodesia.
C. Tanzania.
D. Ivory Coast.

20. Scapolite from Embilipitiya can be distinguished easily from similar-color citrine and feldspar on the basis of

A. fluorescence and birefringence.
B. inclusions and transparency.
C. optic character and immersion microscopy
D. growth zoning and low-relief inclusions.

21. Tanzanite generally can be easily separated from its many imitators by

A. growth-structure analysis.
B. R.I. andS.G.
C. chemical analysis
D. ultraviolet fluorescence.

22. Fine demantoids in commercial size are found almost exclusively in the

A. Ukraine.
B. Volga River.
C. Ural Mountains.
D. Kamchatka Peninsula.

23. One indication that an emerald may be synthetic is the presence of

A. a dominant growth pattern parallel to the *s* plane.
B. Cr lines seen with a hand spectroscope.
C. third-order interference colors.
D. a reaction to long-wave ultraviolet radiation.

24. The De Beers DiamondView™ enables the separation of natural from synthetic diamonds on the basis of

A. cathodoluminescence.
B. the presence of the 415 nm line.
C. the fluorescence image.
D. the colors of fluorescence.

25. The arms of the star in a trapiche ruby are created primarily by

A. oriented rutile needles.
B. chatoyancy.
C. aventurescence.
D. concentrations of inclusions.

GEMOLOGICAL ABSTRACTS

C. W. FRYER, EDITOR

DIAMONDS

Consequences of recycled carbon in carbonatites. D. S. Barker, Canadian Mineralogist, Vol. 34, 1996, pp. 373–387.

The question of the cycling of carbon through the Earth's crust and mantle is one of great interest with regard to the origin and evolution of diamonds. Carbon-bearing phases in the mantle include calcite and dolomite, as well as diamond, graphite, silicon carbide, dissolved methane, carbon monoxide, and carbon dioxide in fluids, and "carbonate components" in magma. The phases that form are a function of the availability of oxygen, as well as carbon, in the mantle.

Evidence has been accumulating that carbon from the crust is recycled deep into the mantle by subduction,- an important destination for this carbon—other than in diamonds—is the igneous rock carbonatite. The carbon isotopes in carbonatites do not match those of either marine carbonates (e.g., from coral reefs) or organic carbon (e.g., from plant debris); however, these isotopes are similar to those in peridotitic diamonds. From the study of trace-element distributions, especially of ultramafic xenoliths in carbonatites, the author concludes that these rocks probably result from repeated interactions of carbonate-rich mag-matic fluids with restricted volumes of metasomatically altered mantle rocks. Several influxes of carbon-rich magma have been implicated in the formation of diamonds at the Premier mine, and of coated diamonds from Africa, Siberia, and Australia. Carbonatites are uncommon in the Earth's crust, but this is probably because the mantle "soaks up" most batches of carbonate-rich magma, and only a few manage to reach the surface. *MLJ*

Southern Africa's offshore diamonds. *Mining Journal, London,* January 26, 1996, p. 63.

An increasing share of South Africa's diamond production comes from offshore deposits; for instance, in 1994, 31% of the country's total output (407,000 carats out of 1.31 million carats [Mct]) came from offshore, and 1995 production probably exceeded 500,000 carats. "Huge quantities" of gem-quality diamonds have been deposited

This section is designed to provide as complete a record as practical of the recent literature on gems and gemology. Articles are selected for abstracting solely at the discretion of the section editor and his reviewers, and space limitations may require that we include only those articles that we feel will be of greatest interest to our readership.

Inquiries for reprints of articles abstracted must be addressed to the author or publisher of the original material.

The reviewer of each article is identified by his or her initials at the end of each abstract. Guest reviewers are identified by their full names. Opinions expressed in an abstract belong to the abstracter and in no way reflect the position of Gems & Gemology or GIA.

along a 1,000 km stretch of Namibia's and South Africa's west coast; the total resource is estimated at 3,000 Met. Most of the deposits are along the Namibian coast because of prevailingly northward currents and waves. To date, about 80 Met have come from these deposits, but on-shore production from marine terraces and beaches in Namibia is expected to decline in the future.

Most offshore diamonds are presently recovered by De Beers Marine, from Namdeb concessions at 100 m depth, about 40 km from the coast. However, Namibian Minerals Corp. (Namco) has the largest exploration program in southern Africa, with concessions at Luderitz Harbor and Hottentots Bay in Namibia and in two areas off South Africa's west coast; its reserves are estimated at 80 Met. Namco is using a converted Russian spy ship to mine in water as deep as 100 m.

Diamond Field Resources (DFR) also has a concession (with BHP/Benguela) in the Luderitz area, between Diaz Point at the south and Hottentots Bay in the north, extend ing from the shoreline to 12 km offshore (water depths to 125 m). On the basis of modest amounts of exploration, a resource of over 1 Met, with an average value of $165/ct, has been confirmed. In 1995, DFR was granted two South African concessions, including the Cape Canyon area (200-500 m depth), which is thought to be a major repository of diamonds carried along a former trajectory of the Orange River. Last, Capetown-based Ocean Diamond Mining is expanding its small-scale mining around the 12 Penguin islands, off Namibia's southern coast. *MLJ*

The typical gemmological characteristics of Argyle diamonds. J. Chapman, G. Brown, and B. Sechos, *Australian Gemmologist,* Vol. 19, No. 8, 1996, pp. 339-346.

The Argyle mine produces more diamonds (about 40 million carats annually) than any other single source in the world. Yet there is a paucity of published data on the gemo-logical properties and characteristics of these diamonds.

Most Argyle diamonds are classified as industrial (45%) or near-gem (50%); only 5% are considered gem quality. Of this small percentage of gem-quality diamonds, the main colors are brown (80%), yellow (16%), colorless (2%), gray (2%), and pink and green (each < 1%). This article provides a valuable compilation of the properties of three color groups of gem-quality material: colorless, brown, and pink-red-mauve.

The following characteristics of these three categories are clearly tabulated and compared: classification (based on nitrogen aggregation), nitrogen content, habit, colors, color zoning, UV fluorescence and phosphorescence, absorption spectra (infrared, visible, and ultraviolet), and characteristic inclusions. Thirteen color photos illustrate surface and internal features, such as etch pits, color zoning, graining, and inclusions.

The authors found that more than 75% of the inclusions were of eclogitic origin, with orange garnet particularly abundant. However, epigenetic graphite lining cleavages and fractures was the most common inclusion in the Argyle diamonds studied. Also summarized is the discovery and geology of the Argyle pipe. Available reserves (if underground mining goes below the 300 m planned for the open pit) total about 100 million tonnes; a diamond con tent of 3.7 ct per tonne is estimated. *AAL*

GEM LOCALITIES

California jade, a geological heritage. A. Pashin, *California Geology,* Vol. 48, No. 6, 1995, pp. 147–154.

Nephrite, and to a lesser extent jadeite, has been found at several localities in California. California jade ranges from white to almost black, but the most common colors are shades of green.

Primary deposits are found throughout the state's extensive serpentinite zones, with significant localities in the counties of Monterey, San Benito, Mendocino, Mariposa, Tulare, Marin, and Siskiyou. However, most of the material recovered comes from secondary alluvial deposits of rivers draining the Klamath Mountains, Coast Ranges, and Sierra Nevada. Jade Cove nephrite can be found in the rough waters of the Pacific Ocean.

Commonly, jade is found in or adjacent to serpentinite bodies. An exception is in Riverside County, where a dark-green-to-black nephrite is found in a contact meta-morphic zone between quartz monzonite and dolomitic limestone. A Mendocino deposit is unique in that jadeite and nephrite are found together, often in the same rock.

The most common California jade simulants are mas sive vesuvianite (idocrase or californite) and serpentine. The vesuvianite varieties have been marketed as "Happy Camp Jade" and "Pulga Jade." A California serpentine called bowenite is marketed as "New Jade." *LBL*

Charoite: A unique mineral from a unique occurrence. M. D. Evdokimov, *World of Stones,* No. 7, 1995, pp. 3-11.

Charoite was first discovered in 1949, but it was not confirmed as a new mineral species until 1978. Unlike some other decorative stones, charoite occurs in several different colors-such as lilac, brown, and gray-often in the same specimen. Contrary to prior beliefs, charoite is not named after the Chara River (the closest bend of which is 70 km from the occurrence). "Instead, it was named for the impression that it gives: *chary*, a Russian word meaning *charms or magic."*

Charoite occu rs in about 25 areas along the Ditmar and Davan streams. The structure and subsequent mineralization of the occurrence are quite complicated. The stages of formation, which began in the early Archean (about 4.6 billion years ago), are described in detail. Charoite formed in breccia zones, the result of a mixture of solutions that was either deposited between the breccia fragments or metasomatically replaced the fragments in the zone. Discussions of the origination of the Murun Alkaline Complex and metasomatic rocks within the Complex complete a complicated and highly technical explanation of the formation of charoite.

Eight structurally diverse varieties of charoite reflect the order in which they were formed. The earliest to form was massive, structureless charoite. This was followed by parallel fibrous, undulatory-fibrous, felted, radial aggregates, mosaic-fibrous, slate-like, and, finally, sheaf-like varieties. Each of these is illustrated by intricate pen-and-ink sketches (which, unfortunately, are not clearly identified with figure numbers). Crystalline charoite has not been seen, so it is impossible to define the crystal structure and exact chemical formula of this mineral. There are at least nine different variations of the proposed formula. *LBL*

Combarbalitá: An ornamental kaolinite from Combarbalá, Chile. R. R. Coenraads, *Australian Gemmologist,* Vol. 19, No. 8, 1996, pp. 325–334.

Combarbalitá, a beautifully colored and patterned ornamental clay material, formed through the deep kaolinitic weathering of a metamorphosed volcanic and sedimentary rock sequence. It is found only in a region near the town of Combarbala, Chile—hence, the material's name. The small town is about 900 m above sea level, 90 km south of Ovalle and 80 km from the Pacific Coast. Mining this ornamental material (by hand) and crafting objects from it are important activities in this small town.

Long before the arrival of the Spanish, the original inhabitants of the area crafted beautiful pieces from this soft, easily worked and polished material. Examples of this somewhat primitive early art include pendants, necklaces, bowls, plates, arrowheads, and figurines. They have been found mainly in the local indigenous cemeteries, or as abandoned domestic items.

Hundreds of small quarries in the hills around Combarbalá produce combarbalita, with each quarry yielding specific colors or patterns. The mines are all close to the surface, the only area from which material can be recovered because weathering has made the original rock soft enough to be worked. The mines are worked by hand with basic tools—crowbars, hammers, and chisels. Pieces larger than 10 cm^3 are collected and tested with a hacksaw blade. If the blade easily saws the material, then it is soft enough to be turned on a lathe or worked by hand.

Most highly favored is a blue combarbalita that varies from a "blue-white" to a "strong sky-blue," very much resembling turquoise. These scarce varieties occur near copper mineralization, which points to copper as the pos sible coloring element. *MD*

Ethiopia: A new source for precious opal. D. B. Hoover, T. Z. Yohannes, and D. S. Collins, *Australian Gemmologist,* Vol. 19, No. 7, 1996, pp. 303–07.

A new source for precious opal has been discovered near the village of Mezezo, Shewa Province, Ethiopia. The deposit is located about 200 km northeast of Addis Ababa, on the Ethiopian plateau in central Ethiopia. Although Africa is not known for precious opal, artifacts show that ancient native cultures used it. Perhaps the source of these artifacts was the North Shewa deposit near Mezezo,- the Kushitic people, a group of stone age farmers, inhabited the region about this time.

Opal-filled lithophysae (hollow, bubble-like structures composed of concentric shells of finely crystalline alkaline feldspar, quartz, and other minerals found in silicic volcanic rock) weather out of the host rhyolite and are found scattered on the ground. The smaller nodules are remarkably spherical, while the larger ones tend to be slightly elliptical. Careful sampling at one site indicated 80 nodules per square meter at the face of the welded tuft host unit. About 10% of the nodules are solidly filled, the remainder have either partial or no opal filling.

The common opal that fills the nodules occurs in many colors- colorless, white, brownish red, orange, yellow, greenish, pale lavender, and an unusual chocolate-brown. The opal can be opaque, or it may be semi-translucent to transparent. Much of the material is transparent enough to facet; some is reminiscent of red Mexican "fire" opal. Precious opal is estimated to be present in about 1% of the nodules, but much of this has a weak play-of-color. Body color is similar to that found in the common opal, but no black opal has yet been found.

More than 50% of the precious opal is of the crystal to semi-crystal type. Typically, the play-of-color covers the spectrum in each piece. Green and blue or only blue play-of-color is rare; red is common. Pinfire patterns are rare; most examples show "flashfire." In better-quality material, the play-of-color is evident in many lighting directions. Some of the opal, both common and precious, has been found to be of the hydrophane type, which becomes more transparent when immersed in liquid. Some specimens of translucent gem hydrophane opal become completely transparent after they have been soaked in water for an hour. At that point, these opals lose most or all of their play-of-color, but they regain their fire once they are dry.

The long-term stability of this new opal is not known. Only a limited amount of material from near the surface has been collected and worked to date. Weathering has already taken its toll. Thus far, the authors of this arti cle have not experienced any major problems, such as frac turing or crazing, during cutting. Government regulations limit opal production to acquisition of representative sam ples for testing and evaluation, in advance of detailed mapping of the deposit and filing of a formal development plan. *MD*

Editor's note: A detailed article on this locality was also published by Johnson et al. in the Fall 1995 issue of Gems & Gemology*, Summer 1996, pp.* 112–120.

Euclase from Colombia showing three-phase inclusions. J. M. Duroc Danner, *Journal of Gemmology,* Vol. 25, No. 3, 1996, pp. 175-176.

This note documents the properties of a greenish blue euclase from Colombia. The specimen was notable for its wealth of "well-shaped" three-phase inclusions, as illus trated by a single photomicrograph. Other properties were characteristic for euclase. *CMS*

Goodletite-a beautiful ornamental material from New Zealand. G. Brown and H. Bracewell, *Journal of Gemmology,* Vol. 25, No. 3, 1996, pp. 211–217.

The ornamental gem material from New Zealand called "goodletite" has been known for more than 100 years. Although mentioned as early as 1962, it has not been detailed in the gemological literature. This is partly because of its rarity. It is a coarsely granular rock consisting of red to blue corundum, green Cr-rich margarite-muscovite mica, and green Cr-tourmaline. Examination of two specimens revealed, not surprisingly, variable properties consistent with the composition of this rock. The best means of identification is magnification, as illustrated by two photomicrographs. No *in situ* deposits have been located yet, and the availability of this material is still extremely limited. *CMS*

Investigations on sapphires from an alkali basalt, South West Rwanda. M. S. Krzemnicki, H. A. Hänni, R. Guggenheim, and D. Mathys, *Journal of Gemmology,* Vol. 25, No. 2, 1996, pp. 90–106.

Yet another new locality for natural blue and treatable sapphire surfaces in this description of material from the Cyangugu district of South West Rwanda. Following summary descriptions of the sapphires' geologic setting and apparent origin from alkali basalts, the results of testing 20 samples is reported. Absorption spectra (visible and infrared), quantitative chemistry (microprobe), and microthermometry were performed on two specially prepared samples. Ten prepared specimens were examined by SEM-EDS for inclusions, and eight rough samples were also studied by SEM for detailed surface analysis. The apparently meticulous methodology yielded high-quality detailed information that is a welcome addition to the gemological literature, despite the small sample size. Numerous illustrations also indicate that this material yields fine-quality gems of brilliant blue color. However, no mention is made of its commercial availability or potential supply. *CMS*

North Carolina's link to the Washington Monument. K. H. Roll, *Rock & Gem,* Vol. 27, No. 2, February 1997, pp. 32–34.

The author relates the little-known story of the five-pound solid aluminum "pyramidion"—made by processing rubies and sapphires mined in North Carolina—that was placed atop the Washington Monument in 1885. This leads to an account of corundum mining in North Carolina and the history of the Corundum Hill mine, once the world's largest producer of commercial corundum.

In the 19th century, aluminum was $1 an ounce and the North Carolina corundum was prized as a source of nearly pure aluminum oxide for use in the manufacture of the newly discovered metal. The Western world's primary source of corundum-based abrasives and jewel bearings before the first World War, the Carolina deposits were played out by the early 1900s. Still, recreational panning for the small gem-quality rubies and sapphires, notable for the distinctive asterism that many reveal, continues to be a tourist attraction in privately owned streambeds around the Corundum Hill area. *AC*

Older and wiser. G. Poinar, *Lapidary Journal,* Vol. 49, No. 10, January 1996, pp. 52–56.

The differences between copal (dried resin) and amber (fossilized resin)—a median of about 200 years versus 2–4 million years—is discussed, along with a simple hot-needletest for separating the two similar-appearing materials. Copal is popular as counterfeit amber. Large, colorful insects or lizards can be pressed into resin, which then hardens into copal in about a month. The author examined copal from deposits in New Zealand and Colombia (the latter is the basis of a bustling "amber" trade). Carbon dating showed that several samples of Colombian copal were between 10 and 500 years old. Nuclear magnetic spectrometry analysis confirmed that the samples did not differ significantly from resin from modern trees. The author concludes that most Colombian "amber" is really copal, found in fields and alluvial soil. Theoretically, amber could be found there, but it would most likely be in sedimentary formations. *AC*

JEWELRY HISTORY

Gleaning treasure from the Silver Bank. T. Bowden, *National Geographic,* Vol. 190, No. 1, July 1996, pp. 90–105.

On October 31, 1641, the Spanish galleon *Nuestra Señora de la Pura y Limpia Concepción struck* a reef north of the (now) Dominican Republic and sank with most of her crew. The *Concepcion* was carrying treasure from the Philippines and Mexico; the reef where she sank was named the "Silver Bank" because the sailors piled treasure from the sinking boat on it. They did this not only to save the treasure but also to provide a higher place to stand, to literally keep their heads above water.

The first successful salvager was William Phips, who hired native pearl divers to recover goods in 1687; the Burt Webber expedition visited the site in 1978. The author of this article returned to the site recently, under a contract with the Dominican Republic's Commission for Underwater Archaeological Recovery, and used ship-mounted vacuum-pumps to expose more artifacts. Shown in the article are gold chains, three gold-and-diamond pendants, a set of diamond-centered gold studs, and an amethyst ring. It is interesting that some of the porcelains recovered from the site show false markings, in an apparent attempt to indicate manufacture in an older (and more desirable) era than the one in which they were actually made. *MLJ*

JEWELRY MANUFACTURING ARTS

Elusive talent. Cathleen McCarthy, *Lapidary Journal,* Vol. 50, No. 10, February 1997, pp. 14-17, 66, 68, 70, 71.

This article gives insight into one of America's most cre-

ative carvers, Steve Walters, a true craftsman who can pick out the right piece of material, look at it, and "see" the design. This rare in-depth interview, well worth reading, covers Mr. Walters' beginnings, influences, and current thoughts on his creative talents and their continuing evolution. (He has no formal art training.) The unpretentious and prolific Mr. Walters insists that he is a craftsman and not an artist. Still, his work is so much in demand that his booth routinely sells out in the first four hours of the week-long Gem and Lapidary Dealers Association show in Tucson each February. How does he come up with his popular and unusual designs? "I don't know why I do it, and I don't know why it works . . . I've lucked out," he says. *AMB*

Making semi-precious precious. C. Frankel, *Art & Antiques,* Vol. 19, No. 9, October 1996, pp. 90–94.

Andrew Grima has long been a force in jewelry design. His use of unusual materials, from the common to the unique, has marked his flamboyant style for the past 50 years. Grima believes that good design need not always use the biggest stones and most costly materials. Originally a draftsman in a civil-engineering firm, he is thankful that he never formally went to school to learn design; he would have ended up turning out the same kinds of pieces as everyone else, he believes. His jewelry, though based on organic forms, tends toward the abstract, with emphasis on textured gold and exotic gems.

Grima's London gallery was opened in 1966. He moved his shop to Gstaad, Switzerland, in late 1993. His clients have included Queen Elizabeth, Jacqueline Onassis, and Elizabeth Taylor. *JEC*

Stuck on glue. A. Oriel, *Lapidary Journal,* Vol. 50, No. 10, February 1997, pp. 34–38, 39, 41, 44.

Andy Oriel talks about a product with which most in the jewelry and gem trade are unfamiliar—adhesives. These adhesives are very different from the gloppy "white" glue of our childhood. According to five jewelers and lapidaries who use high-tech adhesives in their work, the new adhesives stick with a vengeance and last not forever, perhaps, but certainly for a *very* long time. Thomas Harth Ames, Sid Berman, Henry Hunt, Martin Key, and Eugene Millerexplain the different adhesives that each uses and their properties, although they do not detail how the adhesives work chemically. All interviewees agree that adhesive has a place in working with gem materials, and they urge that we rethink the stigma of impermanence sometimes associated with "glue." The use of these new adhesives will allow more jewelry and carving possibilities than ever before. *AMB*

JEWELRY RETAILING

Retail pearl sales increase. *National Jeweler,* February 16, 1997, p. 16.

U.S. retail pearl sales increased an average of 18% in 1996 over 1995, according to a Cultured Pearl Information Center (CPIC) poll. Almost 89% of retailers surveyed reported an increase in their annual cultured pearl sales; 5% reported no change, and 6% reported a decrease. In terms of pearl sales, 41% of the retailers interviewed said they had an excellent year, 32% said they had a good year, 23% said they had a fair year, and 4% rated the year poor. The CPIC cited several reasons for the large increase in 1996, including more money spent on advertising, larger pearl inventories, better-quality pearl jewelry stocked in stores, and greater awareness of Tahitian and South Sea pearls. In addition, pearls appear to have become a more important fashion accessory. Retailers expect an average 14% increase in 1997 over 1996. *MD*

The revised FTC guides-what's permissible, what's not. *Jewelers' Circular Keystone,* Vol. 167, No. 8, August 1996, pp. 152–154.

This article focuses on the many changes present in the newly revised guidelines issued by the Federal Trade Commission for the jewelry industry. Included are reports on some of the commission's internal discussion of the issues involved. Sections on disclosing artificial coloring, misrepresentation of weight and total weight, and misuse of words such as *ruby, sapphire, emerald, and birthstone* are examined. This article is particularly helpful for anyone involved in manufacturing, sales, or appraisals. *JEC*

TREATMENTS

Dyed opalised sandstone and conglomerate: A new product from Andamooka. 1. L. Keeling and I. J. Townsend, *Australian Gemmologist,* Vol. 19, No. 5, 1996, pp. 226–231.

Opal-cemented sandstone and conglomerate from the Andamooka opal fields in south Australia is being treated by a process that is said to differ from the traditional sugar-acid method. The finished material is marketed for use in carvings, inlay work, cabochons, and assembled stones. Because of the high porosity of the sandstone and conglomerate starting material, it was very difficult to remove all traces of acid from the finished product when the conventional sugar-acid treatment was used. The new treatment process, the exact method for which (a "closely guarded secret") is not given in this article, purportedly has solved this problem.

The article did reveal that an organic solution is con verted to carbon in a nonoxidizing environment at tem peratures above 500°C. This produces an overall darker body color in the material, making any play-of-color more apparent. It also results in the production of the typical black microscopic specks of carbon that are associated with the well-known sugar-acid treatment method. These carbon specks made the sandstone and conglomerate treated by this "new" method very easy for this gemolo- gist to identify as treated. However, it may not be possible to distinguish between this "new" treatment method and sugar-acid treatment. *JIK*

On the identification and fade testing of Maxixe beryl, golden beryl and green aquamarine. K. Nassau, *Journal of Gemmology,* Vol. 25, No. 2, 1996, pp. 108-115.

Dr. Nassau discusses his latest findings on the distin guishing characteristics and color stability of Maxixe, golden, and green beryl. Having originally made the distinction between Maxixe and "Maxixe-type" beryl in the 1970s, he now proposes that both be referred to by the term *Maxixe,* on the premise that the distinction "serves no useful purpose in gemmology." Maxixe samples tested in less-than-ideal conditions revealed spectra (680 nm absorption) typical for Maxixe-type beryl. They also responded to color-stability testing with the fading typical of this material.

Similar testing of four "yellow to greenish" beryls produced no fading, but exposure to 100° ± 10°C heat (in darkness) for a week visibly reduced the yellow color component of two out of the four. Eight light-green to greenish yellow beryls proved to be aquamarine-type (pretreat-ment) beryls with no Maxixe component. All of the colors studied could be natural or the result of laboratory irradiation, with no possibility of distinguishing between these origins of color. *CMS*

MISCELLANEOUS

A critical matter. M. Heckenberg, Australian *Gold Gem & Treasure,* Vol. 11, No. 2, February 1996, p. 26.

The working definition of a gemstone's critical angle is the minimum angle at which the gem can be cut before it will have a "fish-eye" effect when viewed through the table. Light generally travels in a straight line, but it travels at different speeds in materials of different optical densities. Thus, light bends at the interface between media of different optical densities (such as air and water—a stick appears bent where it goes through the interface between the two). Light passing at an angle into a different medium is split into two parts: Some bends into the medium, and some reflects off the surface. At an angle greater than the critical angle, no light escapes from the denser medium (gemstone) into the less-dense air; all of it is reflected back into the gemstone.

In cutting a stone, one wants the light coming in through the table to be completely internally reflected by the pavilion facets,- none should "leak out" the back. The higher the optical density of the gem material is, the higher the refractive index—and the smaller the critical angle—will be. If you know the refractive index of a particular gem material, you can look up the critical angle in a book of mathematical tables. It can also be calculated from the nat ural cosecant of the refractive index. *MLJ*

Program to study crust and mantle of the Archean craton in southern Africa. R. W. Carlson, T. L. Grove, M. J. de Wit, and J. J. Gurney, *EOS, Transactions, American Geophysical Union,* July 16, 1996, pp. 273, 277.

A research program has begun that will systematically study the Kaapvaal craton, which covers 1.2 million km^2 (extending across South Africa, Lesotho, Swaziland, and Botswana, and grading into related rocks in Mozambique and Zimbabwe as well). The Kaapvaal craton contains rocks between 3.7 and 2.6 billion years old, and was last disturbed about 2.5 billion years ago; it is cut by kimberlite pipes, including the Jagersfontein, Finsch, Premier, Northern Lesotho, Farm Louwrcnsia, and Ramapfeliso.

Cratons are mysterious because of their long-term stability, which is thought to be caused by different types of sub-basement rocks in the mantle (for instance, the rocks under cratons are colder than other mantle regions at the same depths). Most of the information about these rocks comes from xenoliths in kimberlite pipes; the upcoming study will examine these xenoliths systematically in terms of their chemical and isotopic compositions, petrologies, and petrofabrics. Also, a portable seismic array will be deployed to look at seismic velocities (and their anisotropies) under the Kaapvaal craton. Experimental petrology of lower crustal rock types (that is, growing examples of these rocks at high pressures and temperatures), and studies of the sedimentary history of the Kaapvaal craton, are also planned. *MLJ*

A salty heritage. J. Raloff, *Science News,* April 27, 1996, pp. 264–265.

Chandeliers and life-size statues, altars, and "terrazzo" floors-all have been carved from rock salt (halite, NaCl), underground in Poland's Wieliczka mine. The dry air in the mine has preserved even the earliest carvings, which date to the late 17th century; recently, however, high pollution levels and variable humidity (exacerbated by hordes of tourists) have eroded fine features of the oldest and most valuable works.

An international team of scientists has studied the moisture-related deterioration. They found that, although pure rock salt does not start to pick up water until the relative humidity reaches 75%, pollutant-related salts (suchas ammonium nitrate) that collect on the rock-salt carvings can absorb water at relative humidities as low as 20%. A special dehumidifier has been designed to lower the moisture content of the mine's air—and, it is hoped, protect Wieliczka's unusual art. *MLJ*

What everyone should know about the hardness of diamonds and other minerals. B. Cordua, *Rocks Digest,* 1995, Vol. 8, No. 2, p. 20.

The durability and hardness of minerals can be explained in many different ways. Tests include Mohs and Knoop. Important terms are *brittleness, tenacity,* and strength. This article not only describes these tests and terms, but it also provides some insight into why various rocks can be made up of either hard or soft minerals, yet have very different "strengths" due to internal structure. *CEA*